Lehrstuhl für Zellbiologie der Technischen Universität München
Wissenschaftszentrum Weihenstephan

MIRANDA LOCALIZATION DURING ASYMMETRIC CELL DIVISION OF NEUROBLASTS IN *DROSOPHILA MELANOGASTER*

Veronika Erben

Vollständiger Abdruck der von der Fakultät Wissenschaftszentrum Weihenstephan für Ernährung, Landnutzung und Umwelt der Technischen Universität München zur Erlangung des akademischen Grades eines

Doktors der Naturwissenschaften (Dr. rer. nat.)

genehmigten Dissertation.

Vorsitzender: Univ.-Prof. Dr. Dr. h. c. (Univ. Kaposvári/Ungarn) Johann Bauer

Prüfer der Dissertation: 1. Univ.-Prof. Dr. Bertold Hock, em.
2. Univ.-Prof. Angelika Schnieke, Ph.D. (Univ. of Edinburgh/UK)

Die Dissertation wurde am 08.03.2007 bei der Technischen Universität München eingereicht und durch die Fakultät Wissenschaftszentrum Weihenstephan für Ernährung, Landnutzung und Umwelt am 30.04.2007 angenommen.
.

LIST OF ABBREVIATIONS

α	anti
aa	amino acid
ac	achaete
ACD	asymmetric cell division
ac/sc	achaete–scute complex
A/P	anterior-posterior
APC	adenomatous polyposis coli
aPKC	atypical protein kinase C
ase	asense
Baz	Bazooka
BMP	bone morphogenic protein
BSA	Bovine serum albumin
Cas	Castor
CIAP	calf intestine alkaline phosohatase
CLIP	cytoplasmic linker protein
CNS	central nervous system
CyO	curly wing
d	donkey
DEB	*Drosophila* embryo buffer
DEX	*Drosophila* embryo extract
DIG	digoxygenin
Dlg	Discs large
Dpp	Decapentaplegic
dsRNA	double stranded RNA
DTS	dominant temperature sensitive
DTT	dithiothreitol
D/V	dorsal-ventral
e	ebony
EB1	end-binding protein 1
eGFP	enhanced GFP
EGFR	epidermal growth factor receptor
Elp	Ellipsoid
ER	endoplasmatic reticulum
E(spl)	Enhancer of split
FLP	flippase
FRT	flippase recognition target
FRAP	fluorescence recovery after photobleaching
g	goat

GAL	genes induced by galactose
Gh/Grh	Grainyhead
GFP	green fluorescent protein
GMC	ganglion mother cell
GRP	glucose-regulated protein
Hb	Hunchback
HRP	horseradish peroxidase
hs-flp	heat shock-flippase
IHC	immunohistochemistry
Ind	intermediate neuroblast defective
Insc	Inscuteable
IP	immunprecipitation
KDEL	lysine (K)-aspartic acid (D)-glutamic acid (E)-leucine (L)
Kr	Krüppel
LB	Luria broth
Lgl	Lethal giant larvae
L´sc	Lethal of scute
m	mouse
msh	muscle segment homeobox
NEB	nuclear envelope breakdown
nls	nuclear localization signal
NGS	normal goat serum
NF	nuclear factor
O/N	over night
pa	pro analysis
Par	partitioning defective
PAGE	polyacrylamid gel electrophoresis
PBS	phosphate buffered saline
PBT	phosphate buffered saline with triton
pc	pole cells
PCR	polymerase chain reaction
pdm	POU domain proteins
PTB	phosphotyrosine-binding
PDZ	Post synaptic density protein/Discs large/Zonula occludens protein
Pins	Partner of Inscuteable
PNS	peripheral nervous system
PON	Partner of Numb
PreIS	preimmune serum
PTB	phosphotyrosine binding domain
PVDF	Polyvinylidene fluoride
r	rat

rb	rabbit
RFP	red fluorescent protein
RISC	RNA-induced silencing complex
RKI	Rho-kinase inhibitor
RLC	regulatory light chain
RNAi	RNA interference
ROI	region of interest
RRX	Rhodamine Red-X
RT	room temperature
Sb	Stubble
sc	scute
sca	scabrous
SDS	sodium dodecyl sulphate
SDS-PAGE	sodium dodecyl sulphate polyacryl amid gel electrophoresis
siRNA	small interfering RNAs
SNS	stomatogastric nervous system
SOP	sensory organ progenitor cells
Sp	Sternopleural
Tb	Tubbey
TY	Trypton
UAS	upstream activator sequence
Ubx	Ultrabithorax
VNC	ventral nerve cord
vnd	ventral nervous system defective
w+	white
WB	western blotting
y+	yellow

1 ZUSAMMENFASSUNG

Neuroblasten sind Stammzellen des Zentralnervensystems von *Drosophila*. Aus der inäqualen Zellteilung gehen wiederum ein Neuroblast sowie eine Ganglionmutterzelle hervor, die Vorläuferzelle von Neuronen und Gliazellen. Die inäquale Zellteilung setzt eine ungleichmässige Verteilung von Proteinen und RNA voraus. Neuroblasten sind ein hervorragendes Modellsystem, um die dabei ablaufenden Prozesse zu studieren. Während der Metaphase werden in Neuroblasten zwei Proteinkomplexe auf die gegenüber liegenden Zellpole, d.h. apikal und basal verteilt. Der apikale Proteinkomplex koordiniert die Spindelrotation, die Asymmetrie der Zellgröße und die richtige Lokalisierung eines basalen Protein/RNA-Komplexes in der Metaphase. Innerhalb des basalen Komplexes spielen Miranda als Adaptorprotein für Prospero und „Partner of Numb“ (PON) als Adaptorprotein für Numb eine zentrale Rolle für die Festlegung des weiteren Zellschicksals. Die beiden Adaptorproteine stellen sicher, dass die mit ihnen assoziierten Proteine in der Telophase der Mitose zum basalen Zellpol gelangen und auf diese Weise das Zellschicksal determinieren. Bei der anschließenden Zellteilung werden die Adaptorproteine dann zusammen mit den assoziierten Faktoren nur an die Ganglionmutterzelle weitergegeben. Intensive Forschungsarbeiten in den letzten Jahren konnten dem Aktin-Myosin Zytoskelett eine zentrale Rolle bei der Proteinlokalisierung im Neuroblasten zuweisen. Dennoch blieb der exakte Mechanismus der inäqualen Teilung weiterhin unbekannt. In der vorliegenden Arbeit wird in der komplexe Mechanismus der asymmetrischen Proteinlokalisierung in neuronalen Stammzellen des Zentralnervensystems von *Drosophila* durch die Anwendung konfokaler Fluoreszenzmikroskopie, molekularbiologischer sowie genetischer und biochemischer Arbeitstechniken charakterisiert.

Bereits publizierte Ergebnisse aus Experimenten mit fixiertem Embryonalgewebe weisen auf ein dynamisches Verhalten von Miranda und PON während der Mitose hin. Allerdings ermöglichen experimentelle Ansätze dieser Art nicht, Proteine einer lebenden Zelle während der Zellteilung zu beobachten. Zusätzlich muss mit der Möglichkeit von Fixierungsartefakten gerechnet werden. Im Rahmen dieser Arbeit wurde deshalb eine Methode zur Beobachtung von Proteinen im lebenden Embryo entwickelt. GFP (green fluorescent protein)-Fusionsproteine wurden zellspezifisch exprimiert und mit Hilfe konfokaler Fluoreszenzmikroskopie während der Mitose gefilmt. Hierbei wurde eine dynamische, zytoplasmatische Phase von Miranda-GFP in der Pro/Metaphase entdeckt, während PON-GFP ausschließlich kortikal nachgewiesen wurde. Obwohl Miranda und PON in der Metaphase halbmondförmig basal in einem sog. „Crescent“ kolokalisieren, benutzen sie unterschiedliche „Wege“, zum basalen

Zellpol. Diese Gegensätze deuten auf zwei unterschiedlich regulierte Proteinkomplexe innerhalb des Neuroblasten hin: Einerseits der Miranda/Prospero-Komplex, dessen Komponenten durch das Zytoplasma zum basalen Pol der Zelle gelangen, andererseits der PON/Numb-Komplex, dessen Bestandteile sich entlang des Kortex zum basalen Pol bewegen. Durch die Analyse am lebenden Embryo konnte weiterhin gezeigt werden, dass Miranda in der Prophase kein apikales „Crescent" bildet, wie in einigen fixierten Präparaten zu erkennen ist.

Die Anwendung genetischer sowie immunhistochemischer Methoden und *in situ* Hybridisierung ergaben, dass weder die lokale Translation von *miranda* mRNA am basalen Zellpol noch die apikale Degradation von Mirandaprotein wesentlich zur dynamischen Lokalisierung von Miranda beitragen. Miranda ist auch nicht, wie anfänglich vermutet, mit dem endoplasmatischen Retikulum assoziiert. Die Kinetik von an der inäqualen Zellteilung beteiligten Proteinen wurde mit Hilfe von Bleichexperimenten („Fluorescence Recovery After Photobleaching" (FRAP)) berechnet und deutet auf eine zytoplasmatische Diffusion von Miranda hin. Zur Verringerung der Myosin II- und Myosin VI- Aktivität wurden lebende Embryonen mit RNAi und Proteininhibitoren injiziert und Proteine während der Mitose beobachtet. Die Ergebnisse zeigen, dass Myosin II Miranda vom apikalen Pol ausschließt, während Myosin VI im basalen Zellbereich das diffundierende Protein aufgreift, um es zum basalen Kortex zu transportieren. Die PON Lokalisierung hingegen erfolgt unahängig von Myosin VI. Durch Erzeugung verschiedener transgener *Drosophila* Deletionslinien konnte die Rolle der 314 N-terminalen Aminosäuren für die kortikale Mirandalokalisierung gezeigt werden. Basierend auf diesen Ergebnissen wurde ein Model entwickelt, das die komplexe Regulation von Miranda im Neuroblasten erklärt.

Zusätzlich zur Charakterisierung der Mirandadynamik wurde der Einfluss von Miranda auf die Embryonalentwicklung anhand von Keimbahnklonen („Germline Clones") untersucht. Keimbahnklone ohne funktionales Miranda zeigen einen auffälligen Phänotyp mit fehlender Zellpolarität und abnormaler Zellmorphologie. Dies weist auf eine wichtige Rolle von Miranda bereits während der Embryonalentwicklung hin.

Über den Einfluss posttranslationaler Modifikationen auf die Mirandalokalisierung ist bisher wenig bekannt. In dieser Arbeit konnte erstmals die *in vivo* Phosphorylierung von Miranda an Serin-, Threonin- und Tyrosinresten nachgewiesen werden. An der Mitose von Neuroblasten sind verschiedene Kinasen wie etwa aPKC (atypical protein kinase C) und CdC2 (cell cycle kinase 2) beteiligt. Zukünftige Mutationsexperimente an den vermutlichen Phosphorylierungsstellen von Miranda werden den Zusammenhang zwischen postranslationalen Modifikationen von Miranda und dessen Lokalisierung aufzeigen müssen.

2 ABSTRACT

Drosophila neuroblasts are stem cells in the central nervous system of *Drosophila*. They divide asymmetrically in order to simultaneously self-renew and generate differentiated cells (neurons and glia cells). Asymmetric cell divisions (ACD) can be achieved by localizing cell fate determinants to only one pole of the cell. *Drosophila* neuroblasts provide an excellent model system to study this process. During neuroblast metaphase two different protein complexes are localized to opposite (apical and basal) sides of the cell. The apical protein complex coordinates spindle rotation, size asymmetry, and correct localization of a basal protein/RNA complex. Within the basal complex, the adaptor proteins Miranda and Partner of Numb (PON) were identified to play a major role in establishing cell fate by localizing their respective target proteins and cell fate determinants Prospero and Numb to one side of the cell. Upon cytokinesis, adaptor proteins and associated cell fate determinants are inherited by only one daughter cell which thereby switches its fate. Despite the recent progress that establishes the important role of acto-myosin in the localization of proteins involved in asymmetric cell division (ACD), several questions remain to be answered and were addressed in this thesis. Overall, this thesis elucidates the complex regulatory mechanisms of asymmetric protein localization in neural stem cells by using live imaging combined with molecular biology, genetic and biochemical approaches.

It is known from immunohistochemical studies on fixed embryonic tissue that Miranda and PON exert dynamic localization during ACD of neuroblasts. This method, however, has two major drawbacks. Firstly, it is impossible to follow protein localization over time within the same cell. Secondly, fixation procedures bear the risk of creating artifacts. To overcome these constraints and to improve the understanding of the mechanism underlying ACD a “Live Imaging Set-Up” was developed during this thesis. This new experimental approach enables monitoring of fluorescence fusion proteins in living embryos using time-lapse confocal microscopy. Following Miranda-GFP and PON-GFP in neuroepithelial cells and neuroblasts revealed interesting new features: Although both proteins colocalize to a basal crescent in metaphase they use different routes to translocate there. Miranda-GFP shows a very dynamic behavior that is distinct from PON-GFP, which indicates that the two protein complexes Miranda/Prospero and Numb/PON are regulated differently. Whereas PON-GFP localizes exclusively cortical during all phases of mitosis, Miranda-GFP forms a “cytoplasmic cloud” in pro-metaphase. This cloud moves rapidly through the cytoplasm and precedes basal

crescent formation. Contrary to earlier results gained with fixed embryonic tissue, live imaging revealed that Miranda does not form an apical crescent in prophase.

Using different genetic approaches and *in situ* hybridization combined with immunohistochemistry showed that localized translation of *miranda* mRNA on the basal cortex does not significantly contribute to basal Miranda protein localization. Moreover, Miranda is not associated with the asymmetrically distributed endoplasmatic reticulum (ER) nor is it locally degraded at the apical side of the cell. Fluorescence Recovery After Photobleaching (FRAP) experiments using the "Live Imaging Set-Up" were used to calculate the kinetics of several proteins involved in ACD and revealed a rapid and three-dimensional diffusion of Miranda-GFP in the cytoplasm. Reducing Myosin II and VI activity by injecting RNAi and protein inhibitors into living embryos demonstrated that Miranda is removed from the apical cortex by Myosin II while Myosin VI is required at a subsequent step to relocate Miranda from the cytoplasm to the basal cortex during metaphase. However, PON localization depends on Myosin II but not on Myosin VI, which again indicates that PON and Miranda are differently regulated. Several transgenic fly lines were generated and analyzed revealing a distinctive role of the 314 N-terminal amino acids for cortical Miranda localization. Based on the results of these experiments a new model was developed reflecting the complex regulatory mechanism of proteins involved in ACD in *Drosophila* neuroblasts.

To overcome "maternal contribution" and to analyze the influence of Miranda during early *Drosophila* development, germline clones were generated. Miranda "loss of function" germline clones revealed a strong phenotype manifested in the loss of polarity and abnormal cellular morphology, indicating that Miranda is essential during embryogenesis.

Several kinases like the atypical Kinase C (aPKC) and the cell cycle kinase CdC2 are involved in neuroblast mitosis. However, it is unknown whether phosphorylation of Miranda itself contributes to determining its localization. A biochemical approach in this thesis revealed that Miranda is phosphorylated on serine, threonine, and tyrosine *in vivo*. Future mutation experiments of putative phosphorylation sites will have to demonstrate the exact role of phosphorylation for Miranda localization.

3 INTRODUCTION

3.1 The Development of *Drosophila melanogaster*

Drosophila melanogaster is one of the most commonly used model organisms due to its small size and short generation time. *Drosophila* generation takes about 9 days at 25 °C (Figure 1) and can be slowed down by keeping stocks at 18°C, whereby the development increases up to 20 days (Weigmann et al., 2003). Embryonic development, beginning with fertilization, takes about 24 hours (Table 1). At the end of the first day, the embryo hatches out of the eggshell to become a larva. The larva passes through three stages, known as instars, separated by molts. It synthesizes a new cuticle and releases the old one. At the end of the third instar, the larva pupates. After metamorphosis, a radial remodeling of the body inside the pupa, an adult fly (imago), emerges (Alberts et al., 2002).

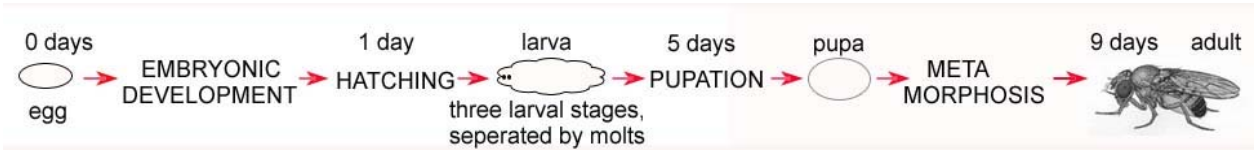

Figure 1: Development of *Drosophila melanogaster.*

3.1.1 Stages of Embryogenesis

Fly development proceeds through a complex series of stages and processes (Figure 1). The "Flybase"* provides comprehensive information covering all aspects of *Drosophila*: genes, proteins, and all developmental processes (Grumbling et al., 2006). In "The Atlas of *Drosophila* Development" (Hartenstein, 1993) several groups of color illustrations follow the main events of embryogenesis and post-embryonic development of *Drosophila.* Volker Hartenstein and Campos-Ortega subdivided embryonic development of *Drosophila* into 17 stages (Figure 2). Staging according to these authors has become a general reference in *Drosophila* research (Weigmann et al., 2003).

3.1.2 Early Development (Oogenesis)

Drosophila begins its development with a series of nuclear divisions without cell division, creating a syncytium (stage 1-4) (Mazumdar and Mazumdar, 2002). The nucleus of the fertilized egg performs 13 rapid divisions, which are synchronous and extremely rapid, occurring

* http://flybase.bio.indiana.edu/

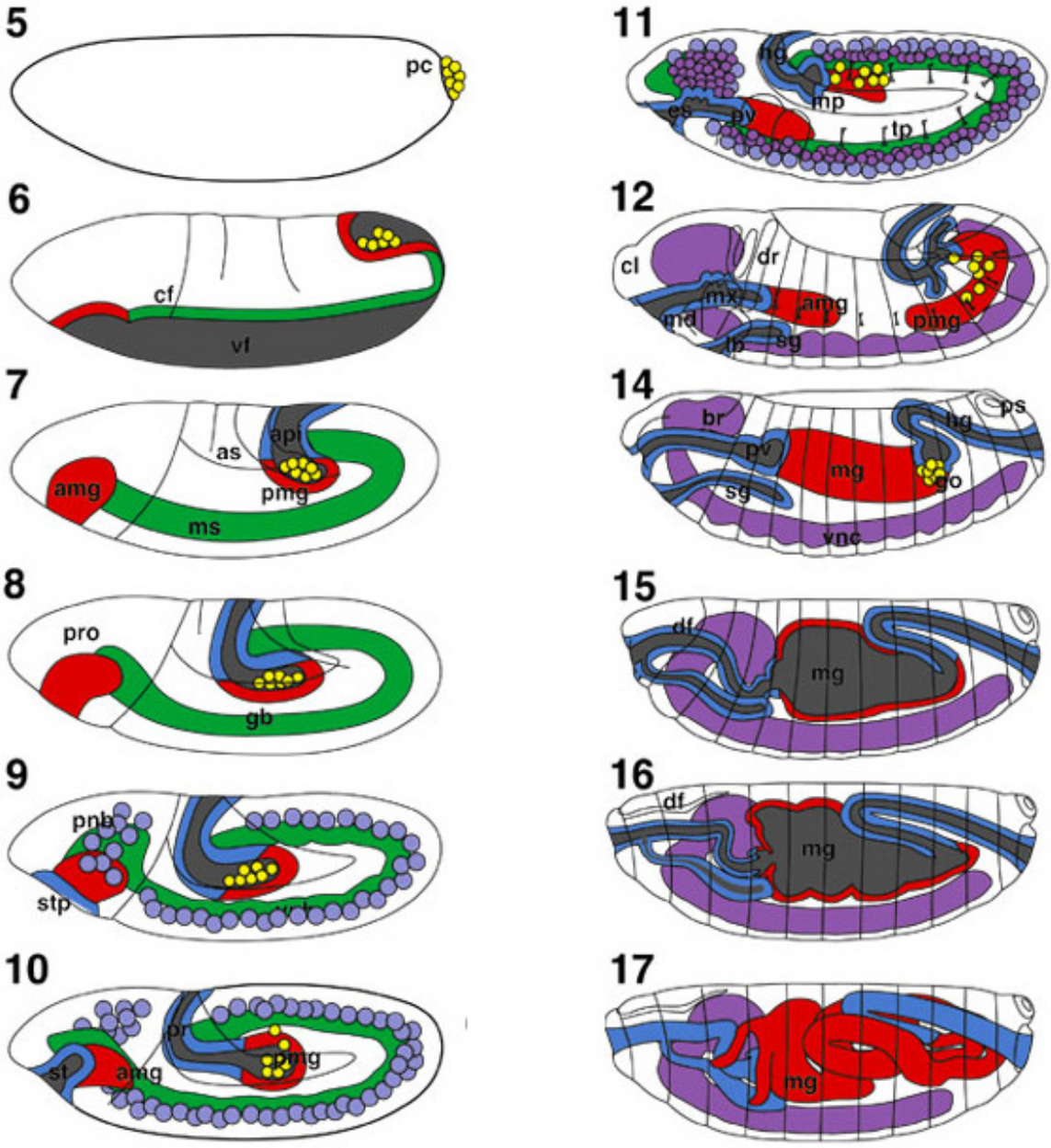

Figure 2: Stages of *Drosophila* embryo development.

Embryos are depicted in lateral view (anterior to the left, posterior to the right). Organs are coloured: endoderm and midgut (red), mesoderm (green), central nervous system (purple), foregut and hindgut (blue) and pole cells (yellow). The following abbreviations were used: anterior midgut rudiment (amg), brain (br), cephalic furrow (cf), clypeolabrum (cl), dorsal fold (df), dorsal ridge (dr), esophagus (es), germ band (gb), gonads (go), hindgut (hg), labial bud (lb), mandibular bud (md), midgut (mg), Malpighian tubules (mg), maxillary bud (mx), pole cells (pc), posterior midgut rudiment (pmg), procephalic neuroblasts (pnb), procephalon (pro), posterior spiracle (ps), proventriculus (po), salivary gland (sg), stomodeal plate (stp), stomodeum (st), tracheal pits (tp), ventral furrow (vf), ventral neuroblasts (vnb), ventral nerve cord (vnc). Adopted from "Atlas of *Drosophila* Development" (Hartenstein, 1993).

Table 1: Timetable of embryogenesis.

Several prominent features define embryonic stages of *Drosophila*. The duration of the various stages refers to embryos developing at 25°C (Weigmann et al., 2003).

STAGE	TIME	DEVELOPMENTAL EVENT
1 - 4	0:00 - 2:10 hr	Cleavage
5	2:10 - 2:50 hr	Blastoderm
6 - 7	2:50 - 3:10 hr	Gastrulation
8 - 11	3:10 - 7:20 hr	Germ band elongation
12 - 13	7:20 - 10:20 hr	Germ band retraction
14 - 15	10:20 - 13:00 hr	Head involution and dorsal closure
16 - 17	13:00 - 22:00 hr	Differentiation

on average every 8 minutes at the beginning (Hartenstein, 1993). Thereby, a cloud of nuclei is generated, most of which migrate from the middle of the egg toward the surface. Arranged in a single layer beneath the egg surface they form a monolayer called the syncytial blastoderm (Hartenstein, 1993; Alberts et al., 2002). Cell membranes are formed around the nuclei and lead to the cellular blastoderm (Table 1; stage 5), a homogeneous cellular sheet surrounding the central yolk (Loncar and Singer, 1995). The pole cells (pc), form a cluster of 34-37 round cells at the posterior embryonic pole (Figure 2) (Hartenstein, 1993). Pole cells are germ-line precursors that will give rise to eggs or sperm later on (Okada, 1998). Development depends largely on stocks of maternal mRNA and protein up to the cellular blastoderm stage, the so-called maternal contribution (3.1.3). The mother therefore loads the egg with most of the gene products because the rapid rate of DNA replication and nuclear divisions gives little opportunity for transcription (Wieschaus, 1996; St Johnston, 2002). After cellularization, cell divisions slow down and the rate of transcription is enhanced. Gastrulation begins shortly before cellularization is complete. Parts of exterior cells sheets invaginate to form the gut, the musculature, and associated internal tissue (Leptin, 1999). The central nervous system is formed shortly after and in another region of the embryo when a separate set of cells immigrates from the surface epithelium into the interior (Alberts et al., 2002). The earliest genes acting in development are maternal genes. They are expressed during oogenesis and their products are stored in the egg. They are required in the egg before the developing embryo starts transcribing its own genes ("zygotic gene expression") (Merrill et al., 1988; Weigmann et al., 2003).

The egg is a highly structured chamber: In the female ovary, the oocyte develops while connected to its sibling nurse (Figure 3)(Mahowald and Kambysellis, 1980). Oocyte and nurse cells are surrounded by a somatic epithelium. Epithelial follicle cells play an impor-

tant role in setting up the initial asymmetries of the oocyte. A complex exchange of signals between the oocyte and the follicle cells define the main axes of the future insect body before fertilization (Riechmann and Ephrussi, 2001). The four egg-polarity signals, provided by *bicoid*, *nanos*, *torso*, and *toll,* define the anterior-posterior (A/P) and dorso-ventral (D/V) axes of the future insect body in form of a morphogen gradient that organize the developmental process in the neighbourhood (Alberts et al., 2002).

3.1.3 Maternal Contribution

During oogenisis, nearly all cytoplasmic components of the early embryo are supplied maternally. The functional unit of oogenesis, the egg chamber, consists of one oocyte and 15 intercellular germline derived nurse cells surrounded by a monolayer of somatic follicle cells (Figure 3) (Gigliotti et al., 2003). Connected by cytoplasmic bridges called ring canals, nurse cells transfer their cytoplsma to the oocyte using a microtubule network that nucleates in the oocyte (Weigmann et al., 2003). Up to stage 10 this process occurs slowly, but during stage 11, the entire cytoplasmic content of the nurse cells is transferred to the oocyte within 30 minutes (Wheatley et al., 1995). This step is known as “dumping” and as demonstrated by drug studies (Gutzeit, 1986) and certain mutations (Cooley et al., 1992; Xue and Cooley, 1993; Cant et al., 1994; Verheyen and Cooley, 1994) depends on an intact cytoskeleton. Nurse cells provide nutrients (e.g. protein, mRNA, ribosomes) and will support the early development of the embryo after the egg is fertilized (Grumbling et al., 2006). After dumping their cytoplasmic contents into the oocyte the nurse cells die by apoptosis (Cavaliere et al., 1998; Foley and Cooley, 1998; McCall and Steller, 1998). The massive cytoplasmic input known as “maternal contribution” can therefore rescue the function of a mutant gene (Perrimon, 1998). This explains why many mutants in *Drosophila* do not show phenotypes in early development despite the abnormalities that they elicit later on. This delay results from the presence of a sufficient amount of wild-type product provided by the mother (Carmena et al., 1991).

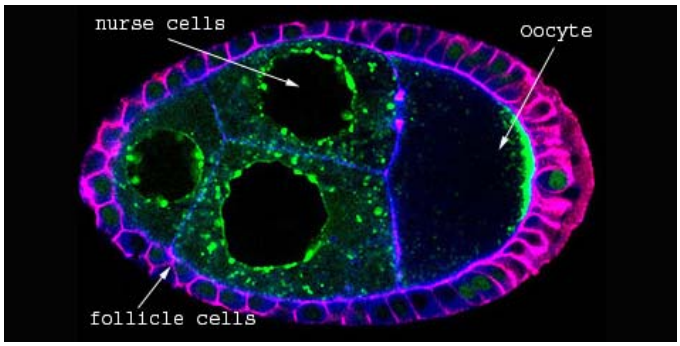

Figure 3: Drosophila egg chamber.

Nurse cells and follicle cells are associated with the Drosophila oocyte. The confocal image of a Drosophila egg chamber was stained for Staufen (green), actin (blue) and spectrin (red). Source: Herman Lopez-Schier, University of Cambridge, UK.

3.2 The Nervous System of *Drosophila melanogaster*

3.2.1 Structure of the Nervous System

The nervous system consists of three different subtypes:

- The **central nervous system (CNS)** consists of the brain and the ventral nerve cord (VNC). It is derived from neuroblasts and midline progenitor cells.
- The **peripheral nervous system (PNS)** builds up the sensory system and derives from sensory organ progenitor cells (SOP´s).
- The **stomatogastric nervous system (SNS)** derives from three evaginations on the dorsal side of the stomodeum (Weigmann et al., 2003).

3.2.2 Development of the Ventral Nerve Cord

3.2.2.1 Overview

The central nervous system (CNS), which encompasses the brain and ventral nerve cord (VNC), develops from a bilateral neuroectoderm (Urbach and Technau, 2003). Neuroectodermal cells localized at the ventral-lateral region of the embryo form the future VNC. Patterning genes which are acting along the anterior–posterior (A/P) and dorsal–ventral (D/V) axes subdivide this region into a pattern of neural equivalence groups (Figure 4 a,b, detailed description 3.2.2.2). Through interaction among cells of each equivalence group one cell is selected to acquire CNS stem cell or neuroblast fate. The neuroblast then enlarges and delaminates into the interior of the embryo whereas remaining cells either retain their undifferentiated state or acquire an epidermal fate (Figure 4 c, detailed description 3.2.2.3). Neuroblast segregation occurs in 5 sequential waves which results in the formation of an invariant pattern of 30 neuroblasts per hemisegment (a hemisegment is defined as the bilateral half of a segment and is the developmental unit of the VNC). After delamination each neuroblast divides repetitively and asymmetrically in a stem cell manner to generate chains of smaller secondary precursor cells known as “ganglion mother cell”s (GMC) into the interior of the embryo (Figure 4 d; detailed description 3.2.2.4). GMC divide only once more asymmetrically to produce two postmitotic neurons and/or glia cells. Consequently, in each VNC hemisegment an identified set of 30 neuroblasts generates a large pool of GMCs giving rise to about 400 postmitotic neurons and glia. Each postmitotic cell expresses special regulatory genes resulting in individual neurons and glia cells with distinct morphologies, synaptic targets, ion channels, neurotransmitters and neuropeptides (Figure 4 e,f; detailed description 3.2.2.5 and 3.2.2.6). The sequential action of all these processes generates a three-dimensional and func-

tionally integrated CNS out of uniform neuroectodermal cells in less than 24 hours (Skeath and Thor, 2003).

3.2.2.2 Patterning of the Ventral Nerve Cord

Genetic cascades that pattern the neuroectoderm along its A/P and D/V axes were identified by complex molecular genetic studies (Figure 4 a,b) (Anderson et al., 1985; Frohnhofer et al., 1986; Schupbach and Wieschaus, 1986; St Johnston and Nuesslein-Volhard, 1992). The location of each A/P stripe of segment-polarity gene expression in a segment is defined by the sequential action of the maternal A/P coordinate, *gap* and *pair-rule* genes (Akam, 1987). The "segment-polarity" genes such as *wingless* (Baker, 1987), *hedgehog* (Ma et al., 1993), *gooseberry* (Gutjahr et al., 1993), and *engrailed* (Kornberg, 1981), control gene expression along the A/P axis and enable neuroblasts that form in different A/P rows to acquire different fates (McDonald and Doe, 1997; Bhat, 1999). Simultaneously to A/P patterning, three signaling pathways, namely the nuclear factor NF-κB, known as Dorsal in *Drosophila*, bone morphogenic protein (BMP) named Decapentaplegic (Dpp) in *Drosophila*, and epidermal growth factor receptor (EGFR), converge to determine the D/V borders of the neuroectoderm and subdivide the embryo into specific tissue types: mesoderm, neuroectoderm, dorsal, epidermis, PNS, and amnioserosa (von Ohlen and Doe, 2000). Each tissue is further subdivided into more precise D/V domains. In the neuroectoderm expression of one of the three homeodomain-containing "columnar genes" *ventral nervous system defective* (*vnd*), *intermediate neuroblast defective* (*ind*) and *muscle segment homeobox* (*msh*) in adjacent columns control the formation of three D/V domains (Jimenez et al., 1995; Mellerick and Nirenberg, 1995; D'Alessio and Frasch, 1996; Isshiki et al., 1997; Weiss et al., 1998). These "columnar genes" regulate gene expression along the D/V axis and enable neuroblasts that form in different D/V columns to acquire different fates. A/P and D/V patterning events subdivide the neuroectoderm of each hemisegment into a checkerboard pattern of neural equivalence groups each of which contains a unique combination of segment-polarity and columnar gene activities (Figure 4 a,b). Each unique combination of gene activities results in the expression of a distinct set of genes which control the identity of the neuroblast that segregates from the neuroectoderm (Skeath and Thor, 2003).

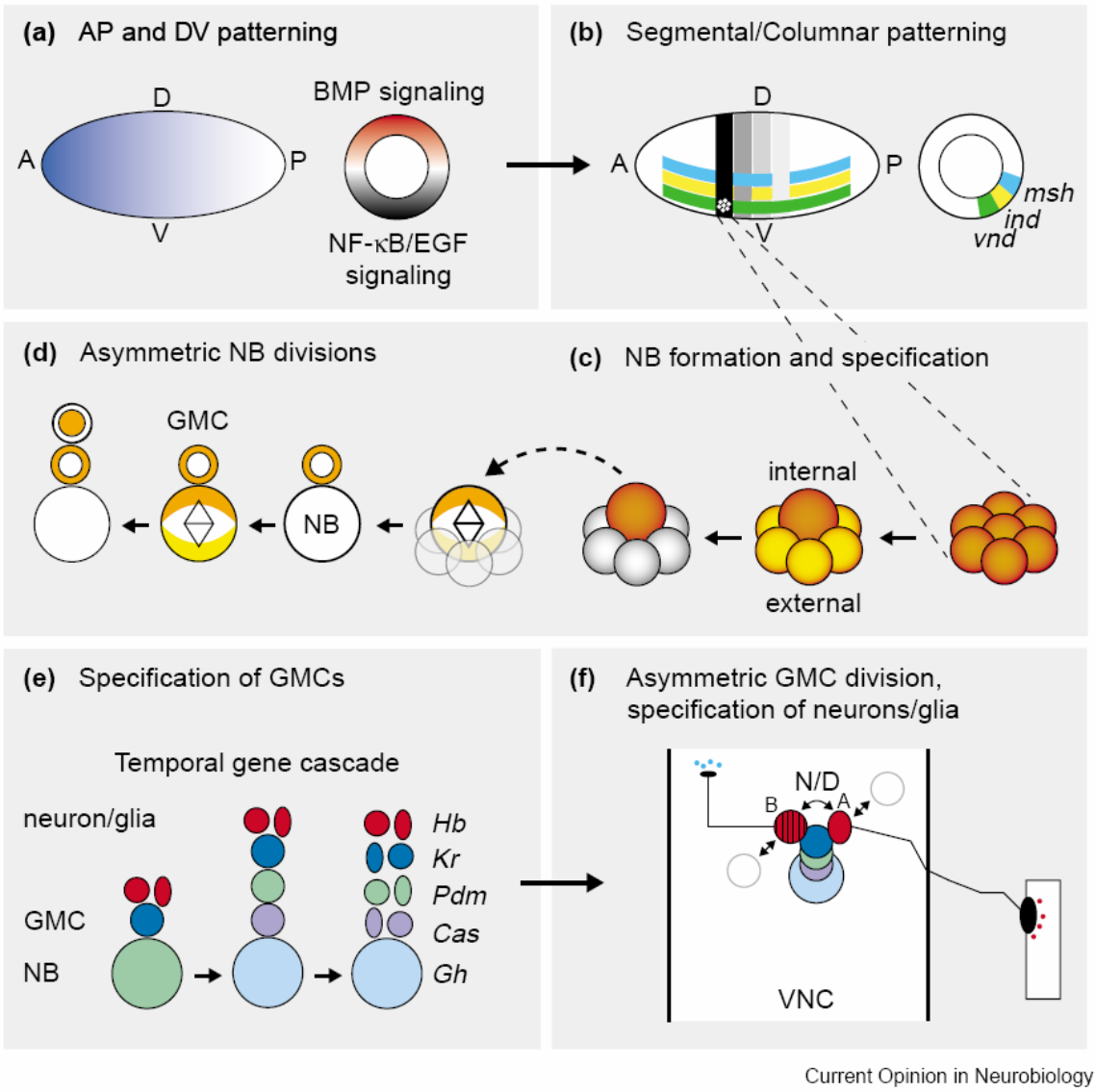

Figure 4: Development of the *Drosophila* ventral nerve cord (VNC).

Adopted from Skeath and Thor, 2003.

3.2.2.3 Neuroblast Formation

Neuroblast formation is regulated by two important classes of genes: Proneural genes promote neuroblast formation (Garcia-Bellido, 1979; de-la-Concha et al., 1988; Ghysen and Dambly-Chaudiere, 1989; Romani et al., 1989; Brand et al., 1993; Dominguez and Campuzano, 1993; Jarman et al., 1993), whereas the neurogenic genes inhibit neuroblast formation (Campos-Ortega, 1993). The proneural genes *achaete (ac)*, *scute (sc)*, *lethal of scute (l'sc)* and *asense (ase)*, collectively known as the "*achaete–scute*" complex genes *(ac/sc)* (Garcia-Bellido and Santamaria, 1978) encode a family of basic helix-loop-helix transcription factors and are necessary and required to commit ectodermal cells to the neuroblasts fate (Villares and Cabrera,

1987). Proneural genes are expressed in 4-6 cell clusters (proneural cluster) at specific positions within the neuroectoderm (Figure 4 b,c). In each proneural cluster, all cells acquire neural potential through the expression and function of the proneural genes (Garcia-Bellido and Santamaria, 1978), but one cell will express the *ac/sc* genes to the highest level. This cell is singled out to become a neuroblast whereas the remaining cells stay in the epithelium (Cubas et al., 1991).

The presumptive neuroblast inhibits neural gene expression in the surrounding cells by triggering the Notch pathway. A process known as "lateral inhibition" extinguishes *as/sc* expression in the remaining cells of the cluster and shifts them towards epidermal development. Lateral inhibition is based on a regulatory loop between adjacent cells and is regulated by the Delta/Notch signaling pathway (Muskavitch, 1994). Both *Notch* and *Delta* are neurogenic genes encode transmembrane proteins (Portin, 2002). The future neuroblast expresses the Notch ligand, Delta on its surface. Binding of Notch to Delta initiates signal transduction, which involves proteolytic release and nuclear translocation of the intracellular domain of Notch (Lieber et al., 1993; Struhl and Adachi, 1998) resulting in the expression of repressors such as the *"Enhancer of split"* (*E*(*spl*)) complex genes (Wurmbach et al., 1999) that directly downregulate proneural gene expression (Knust, 1994). Consequently proneural gene expression is restricted to single cells that becomes a neural stem cell and divides asymmetrically to give rise to neurons and glia cells, whereas the others form the epithelium (Skeath and Carroll, 1994; Artavanis-Tsakonas et al., 1999).

3.2.2.4 Neuroblast Delamination and Division

Neuroblasts are enlarged cells that undergo a cell shape change before delaminating from a polarized neuroectodermal epithelium (Lu et al., 2001; Justice et al., 2003). Accompanied by localization of two protein complexes to opposite poles and a programmed rotation of the mitotic spindle neuroblasts divide asymmetrically into a larger neuroblasts and a smaller ganglion mother cell (GMC) (Chia and Yang, 2002). The neuroblast continues to divide in a stem cell-like fashion again into neuroblast and GMC whereas the GMC divides only once and differentiates in neuron and glia cells (Doe and Bowerman, 2001; Betschinger and Knoblich, 2004; Wodarz, 2005). An apical complex coordinates basal transport of a protein/RNA complex consisting of cell fate determinants and their adaptors such as Miranda and positions the mitotic spindle along the apical-basal axis (Figure 5) (Wodarz and Huttner, 2003).

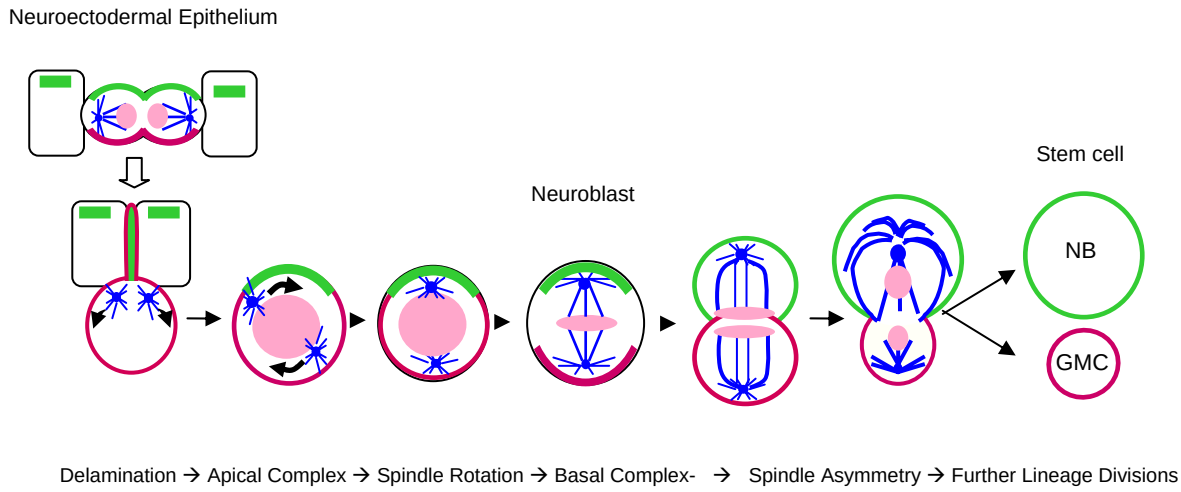

Figure 5: Neuroblast mitosis.

Neuroblasts delaminate from a polarized epithelium and rotate their spindle by 90°C. Two protein complexes (green and red) are localized to opposite poles of the cell and inherited asymmetrically by a larger neuroblast (NB) and a smaller ganglion mother cell (GMC). The neuroblast continues to divide in a stem cell-like manner, the GMC, which inherits cell fate determinants, produces differentiated neurons and glia cells.

3.2.2.5 Neuroblast Specification

As described above each neuroblast acquires a unique identity depending on positional information in the neuroectoderm, provided by the products of early patterning genes (Bhat, 1999; Skeath, 1999). Beside the time and position of its delamination from the neuroectoderm, neuroblasts identity genes, such as *as/sc*, *huckebein*, *runt* and *msh* are each expressed in distinct subsets of equivalence groups (Figure 4 b) (Duffy et al., 1991; Brand et al., 1993; D'Alessio and Frasch, 1996; McDonald and Doe, 1997). However, none of them is deterministic for a specific neuroblast fate. Rather, each identity gene seems to regulate a certain set of features that distinguishes specific neuroblasts from each other. Neuroblast identity genes encode transcription factors. Thus, identity seems to be largely determined at the transcriptional level. However, the logic underlying the molecular mechanism through which distinct sets of transcription factors trigger specific neuroblast identities remains unknown (Skeath and Thor, 2003).

3.2.2.6 Ganglion Mother Cell Specification

Ganglion mother cells (GMC) are secondary precursors, which arise from asymmetric cell division (ACD) of neuroblasts. They divide and produce postmitotic neurons that take on different cell fates (Buescher et al., 1998). Nearly each GMC acquires a unique fate. A temporal transcription factor cascade, consisting of *Hunchback* (*Hb*)→ *Krüppel* (*Kr*)→ *POU domain proteins* (*Pdm*)→ *Castor* (*Cas*)→ *Grainyhead* (*Gh* or *Grh*) (Figure 4 e), has been found in

most neuroblast lineages (Kambadur et al., 1998; Brody and Odenwald, 2000; Isshiki et al., 2001; Novotny et al., 2002; Pearson and Doe, 2003). Neuroblasts sequentially express these transcription factors resulting in differentiated progeny maintaining the transcription factor profile present at their birth. *Hunchback* as an example is necessary and sufficient for first-born cell fates, whereas *Krüppel* is necessary and sufficient for second-born cell fates (Isshiki et al., 2001). This orderly progression of gene activity results in a layered pattern of gene expression in the neurons and glia produced by each neuroblast. *Hb*-positive neurons are located at the basal edge of the VNC whereas *Gh*-positive neurons are located at the apical edge, with *Kr*-, *Pdm*- and *Cas*-positive neurons sandwiched in between (Skeath and Thor, 2003).

3.3 Asymmetric Cell Division

3.3.1 Mechanism of Asymmetric Stem Cell Division

During recent years stem cells have received much attention due to their unique capabilities for self renewal and their multi potency (Temple and Alvarez-Buylla, 1999; Temple, 2003). These features make stem cells and their more committed progeny such as neural or glia progenitor cells very attractive tools for regenerative medicine. Stem cells possess the unique ability to make more stem cells ("self-renewal"), and the ability to produce cells that differentiate (Morrison and Kimble, 2006). One strategy by which stem cells can accomplish these two tasks is asymmetric cell division (ACD) (Doe and Bowerman, 2001; Betschinger and Knoblich, 2004; Clevers, 2005; Yamashita et al., 2005). Mechanism governing ACD can be divided into two main types (Figure 6). The "extrinsic" mechanism involves asymmetric placement of daughter cells relative to external cues. The second, known as "intrinsic" mechanism, relies on the asymmetric partitioning of cell fate determinants (Morrison and Kimble, 2006).

The *Drosophila* germline stem cell provides a classic example of an asymmetric division that is controlled by an extrinsic mechanism. It divides with a reproducible orientation to generate one daughter cell that remains in the stem cell niche and retains stem cell identity. The other daughter is removed from the niche and therefore begins to differentiate (Yamashita et al., 2005). A typical example of ACD controlled by an intrinsic mechanism is provided by the *C. elegans* zygote. Asymmetrically localized Par proteins govern both mitotic spindle orientation and asymmetric segregation of cell fate determinants (Gönczy and Rose, 2005). *Drosophila* neuroblast division is controlled by a closely related mechanism (Doe and Bowerman, 2001; Wodarz, 2005). Although this early embryonic lineages do not display a traditional stem cell they provide a model for asymmetric stem cell divisions. Both rely on mechanisms

that are widely used by asymmetrically dividing stem cells and progenitors (Morrison and Kimble, 2006).

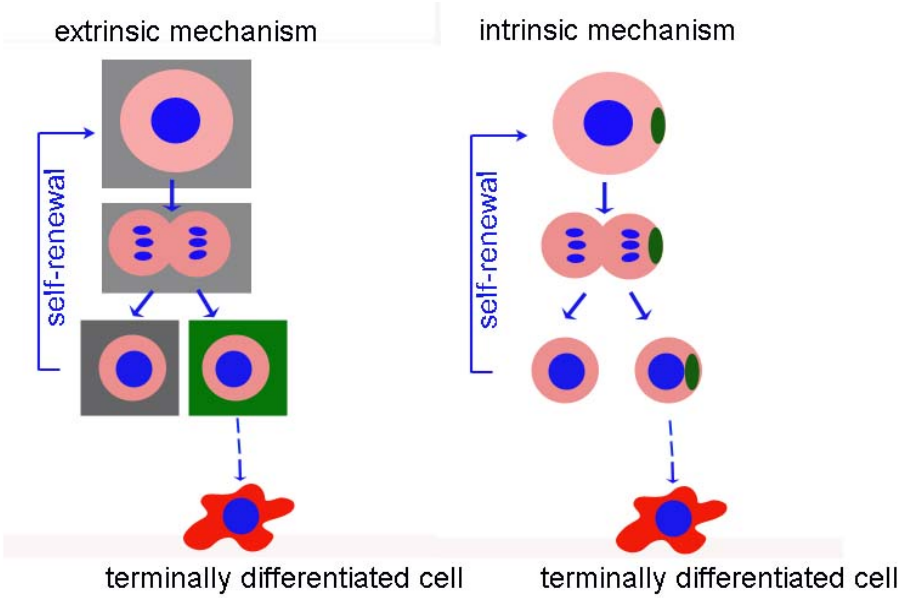

Figure 6: Two ways for a stem cell to produce different daughter cells.
In an asymmetric division regulated by a cell-intrinsic process, the two daughter cells acquire different cell fates right after birth. In a symmetric division, cells are initially identical but due to differences in their microenvironment acquire different fates later on (extrinsic mechanism). Model following Alberts et al., 2003.

3.3.2 Asymmetric Cell Division in *Drosophila* Neuroblasts

3.3.2.1 Regulation of Cell Division by an Apical Protein Complex

Asymmetric cell division (ACD) of *Drosophila* neuroblasts requires the localization of an apical complex (Figure 7, green), which acts downstream of the G protein Gβ13F (Fuse et al., 2003; Yu et al., 2003) in two parallel pathways to control the size asymmetry of neuroblast divisions (Cai et al., 2003). The non-conserved protein Inscutable (Insc) can direcly interact with two highly conserved protein complexes, the Par proteins (for partitioning-defective) and Partner of Inscutable (Pins), and the associated heterotrimeric G protein subunit Gαi. Early in the neuroblast cell cycle the Par protein complex, consisting of the conserved PDZ domain protein Bazooka (Par-3) (Kuchinke et al., 1998; Schober et al., 1999; Wodarz et al., 1999), *Drosophila* atypical protein kinase C (aPKC) (Wodarz et al., 2000) and Par-6 (Petronczki and Knoblich, 2001), localizes to the apical pole. This Par complex recruits Inscuteable (Insc) (Kraut and Campos-Ortega, 1996; Kraut et al., 1996), which directly interacts with a second complex consisting out of Partner of Inscuteable (Pins) (Parmentier et al., 2000; Schaefer et al., 2000; Yu et al., 2000) and Gαi (Schaefer et al., 2001). All these apical complex compo-

nents are key molecules, which act to facilitate apical-basal spindle orientation as well as the basal localization and segregation of cell fate determinants (Wang and Chia, 2005). However, it appears that the asymmetric localization of basal components depends primarily on the activation of Par proteins, wherease Pins-Gαi play a predominant role in mediating the orientation of the mitotic spindle. However, even when Par protein function is comprised, basal proteins like Miranda concentrate to the GMC in telophase neuroblasts. This phenomenon is called "telophase rescue" (Schober et al., 1999; Peng et al., 2000).

The basal complex (Figure 7; red) consists of cell fate determinants Prospero, a homeodomain transcription factor (Doe et al., 1991), *prospero* RNA (Broadus et al., 1998) and Numb (Rhyu et al., 1994), a phosphotyrosine-binding (PTB)-domain containing signaling molecule and the adaptor proteins Miranda (Shen et al., 1997), the RNA binding protein Staufen (Li et al., 1997) and Partner of Numb (PON) (Lu et al., 1998), which are themselves localized to the basal pole in metaphase. Upon neuroblast division, the basal complex is inherited almost exclusively by the ganglion mother cell (GMC). It thereby determines the identity of the GMC and differentiates it from its neuroblast sister (Figure 5) (Jan and Jan, 1998; Knoblich, 2001; Wodarz and Huttner, 2003).

In addition to the apical and basal components, two other classes of molecules have been identified which act to facilitate the basal complex formation but are not required for apical complex formation. These molecules include two tumor suppressors (Lgl and Dlg) as well as two myosins (Myosin II and Myosin VI). The two uniformly cortically localized tumor suppressor proteins, Lethal giant larvae (Lgl) and Discs large (Dlg) regulate basal protein localization (Ohshiro et al., 2000; Peng et al., 2000). Phosphorylation of Lgl by aPKC is supposed to inhibit Lgl activity on the apical pole, thereby restricting functional Lgl and the recruitment of basal proteins, like Miranda, to the basal side of the neuroblast (Betschinger et al., 2003). It has been shown that an intact actin cytoskeleton (Knoblich et al., 1997; Lu et al., 1999), the unconventional Myosin VI (Petritsch et al., 2003) and non-muscle Myosin II (Barros et al., 2003) are required for basal protein localization. The pointed-end directed motor protein Myosin VI directly binds to Miranda and its distribution partially overlaps with Miranda localization in neuroblasts, suggesting that Miranda and the complex including Prospero, Staufen and *prospero mRNA* may be a cargo for Myosin VI (Petritsch et al., 2003). The barbed-end directed Myosin II directly binds to Miranda (Petritsch et al., 2003) and to Lgl which negatively regulates filament formation and Myosin II activity (Barros et al., 2003). Myosin II has been shown to be asymmetrically localized itself and to play a role in restrict-

ing proteins to the basal crescent probably by apical exclusion (Barros et al., 2003). Despite the recent progress, several questions regarding the mechanism remain to be answered.

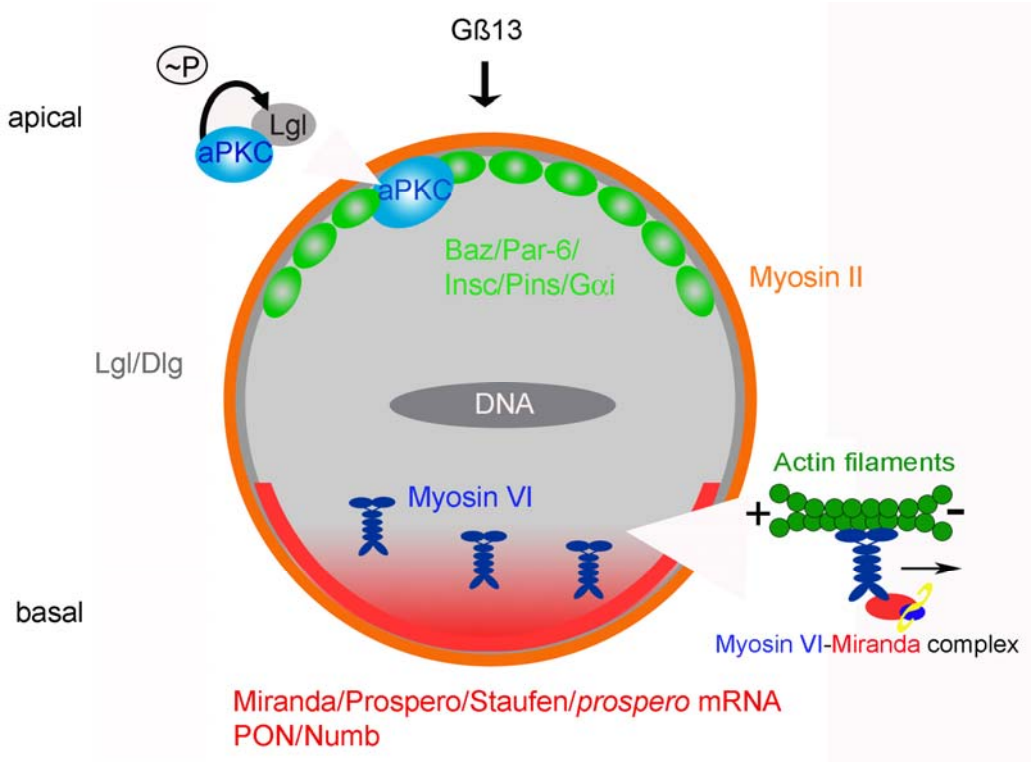

Figure 7: Model for regulation of basal protein transport.

Gß13 F and the apical complex (green) regulate spindle orientation, size asymmetry and the localization of a basal complex (red) during neuroblast division. Dlg (grey) is required for cortical localization of Lgl (grey) and both are essential for basal protein localization in metaphase (red). aPKC (turquoise) within the apical complex phosphorylates Lgl and thereby inhibits Lgl binding to the apical complex. Lgl cannot bind to Myosin II and is released from the apical side. Cytoplasmic Myosin VI (blue) moves along actin filaments towards the pointed end and is required for basal Miranda localization.

3.3.2.2 Proteins show Dynamic Localization during Neuroblast Mitosis

Numerous proteins are involved in neuroblast mitosis and several show dynamic and distinct localization (Figure 8 and Figure 10). According to a widely accepted model the Par complex, Miranda, Prospero, Staufen, and *prospero mRNA* (Spana and Doe, 1995; Li et al., 1997; Shen et al., 1998) accumulate apically in interphase (Schaefer et al., 2000; Yu et al., 2000) and during early prophase while PON and Numb localize uniformly cortical (Lu et al., 1999). At metaphase, Par proteins stay apically, whereas Miranda, Prospero, Staufen, Prospero, and *prospero mRNA* are localized to the basal cortex where they colocalize with Numb and PON. Basal proteins form a tight crescent and are exclusively inherited by the GMC. After comple-

tion of neuroblast division Miranda releases Prospero, which then translocates to the GMC nucleus to activate specific genes (Lu et al., 2000). Recent data show that an actin-myosin network is involved in basal protein targeting (Knoblich et al., 1997; Lu et al., 1999; Barros et al., 2003; Petritsch et al., 2003). However, the exact mechanism how the proteins move to the opposite side of the cell is unknown (Lu et al., 2000).

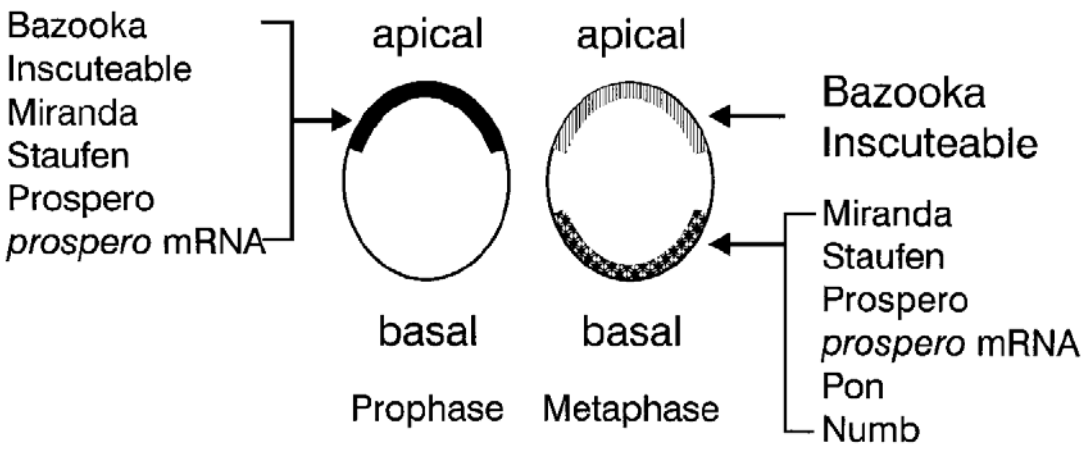

Figure 8: Asymmetrically localized proteins and RNA in *Drosophila* neuroblasts.
At interphase and early prophase, Bazooka and Inscuteable are localized to the apical cortex. Subsequent to this, Miranda, Staufen, Prospero, and *prospero* mRNA are also localized to the apical cortex. Later during mitosis, Miranda, Staufen, Prospero, and *prospero* mRNA are localized to the basal cortex by an unknown mechanism and colocalize with Numb and PON, whereas Bazooka and Insc stay at the apical cortex. Adopted from Lu et al., 2000.

3.3.2.3 Characterization of the Miranda Protein

Miranda was identified in a yeast two-hybrid screen (Bartel et al., 1993) interacting with the asymmetric localization domain of Prospero. The name arises from Shakespeare's play *The Tempest* where Miranda is Prospero's daughter and companion in exile. The Miranda gene produces at least two different transcripts, probably due to alternative splicing. The long form encodes a protein with 830 amino acids. The short form has the same sequence apart from a 30 amino acid internal deletion (Shen et al., 1997). Miranda protein exhibits extensive regions of predicted coiled-coil structure (140–680 aa) which are implicated in mediating protein-protein interaction (Figure 9) (Fuerstenberg et al., 1998). The carboxy-terminal half of the protein contains two leucine-zipper motifs and eight consensus sites for phosphorylation by protein kinase C (PKC). Based on sequence analysis of Miranda alleles it is thought that these PKC sites may regulate the ability of Miranda to bind Prospero (Ikeshima-Kataoka et al., 1997).

Miranda protein contains an amino-terminal asymmetric localization domain which interacts with Inscuteable, a central Numb interaction domain, and a carboxy-terminal Prospero interaction domain (Shen et al., 1998). The analysis of hypomorphic and loss of function *miranda* alleles revealed a C-terminal domain regulating Miranda degradation and release of Prospero/Staufen cargo from the GMC cortex; a central domain regulating Miranda apical localization and Prospero/Staufen cargo binding; and an N-terminal domain sufficient for cortical association and basal localization of Miranda (Fuerstenberg et al., 1998). Miranda protein may be degraded in a cell cycle dependent fashion, due two four potential destruction boxes.

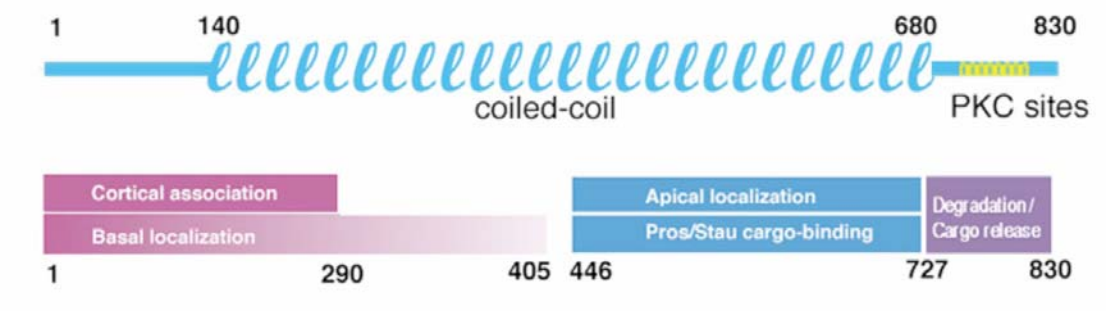

Figure 9: Summary of Miranda domains, protein localization, and function.

Summary of Miranda domains, protein localization, and function. (A) Miranda encodes a predicted 830-aa protein with a central coiled-coil domain (140–680 aa) and seven predicted PKC sites in the N-terminal 100 aa (yellow). An N-terminal domain is sufficient for cortical association (pink); a slightly larger N-terminal domain has distributed elements regulating basal localization in mitotic neuroblasts (graded pink). A central domain is required for both Prospero/Staufen cargo binding and apical localization in interphase neuroblasts (turquoise). A C-terminal domain is necessary for timely Miranda degradation and Prospero/Staufen cargo release in newborn GMCs (purple). Adopted from Fuerstenberg et al., 1998.

Whole-mount embryo RNA *in situ* hybridization revealed Miranda transcripts in the embryo at stage 3, probably due to maternal contribution. At stage 8, transcripts start to accumulate in the procephalic and ventral neurogenic region. Subsequently Miranda is expressed in delaminating neuroblast cells in the posterior midgut primordial and SOP cells in the developing PNS. After germband retraction transcripts can only be detected in the brain lobes and ventral region of the ventral nerve cord where cell divisions continue to take place (Shen et al., 1997). Miranda has been mapped by recombination to the chromosome 3 and cytologically to 92C. Loss of function embryos have been isolated with sever effects on CNS and are recessive lethal (Shen et al., 1998). Analysis of *miranda* mutations allowed to discover the effect that lack of *miranda* function has on CNS development (6.2.3).

3.3.2.4 The Miranda Complex

Miranda directly associates and colocalizes with the transcription factor Prospero (Hirata et al., 1995) and the RNA binding protein Staufen (Broadus et al., 1998). It thereby acts as an adaptor that is essential for the localization of Prospero and Staufen to the plasma membrane and their asymmetric localization segregation into only one daughter (Ikeshima-Kataoka et al., 1997; Shen et al., 1997; Matsuzaki et al., 1998; Schuldt et al., 1998; Shen et al., 1998). Prospero is a homeodomain containing transcription factor. Shortly after neuroblast mitosis it is released from the membrane and from Miranda and translocated into the nucleus of the GMC where it induces and represses various cell type specific target genes (Doe et al., 1991; Vaessin et al., 1991; Karcavich, 2005). Staufen binds to *prospero RNA* and localizes it into the GMC. Although localization of *prospero* RNA is not essential it is thought to serve as an important backup mechanism for Prospero protein localization (Broadus et al., 1998). While Staufen is dispensable for neuronal specification, Prospero controls GMC specific genes in some neuroblast lineages (Vaessin et al., 1991; Doe and Bowerman, 2001). Recently the tumor suppressor Brat was identified as a Miranda binding partner. Brat cooperates with Prospero to establish GMC fate in the embryonic nervous system and controls proliferation in the larval brain (Betschinger et al., 2006; Lee et al., 2006).

3.3.2.5 Miranda Localization Depends on Myosin II and Myosin VI

Basal Miranda localization requires the barbed-end directed Myosin II (Barros et al., 2003) and the pointed-end directed Myosin VI, known as Jaguar in *Drosophila* (Petritsch et al., 2003). Myosin VI is a dimeric protein with an N-terminal head domain, consisting of the ATP binding motor domain, the actin binding region, a long helix-loop-helix region serving as a dimerisation domain and the tail region, that has been shown earlier to interact with membrane structures and additional proteins (Buss et al., 2001; Aschenbrenner et al., 2003). *Drosophila* Myosin VI specifically interacts with the first 300 amino acids of the Miranda N-terminus (Petritsch et al., 2003), representing the asymmetric localization domain (Fuerstenberg et al., 1998; Shen et al., 1998; Petritsch et al., 2003). Reducing Myosin VI activity by several genetic approaches resulted in Miranda mislocalization and spindle misorientation in *Drososphila* neuroblasts. Myosin VI appears to act synergistically with Lgl, downstream or in parallel with apical complex, to localize Miranda and its cargo (Petritsch et al., 2003). The barbed end-directed Myosin II is activated by a kinase (Barros et al., 2003). Phosphorylation of the regulatory light chain (RLC) of Myosin II, and inhibition of phosphatase-mediated dephosphorylation of the regulatory chain by Rho-kinase enables Myosin II to as-

semble into bipolar filaments and increases myosin's actin-dependent ATPase activity (Tan et al., 1992). Myosin II is asymmetrically localized itself but does not colocalize with Miranda. The predicted function therefore is excluding proteins from the apical side of the cell rather than active transport (Barros et al., 2003).

3.3.2.6 The PON/Numb Complex

Numb, an evolutionarily conserved cell fate-determining factor plays a pivotal role in the development of *Drosophila* and the nervous systems of other vertebrates. Numb localizes asymmetrically in mouse, rat and chicken neuronal progenitor cells (Zhong et al., 1997; Wakamatsu et al., 1999; Cayouette et al., 2001; Shen et al., 2002). In *Drosophila*, Numb is a cell fate determinant that is asymmetrically distributed during neural and muscle precursor divisions (Rhyu et al., 1994; Knoblich et al., 1995; Spana et al., 1995; Kraut et al., 1996; Buescher et al., 1998; Carmena et al., 1998). Numb is membrane-associated and contains a phosphotyrosine binding (PTB) domain. Its proper localization depends on its interaction with the adapter protein PON. In *pon* mutant embryos the formation of Numb crescent is delayed in neuroblasts and disrupted in muscle progenitor cells (Lu et al., 1998). Similar to Miranda, PON and Numb colocalize to a basal crescent in metaphase which requires an intact actin cytoskeleton (Knoblich et al., 1997). Another Numb-interacting protein NIP has been discovered and it is suggested to anchor Numb to the cortex (Qin et al., 2004).

3.3.2.7 Regulation of the Mitotic Spindle during Neuroblast Mitosis

Spindle rotation has to be coordinated with basal localization of a protein/RNA complex. The protein complex, that remains on the apical pole throughout the neuroblast cell cycle, controls all three aspects of asymmetric neuroblast division: basal transport, spindle orientation and together with the G protein Gβ13F size asymmetry (Figure 7) (Fuse et al., 2003; Yu et al., 2003). Neuroepithelial cells divide symmetrically and within the epithelial plane to produce equally sized daughters (Figure 5). Therefore a symmetric mitotic spindle is oriented parallel to the surface by recognizing a planar polarity cue regulated by the adherens junction and a *Drosophila* homologue of Adenomatous polyposis coli (APC) tumor suppressor protein and microtubule associated End-binding protein 1 (EB1). In neuroblasts, as the bipolar spindle forms, it starts to rotate by 90° and aligns along the apical/basal axis (Kaltschmidt et al., 2000; Kaltschmidt and Brand, 2002) in metaphase. In anaphase the spindle itself becomes asymmetric due to elongation of the apical intra-centrosomal arm of the spindle (Kaltschmidt et al., 2000). It has been generally accepted that proper orientation of the neuroblast mitotic spindle

requires all of the apical components. Mutations in any apical component can cause defects in apical-basal spindle orientation (Kraut et al., 1996; Wodarz et al., 1999; Yu et al., 2000; Petronczki and Knoblich, 2001; Yu et al., 2003). However, Izumi et al., (2004) showed that Gαi-Pins play a predominant role in orientating the mitotic spindle. In neuroblasts the mitotic spindle always points to the localization of Pins regardeless of where the Par proteins are localized. In wild type epithelial cells in which Gαi-Pins are localized to the lateral cortex wherease Par proteins are apically localized, the mitotic spindle is orientated to the lateral cortex and the cells divide symetrically and in parallel to the epithelial surface. In neuroblasts the primary role of the Par proteins may be to place Gαi-Pins to the apical cortex. Only when Gαi-Pins is absent the Par proteins play a role in orientating the spindle suggesting that the proteins are functionally redundant (Wang and Chia, 2005). Gβγ controls Gαi protein stability and thereby affects spindle positioning (Schaefer et al., 2001; Yu et al., 2003; Izumi et al., 2004). Pins is proposed to activate heterotrimeric G proteins in an receptor independent fashion by binding Gαi and thus interrupting interaction (Kimple et al., 2004).

A central role for spindle positioning has so far been demonstrated for Inscuteable (Insc). When Inscuteable is ectopically expressed in neuroepithelial cells they reorient their spindle along the apical-basal axis, like neuroblasts, which suggests that Inscuteable might provide an apical cue (Kraut et al., 1996).

Recent studies suggest that a microtubule/Khc-73/Dlg pathway that acts in parallel to the Inscuteable-Par pathway links the spindle with the neuroblasts cortex. Kinesin heavy chain (Khc)-73, a plus-end motor protein which localizes to astral microtubule, can interact with Dlg *in vivo*, thereby localizing Pins-Gαi asymmetrically to the apical side and linking the spindle with apical proteins (Siegrist and Doe, 2005). Since reduced *Drosophila* Myosin VI (Jaguar) activity results in spindle misorientation and Myosin VI associates with a microtubule-binding protein CLIP-190 (cytoplasmic linker protein), Jaguar might be involved in linking microfilaments to microtubules (Petritsch et al., 2003).

Most likely, multiple interactions between cortical polarity cues and the mitotic spindle are responsible for linking microtubles to the cortex and orientating mitotic spindle during ACD.

4 AIM OF THE WORK

Despite the recent progress that establishes the important role of acto-myosin in the localization of proteins involved in asymmetric cell division (ACD) of *Drosophila* neuroblasts several questions remain to be answered and will be addressed in this thesis.

Immunohistochemical analysis of fixed embryonic tissue revealed that Miranda and PON exert dynamic localization during asymmetric cell division of neuroblasts. This method, however, has two major drawbacks. Firstly, following Miranda localization over time within the same cell is impossible. Secondly, fixation procedures bear the risk of creating artifacts. PON and Miranda are both localized to an overlapping basal cortical crescent in metaphase but since only PON localization has been studied by time-lapse analysis, it is still unknown whether Miranda and PON are localized by similar mechanisms. The molecular details of asymmetric Miranda localization is the central question of this thesis and will be approached with live imaging, genetic, and biochemical tools.

The exact mechanism of Myosin VI and Myosin II directed basal protein localization is not yet fully understood. This question will be addressed by studying Miranda and PON dynamics in living embryos that exert reduced Myosin VI and Myosin II activity.

Despite analysis of several Miranda alleles, the effect of complete loss of Miranda function on embryonic development has not been demonstrated so far, due to the potential activity of the maternally contributed *miranda* mRNA. To remove the maternal contribution of Miranda, germline clones lacking Miranda gene expression will provide an answer to this question.

Phosphorylation is linked to neuroblast mitosis. Several proteins regulating asymmetric cell division are phosphorylated. However, nothing is known about the regulation of Miranda by post-translational modification.

5 MATERIAL AND METHODS

5.1 Chemicals and Other Materials

5.1.1 Chemicals

All chemicals had *pro analysis* grade and were purchased from the following manufacturers if not stated:
AmershamPharmacia Biotech, Freiburg, Germany; *Biomol*, Hamburg, Germany; *Bio-Rad*, Munich, Germany; *Fluka Chemie AG,* Deisenhofen, Germany; *Gibco/BRL Life Technologies*, Karlsruhe, Germany; *Merck*, Darmstadt, Germany, *Roth*, Karlsruhe, Germany; *Roche Diagnostics GmbH,* Mannheim, Germany, *Sigma-Aldrich*, Steinheim, Germany.

5.1.2 Ready-to-Use Systems

- **QIAquick PCR Purification Kit**, *Qiagen*, Hilden, Germany
- **QIAquick Gel Extraction Kit,** *Qiagen*, Hilden, Germany
- **QIAprep Spin Miniprep Kit,** *Qiagen*, Hilden, Germany
- **HiSpeed Plasmid Midi Kit,** *Qiagen*, Hilden, Germany
- **Qiagen Plasmid Purification Kit**, *Qiagen*, Hilden, Germany

5.1.3 Vectors

- **pBluescript KS+/SK+:** vector for PCR of *miranda* and *myosin VI* (*Stratagene,* Heidelberg, Germany)
- **pUChsπΔ2-3**: "helper- plasmid" for transformation of *Drosophila*, codes for transposase (Laski et al., 1986)
- **pUAST**: vector for generation of UAS-lines in *Drosophila* (Brand and Perrimon, 1993)

5.1.4 Bacterial Strains

$CaCl_2$ competent *E. coli* strain DH5α was used for transformation.

5.1.5 Molecular Weight Markers

Following protein and DNA ladders were purchased from *Fermentas GmbH,* St. Leon-Rot, Germany:

- PageRuler™ Prestained Protein Ladder
- GeneRuler™ DNA Ladders Mix

5.1.6 Enzymes

All enzymes were purchased from *MBI Fermentas*, St. Leon-Rot, Germany.

5.1.7 Antibodies

Antibodies were purchased from following companies, otherwise mentioned: *ACCURATE CHEMICAL & SCIENTIFIC CORPORATION*, Westbury, USA; *DAVIDS BIOTECHNOLOGY*, Regensburg, Germany; *Developmental Studies Hybridoma Bank (DSHB),* Iowa, USA; *Jackson Immuno Research Laboratories* purchased from *Dianova,* Hamburg, Germany; *Merck*, Darmstadt, Germany; *Molecular Probes*, purchased from *Invitrogen*, Karlsruhe, Germany**;** *Santa Cruz Biotechnology*, Heidelberg, Germany; *Sigma-Aldrich*, Steinheim, Germany; *Zymed*, purchased from *Invitrogen*, Karlsruhe, Germany.

5.1.7.1 Primary Antibodies

Table 2: Primary antibodies used in this study.

Following abbreviations were used: anti (α); Discs-Large (Dlg), endoplasmatic reticulum (ER), green fluorecent protein (GFP), lysine (K)-aspartic acid (D)-glutamic acid (E)-leucine (L) (KDEL); mouse (m), protein kinase C (PKC), rabbit (rb), rat (r), western blotting (WB), immunohistochemistry (IHC).

Name	Additional Information	Dilution	Origin/Reference
mαDelta	monoclonal; against extracellular domain of Delta	WB: 1:4000	*DSHB*
mαDlg	monoclonal; against Discs-Large (Dlg)	IHC: 1:500	*DSHB;* Parnas et al., 2001
mαF2F	monoclonal; recognizes Cyclin B	IHC: 1:3	*DSHB;* Lehner and Knoblich, 1993
mαGFP	monoclonal; against full length GFP	IHC: 1:200	*Santa Cruz Biotechnology*
rbαGFP	polyclonal; against full length GFP	IHC: 1:200 WB: 1:400	*DAVIDS BIOTECHNOLOGIE*
rbα$G\alpha_i$	polyclonal	IHC: 1:150	Knoblich Lab; unpublished
rbαInscutable	polyclonal	IHC: 1:500	Chia Lab
mαKDEL	monoclonal; marker for the ER	IHC: 1:50	*Merck*
mαMiranda	monoclonal; against C-terminus of Miranda	IHC: 1:2	Matsuzaki Lab; Oshiro et al., 2000
rbαMiranda	polyclonal; against C-terminus (781-803) of Miranda	WB: 1:500	*DAVIDS BIOTECHNOLOGIE;* Shen et al.,1997

rbαMiranda	polyclonal; against N-terminus (aa 96-118) of Miranda	IHC: 1:200 WB: 1:300	*DAVIDS BIOTECHNOLOGIE;* Shen et al., 1997
rbαNumb	polyclonal; against aa 517-546 of NUMB	WB: 1:500	Jan Lab; Rhyu et al., 1994
rbαPKC	polyclonal; against C-terminus of atypical Protein Kinase C (aPKC)	IHC: 1:200	*Santa Cruz Biotechnology*
rbαphosphoserine	polyclonal; against phosphorylated serine	WB: 1:4000	*Zymed*
rbαphospho-threonine	polyclonal; against phosphorylated threonine	WB: 1:4000	*Zymed*
mαphospho-tyrosine	monoclonal; against phosphorylated tyrosine	WB: 1:2000	*Zymed*
$r\alpha_{\alpha}$ tubulin	monoclonal, recognizes α-subunit of tubulin	IHC: 1:10	*Accurate*
$m\alpha_{\alpha}$tubulin	monoclonal; recognizes α- subunit of tubulin	WB: 1:2000	*Sigma Aldrich*
$rb\alpha_{\gamma}$tubulin	polyclonal; centrosome marker; recognizes γ- subunit of tubulin	IHC: 1:500	*Sigma Aldrich*
mαProspero	monoclonal; recognizes C-terminal of Pros-pero	IHC: 1:5	*DSHB*

5.1.7.2 Secondary Antibodies

Table 3: Secondary antibodies used in this study.

Following abbreviations were used: anti (α); donkey (d), goat (g), horseradish peroxidase (HRP), mouse (m), rabbit (rb), rat (r), rhodamine red-X (RRX), western blotting (WB), immunohistochemistry (IHC).

Name	Dilution	Origin
gαrbAlexa488	IHC: 1:400	*Molecular Probes*
dαrbAlexa488	IHC: 1:400	*Molecular probes*
gαmCy3	IHC: 1:200	*Jackson ImmunoResearch*
dαrCy3	IHC: 1:200	*Jackson ImmunoResearch*
dαmRRX	IHC: 1:200	*Jackson ImmunoResearch*
gαrRRX	IHC: 1:200	*Jackson ImmunoResearch*
dαrbRRX	IHC: 1:200	*Jackson ImmunoResearch*
gαrCy5	IHC: 1:200	*Jackson ImmunoResearch*
dαm-HRP	WB: 1:5000	*Jackson ImmunoResearch*
gαrb-HRP	WB: 1:5000	*Jackson ImmunoResearch*

5.2 Cultivation of *Drosophila Melanogaster*

5.2.1 Keeping *Drosophila*

Flies were kept in plastic vials containing different amount of food, a mixture of dried yeast molasses sugar and cornmeal, thickened with agar (5.2.2.1). Stock flies were kept at 18°C and 60% humidity. They were transferred to new 23 ml vials every 4 weeks. Before adding flies to the vials, the food was coated with a viscous paste of dry yeast and propionic acid (0.5%)

("yeast-paste"). The vials were stoppered with cotton wool. To amplify a stock, flies were transferred to 175 ml beaker (including "yeast-paste"), stoppered with cellular material (*Greiner bio-one,* Frickenhausen, Germany), until embryos covered the surface of the food (white layer). Vials were emptied and embryos developed into adults within 10 days at 25°C. To cultivate large amount of wild type flies (Oregon R), 1 l plastic vials were filled with paper tissue, soaked with liquid yeast-sugar-water solution (5.2.2.3). Large amounts of dechorinated embryos were absorbed in ethanol (70%) and pipetted onto the surface of the wet paper. They developed into adult flies during ca 10 days at room temperature. The 1 l vials were sealed with a reticule lid, a custom product of the garage of the Gene Centre. When adult flies hatched, they were transferred in large "biochemistry cages" (RT; V~50 l), also a custom product of the garage. This set-up allows collecting large amounts of wild type embryos to produce embryo extract for biochemical experiments (5.7.1). To "harvest" embryos, large Petri dishes filled with apple agar (5.2.2.2) and brushed with "yeast-paste" were placed in the "biochemistry cages" and changed twice a day. To collect small amount of staged embryos of a particular stock, flies were transferred into "collection vials". A 175 ml plastic beaker including vent holes was covered with a Petri dish, filled with "apple agar" and "yeast paste". The Petri dish was fixed with tape on the outside of the vial and changed regularly.

5.2.2 Fly Food

5.2.2.1 Standard Fly Food

For 10 liters

Fiber-agar was boiled in 4 l of distilled water. Soya flour and brewer's yeast were dissolved in 1.5 l cold distilled water. Polenta, sugar beet molasses, and malt essence were heated in 4 l distilled water. The soya-yeast solution and the dissolved agar was added and everything was boiled for approximately 40 minutes. After cooling down the homogenate to 70°C, hydroxypropyltrimonium were dissolved in ethanol and added to the food with propionic acid. Subsequently the appropriate amount of food was pumped in plastic vials:

175 ml vials (*Greiner bio-one* Frickenhausen, Germany)	→	40-42 ml food
23 ml vials (*Sarstedt*, Nümbrecht, Germany)	→	6-7.7 ml food

The vials were completely covered with net material, food was dehumidified at room temperature over night and then stored in plastic bags at 4°C.

Material:

80 g fiber agar (*ProBioGmbH,* Eggenstein, Germany), 100 g soya flour (*Spielberger,* Brackenheim, Germany), 180 g brewer's yeast, 800 g polenta (*Antersdorfer Mühle*, Simbach, Germany), 220 g sugar beet molasses (*Bauckhof,* Rosche, Germany), 200 g malt essence *(Linco*, Heilbronn, Germany), 7.5 g hydroxypropyltrimonium, 50 ml ethanol (99,8% p.a.), 63 ml propionic acid (99%), 9.5 l distilled water;

5.2.2.2 Apple Agar

For 10 liters

Bacto-agar were autoclaved in 5.5 l tap water to solubilize the agar. The liquid agar was filled up to 7 l final volume with water (additional 3 l of water were autoclaved). White sugar was dissolved in apple juice in a 5 l Erlenmeyer beaker at 60°C (water bath). Hydroxypropyltrimonium was solubilized in ethanol. All ingredients were mixed in a 10 l beaker and aliquots were transfered in 500 ml Schott bottles (300-400 ml each).

Material:

284 g bacto agar (*Becton Dickinson GmbH*, Heidelberg, Germany), 8.5 l water, 2.6 l unfiltered apple juice, 260 g white sugar, 15.8 g hydroxypropyltrimonium, 63 ml ethanol (99.8%);

5.2.2.3 Yeast-Sugar Solution

For 5 liters

Sugar and brewer's yeast were solubilized in 3.75 l distilled water. Propionic acid (99%), nipargin and orthophosphoric acid were added. The mixture was stirred at room temperature without heating.

Material:

490 g sugar, 700 g brewer´s yeast, 5.5 ml propionic acid, 7.5 g hydroxypropyltrimonium, 37.5 g orthophosphoric acid;

5.3 Genetics

5.3.1 *Drosophila* Stocks

5.3.1.1 UAS-Lines

Table 4: *Drosophila* UAS- lines used in this study.

Following abbreviations were used: dominant temperature sensitive (DTS), genes induced by galactose (GAL), green fluorescent protein (GFP), Lethal giant larvae (Lgl), Miranda (Mira), Partner of Numb (PON), red fluorescent protein (RFP), scabrous (sca), upstream activator sequence (UAS).

Stock	Chromosome	Information/ Application	Reference	Origin
UAS-*Mira*-GFP	1	expression of full length Miranda eGFP	Ohshiro et al., 2003	Matsuzaki Lab
UAS-*Mira1*-GFP	3	aa 1-400; C-terminally fused to 3xeGFP	not published	Jan Lab
UAS- *Mira2*-GFP	2	aa 1-314; N-terminally fused to eGFP	not published	Petritsch Lab (Erben)
UAS-*Mira3*-GFP	2	aa 1-209; N-terminally fused to eGFP	not published	Petritsch Lab (Erben)
UAS-*Mira4*-GFP	2	aa 83-314; N-terminally fused to eGFP	not published	Petritsch Lab (Erben)
UAS-*Mira5*-GFP	3	aa 206-314; N-terminally fused to eGFP	not published	Petritsch Lab (Erben)
UAS-*Mira*-GFP; Histone-RFP	1;2	full length Miranda eGFP combined with Histone mRFP	Oshiro et al., 2000; Pandey et al., 2005	Petritsch Lab (Erben)
UAS-*DTS5-1*	2	dominant negative temperature sensitive mutation in the ß2 proteasome subunit	Schweisguth, 1999	Schweisguth Lab
UAS-*Lgl3a*	2	serine residues 656, 660 and 664 mutated to alanine; non-phosphorylatable	Betschinger et al., 2003	Knoblich Lab
UAS-*eGFP*	2	eGFP not bound to any subcellular structures		Bloomington Stock center
UAS-*PON*-GFP,*sca*GAL4	2	UAS PON expressed by *scabrous* GAL4	Roegiers et al., 2001	Jan Lab

5.3.1.2 GAL4-Lines

Table 5: *Drosophila* GAL4-lines used in this study.

Following abbreviations were used: curly wing (CyO), genes induced by galactose (GAL), green fluorescent protein (GFP), Krüppel (Kr), Stubble (Sb), upstream activator sequence (UAS).

Stock	Chromosome	Information/ Application	Reference	Origin
*neuralized*GAL4/ TM3SbKrG4GFP	3	used for expression of UAS constructs mainly in neuroectodermal cells and randomly in neuroblasts; 3rd chromosome balanced over GFP	Bellaiche et al., 2001	Jan Lab
*prospero*GAL4	3	used for neuroblast specific expression of UAS constructs	Pearson and Doe, 2003	Jan Lab
*scabrous*GAL4/ CyoKrGFP	2	used for expression of UAS constructs in neuroectodermal cells and neuroblasts; 2nd chromosome balanced over GFP	Nakao and Campos-Ortega, 1996	Jan lab

5.3.1.3 Other Stocks

Table 6: Other stocks used in this study.

Following abbreviations were used:ebony (e), flippase recognition target (FRT), green fluorescent protein (GFP), heat-shock flippase (hs-flp), krüppel (Kr), miranda (mira), nuclear localization signal (nls), P-element (P), red fluorescent protein (RFP), spaghetti squash (sqh), Stubble (Sb), Tubby (Tb), yellow (y^+).

Stock	Chromosome	Information/ Application	Reference	Origin
DTS5/TM6	3	dominant negative temperature sensitive mutation in the ß2 proteasome subunit;	Schweisguth, 1999	Schweisguth Lab
Histone-mRFP	2	red fluorescence protein fused to histone; cell cycle marker for live imaging	Pandey et al., 2005	Lehner Lab
sqh^{AX3}; P[w, sqh-GFP42]	2	regulatory light chain of Myosin II fused to GFP	Barros et al., 2003, Royou et al., 2002	Brand lab
hs-flp; FRT82B, $mira^{ZZ176}$,e,y^+/Tm3Sb, e	1,3	germline clones	Ikeshima-Kataoka, 1997	Jan Lab
FTR82B,nlsGFP/ Tm6B,Tb, e	3	germline clones	Ikeshima-Kataoka, 1997	Jan Lab
FRT82B, $mira^{ZZ176}$,e,y^+/ Tm3, Sb, KrG4GFP	3	germline clones	Ikeshima-Kataoka, 1997	Jan Lab

5.3.1.4 Balancer Stocks

Table 7: Balancer used in this study.

Following abbreviations were used: ebony (e), green fluorescent protein (GFP), Krüppel (Kr), Sternopleural (Sp), Stubble (Sb), Tubby (Tb), Ultrabithorax (Ubx), white (w^-).

Stock	Chromosome	Information/ Application	Origin
TM3Sb,e/TM6Tb,e	3	balancing of mutations on 3rd Chromosome	Jan Lab
w^-;Sp/Tm2CyO; Ubx,e/Tm3Tb,e	1,2,3	balancing of transgenic flies	Jan Lab

5.3.2 Genetic Methods

5.3.2.1 The Basics of a Cross

Females can mate with more than one male and store sperm from multiple mating. Therefore, geneticists are forced to use virgins for crosses. Using non-virgins the progeny will not have the "Mendel" predicted genotype. Newly hatched females will remain virgins for approximately 6 hours at 25°C, 12 hours at 21-22°C, and 18 hours at 18°C.

5.3.2.2 Nomenclature

The extensive nomenclature of *Drosophila* is listed on the Flybase (http://chervil.bio.indiana.edu:7092/docs/nomenclature/lk/nomenclature.html#Introduction) and refers to (Lindsley and Zimm, 1992). Using the standard rules one can properly and clearly describe the complete genotype of a fly stock. A few are listed below.

- Chromosomes are written in order, a semi-colon separates each chromosome from each other (e.g. X/Y; 2; 3; 4)
- Only mutations are listed and are italicized
- Anything not listed is assumed to be wild type
- Recessive mutations are written in lower case (e.g. e for ebony)
- Dominant mutations are capitalized (e.g. Sb for stubble)
- Particular alleles are superscripted (e.g. $mira^{ZZ176}$)
- Homozygous mutations are just written once (e.g. $mira^{ZZ176}$ heterozygous are separated by a slash (e.g. jag^{322}/TM2)

5.3.2.3 Genetic Tools

There are three genetic tools, which help to perform *Drosophila* crosses:

- Phenotypic markers
- Balancer chromosomes
- No recombination in males

Markers

Phenotypic markers make genetics in *Drosophila* unique and easy compared to other organisms. Markers often affect prominent body features, like bristles, eyes, or wings. Characteristics of specific markers are listed in the Flybase or can be looked in (Lindsley and Zimm, 1992). *Drosophila* genetics is replete with both recessive and dominant markers that allow by using Mendel's laws directly (selection for) and indirectly (selection against) to follow (hidden) mutations throughout a multiple generation cross. The following markers were used:

Curly wing (CyO): Dominant Marker on the second chromosome, which causes curly wings. CyO is homozygous lethal.

Ellipsoid (Elp): dominant marker on the second chromosome with ellipsoid eye phenotype. Elp is homozygous viable.

ebony (e): Recessive marker on the third chromosome with affect to a dark body color. e is homozygous viable.

Stubble (Sb): marker of the third chromosome with the dominant phenotype of short bristles. Sb is homozygous lethal.

Sternopleural (Sp): Dominant marker on the second chromosome, which increases the Number of sternopleural bristles. Sp is homozygous lethal.

Tubby (Tb): Dominant marker of the third chromosome, which produces a short squat. *Drosophila*. Tb is homozygous viable.

Ultrabithorax (Ubx): Dominant marker on the third chromosome that produces bristles on the halteres. Ubx is is homozygous lethal.

white (w^+): Recessive marker with effect on the eye color (red). w^+ is homozygous viable.

white (w^-): Recessive marker with effect on the eye color (white). w^- is homozygous viable.

yellow (y^+): Recessive marker, which controls the pigment pattern of the cuticle of the adult fly. y^+ is homozygous viable.

Balancers

Balancers are used to avoid recombination between homologous chromosomes. One or more inverted segments (inversions) within the same chromosome suppress recombination. Most of them are homozygous lethal. To make balancer phenotypically visible most of them carry dominant markers, which make them useful for genetic crosses. Since most recessive mutations have no influence on the phenotype, balancers allow to indirectly following the recessive mutation (due to dominant markers) without losing the mutation (due to inhibited recombination). Furthermore, balancers allow maintaining chromosomal deficiencies or mutations that would otherwise be lethal. Following balancers were uses:

CHROMOSOME	BALANCER	MARKER
2	CyO	Curley wings (CyO)
3	TM3	Stubble (Sb)
3	TM3B	Tubby (Tb)

Absence of recombination in males

Since there is (nearly) no recombination in males one does not need to worry about losing a gene of interest in the unbalanced state.

5.3.2.4 Microinjection of *Drosophila* Embryos

Microinjection is most frequently used to introduce foreign DNA into developing germ cells of embryos to generate transgenic flies. However, there are also other applications such as RNAi (5.3.2.5) or injection of drugs (5.3.2.6).

5.3.2.4.1 Germline Transformation

The syncytial blastoderm of *Drosophila* is an excellent target for gene transfer (Parks et al., 1986). Integration of "new" DNA into the genome is facilitated by cloning the transgene into a transposable element-based vector (e.g. pUAST) (Brand and Perrimon, 1993) where it is flanked by 31 bp long terminal repeat sequences. These "inverted repeats" are recognized by the P-element transposase, an enzyme which can bind to them at each end, make a copy and jump or transpose the copy to a new location in the genome. For germline transformation the transposase and the transgenic DNA are localized on two different plasmids. The "transgenic vector" where the transgenic DNA is flanked by "inverted repeats" also contains a sequence for the eye color marker gene (w^+). The second plasmid, so-called "helper plasmid" (pUChsπΔ2-3) (Laski et al., 1986) codes for the transposase. By co-injection of both vectors

into the egg the transposase from the helper plasmid catalyses integration of the transgenic DNA into the fly's genome. Offspring derived from a transgenic sperm or egg can be identified using the marker gene phenotype eye color.

5.3.2.4.2 Production of Injection Mix

The DNA of the pUAST vector as well as DNA of the helper plasmid (pUChspΔ2-3) were isolated by Midiprep, using the Qiagen® Plasmid Purification Kit. For each injection 3 µg of the pUAST vector and 1 µg of the pUChspΔ2-3 were mixed, filled up to 100 µl with water, ethanol precipitated and resuspended in 20 µl injection buffer (0.1 mM).

Solutions:

Injection buffer (1 mM): 5 mM KCl, 0.1 mM Na-Phosphat buffer, pH 6.8;

5.3.2.4.3 Injection Needles

Before filling the capillary, the injection mix was centrifuged for 5 min at 13000 rpm to separate airborne particles, which could block the needle. 3-5 µl of injection mix were filled in sterile Femptotips (Eppendorf, 5242 952.008) which were clamped in the in the mechanical micromanipulator (*LeicaMicrosystems AG,* Wetzlar, Germany). Needles were focused and broken at the border of the slide.

5.3.2.4.4 Microinjection

For the injections 0-1 hr old w^- embryos (w^{1118}) were used. Because the pUAST vector carries a w^+ gene, all transgenic flies can be identified due to the eye color (varying from light yellow to dark red, depending on the integration site). Injections in the posterior side of the embryo were performed before pole cell formation. These cells will form later on the germline of the embryo. In this way, “new” DNA can be internalized during cell formation and is integrated into the genome of the pole cells. This can only be done until 1.5 hr after fertilization, during which time the embryo forms a syncytium of dividing nuclei (Campos-Ortega and Hartenstein, 1997). To increase and synchronize egg laying, w^- flies were transferred into collection vials (5.2.1) two days before injection. Apple agar plates were changed regularly. w^- embryos were collected on apple agar plates for 1 hr and dechorinated with 5% sodium hypochlorite. They were strung (with tweezers) in the same orientation on apple agar blocs and transferred to a cover slip. The cover slip was bonded with a double-faced scotch tape before or alternatively (for live imaging) brushed with sticky paste (tape solubilized in n-heptane). Then embryos were dried for 8 min, the cover slip was fixed on a slide (with a drop of oil), and em-

bryos were mounted in halocarbon oil (Voltalef 10S, *Lehmann+Voss+Co*, Hamburg, Germany). Injections were carried out under the microscope with optimized micromanipulator.

5.3.2.4.5 The "Set-Up"

The microinjection set-up was installed in a cool room (18˚C) to give more time flexibility as the embryos develop more slowly and the appropriate stage for injection lasts longer. The injection set-up consists of two parts: an inverted microscope (Leica DMIRE2, *LeicaMicrosystems AG,* Wetzlar, Germany) equipped with a 10 x lens and a micromanipulator, and an air-pressure injecting device (Femptojet, *Eppendorf*, Hamburg, Germany), connected to the micromanipulator (*LeicaMicrosystems AG,* Wetzlar, Germany). Once the needles are suitable to penetrate the embryos smoothly, the amount of injection mix coming out can be adjusted by varying the injection time (should be between 10 and 40 ms) and the injection pressure knobs.

5.3.2.4.6 Isolation and Balancing of Transgenic Flies

G0 flies do not show whether the injected DNA was integrated into the genome because insertion only occurs in the germline. Therefore, each G0 fly was crossed against 3 w- flies. The progenitors of this cross (G1) show red eyes only if germline transformation in G0 occurred. To determine on which chromosome the P-element was integrated, every transgenic fly (of the G1) was crossed against 3 flies of w-/w-(Y); Sp/CyO; Ubx,e/Tm3Tb,e (w- flies with dominant Markers on 2^{nd} (Sp) and 3^{rd} (Ubx) and Balancer with dominant Markers on 2^{nd} (CyO) and 3^{rd} (Tm3Tb) Chromosome). Red eyed females (w+) from the F2 carrying the 2^{nd} (CyO) and 3^{rd} (TM3Tb,e) chromosome balancer (to avoid recombination) were then crossed against red eyed males (w+) from the F2, carrying a dominant marker (no recombination in males) on the 2^{nd} (Sp) and 3^{rd} (Ubx) chromosome. According to Mendel law, dominant markers and red eye color show a ration, depending on the chromosome on which the DNA was integrated. Of each construct several independent lines were generated and tested. Depending on the expression level, the strongest (usually correlating with dark eye color) were added to the stock collection.

5.3.2.5 RNA Interference

5.3.2.5.1 Mechanism of RNAi

RNA interference (RNAi) by double stranded RNA (dsRNAs) molecules is a powerful method for preventing the expression of a particular gene. The technique was first developed

in *C. elegans* (Fire et al., 1998), and then rapidly applied to a wide range of organisms, including flies. dsRNA dominantly silences gene expression in a sequence-specific manner by causing the corresponding endogenous mRNA to be degraded. Upon introduction, the long dsRNAs enter a cellular pathway that is commonly referred to as the RNA interference (RNAi) pathway. First, dsRNAs are processed into 20-25 nucleotide small interfering RNAs (siRNAs) by an RNase III-like enzyme called Dicer (Carmell and Hannon, 2004). The siRNAs assemble into endoribonuclease-containing complexes known as RNA-induced silencing complexes (RISC). The siRNA strands subsequently guide the RISCs to complementary RNA molecules, where they cleave and destroy the cognate RNA (effecter step). Cleavage of cognate RNA takes place near the middle of the region bound by the siRNA strand (Matzke and Birchler, 2005).

5.3.2.5.2 RNAi of Myosin VI in *Drosophila* Embryos

For knocking down Myosin VI activity, living embryos were injected (5.3.2.4) with myosin VI RNA (Petritsch et al., 2003). Double-stranded DNA was produced by *in vitro* transcription from PCR- generated templates tagged with T7 RNA polymerase promoter sequence and injected into embryos expressing Miranda-GFP/*sca*-GAL4 and Histone-mRFP. Embryos were aged for 3 hr at 29°C and live imaging was performed by confocal microscopy (5.5).

5.3.2.6 Injection of Rho-Kinase Inhibitor (RKI)

The Rho-kinase inhibitor (RKI) Y-27632 specifically inhibits Myosin II in *Drosophila* neuroblasts (Barros et al., 2003). For knocking down Myosin II activity stage 9 embryos expressing Miranda-GFP/*scabrous (sca)*-GAL4 and Histone-mRFP were injected (5.3.2.4) with RKI (17 mg/ml in water; *TOCRIS Bioscience*, Bristol, United Kingdom) laterally and live imaged by confocal microscopy (5.5).

5.4 Immunohistochemistry

5.4.1 Embryo Staining with Antibodies

This method is used to visualize cellular or tissue constituents by antigen-antibody interactions. A fluorescence labeled secondary antibody binds to a primary antibody directed against the protein of interest (e.g. Miranda).

Standard protocol

Embryos, washed from apple agar plates with embryo wash, were “dechorinated” in 5% sodium hypochlorite for 2 minutes and transferred to 1.5 ml tubes in PBT.

Fixation 1: Embryos were fixed in 500 µl heptane (100%) and 500 µl formaldehyde (37%) for 4 min on the "Multireax" (*Heidolph Instruments GmbH & Co. KG,* Schwabach, Germany) at level 7, alternative

Fixation 2: Embryos were fixed in 500 µl heptane (100%) and 500 µl PBS-formaldehyde (4%) for 20 min on the Multireax at level 7.

For devitalisation, the lower phase was removed and replaced by 500 µl methanol (100%). Each sample was vortexed hard for 30 sec and supernatant was removed after the embryos sank to the bottom of the tube. Embryos were rinsed two times with 500 µl methanol, and washed two times short and two times 5 min in PBT. After blocking for 1 hr at RT in 5% normal goat serum (NGS), primary antibodies were diluted in blocking solution and incubated O/N at 4°C. The next day antibody was removed and embryos were washed 6 x 5min in 1 ml PBT at RT. Secondary fluorescent antibodies were centrifuged for 10 min at 4°C and 13000 rpm. Secondary antibody solution was incubated in the dark at RT. After 1 hr, solution was removed and samples were washed again 6 x 5 min. To stain DNA TOTO3 was diluted 1:1000 (in PBT) and incubated for 10 min. Supernatant was removed and embryos were washed 2 x 10 min in 1 ml PBT and 2 x 2 min in 1ml PBS. Embryos were mounted in 50-100 µl Vectashield and transferred to a slide (cut the tip to avoid damage). Embryos were spaced carefully and covered with a cover slip, which was fixed by nail polish. Dried samples were stored at -20°C or directly analyzed at the confocal fluorescent microscope (5.5.1).

Solutions:

Embryo wash:	0.7% NaCl, 0.03% TritonX-100;
PBS (10 x):	1.3 M NaCl; 70 mM NaHPO4; 30 mM NaH2PO4;
PBT:	PBS , 0.1% TritonX-100;
Fixing solution 1:	500 µl heptane (100%), 500 µl formaldehyde (37%);
Fixing solution 2:	500 µl heptane (100%), 54 µl formaldehyde (37%), 446 µl PBS;
Blocking solution:	PBS, 5% NGS;
Mounting medium:	50 µl VECTASHIELD mounting medium (*Vector Laboratories*, Burlingame, USA);
DNA staining solution:	Toto3 (*Molecular Probe* purchased from *Invitrogen*, Karlsruhe, Germany) 1:1000 in PBT;

5.4.2 *miranda* ^{ZZ176} Germline Clones

F2 embryos were sorted under the stereo fluorescence microscope (Leica MZ16 FA, *Leica Microsystems AG*, Wetzlar, Germany). An appropriate long-pass emission filter was used to visualize GFP fluorescence of "green balancers" (Kr G4 GFP) and distinguish between the yellow fluorescence derived from embryonic yolk and gut, and the green GFP fluorescence.

Embryos homozygous for the *miranda*^{ZZ176} mutation were separated, fixed and stained (5.4.1).

5.4.3 Whole Mount *In-situ* Hybridization

In situ hybridization is used for detecting specific mRNA sequences by hybridizing the complementary strand of a nucleotide probe to the sequence of interest. Whole mount *in situ* hybridization was done according to a protocol by (Tautz and Pfeifle, 1989), available from *Roche*:
http://www.roche-applied-science.com/PROD_INF/MANUALS/InSitu/pdf/ISH_208-215.pdf
An antisense RNA probe derived from *miranda* cDNA was labeled with digoxygenin (DIG)-UTP Embryos were hybridized at 65°C O/N in hybridization solution, followed by incubation with mouse anti-DIG (1:2000) and rabbit anti-Miranda (1:100). Miranda protein and DNA were visualized as described above (5.4.1).

5.5 Live Imaging and Fluorescence Recovery After Photobleaching

5.5.1 Technical Data

All described experiments were performed using the Confocal Laser Scanning Microscope Leica SP TCS_SP2 (*Leica Microsystems*, Heidelberg GmbH, Germany). Room temperature varied between 18-25 °C depending on the season. The HCL PL APO lbd.BL 63.0x1.40 Oil objective was used. The numerical aperture was fixed on 1.4.

5.5.2 Live Imaging

The commonly available method to detect protein localization by immunostaining of fixed embryos only provides static images of the proteins in different cells. Therefore, a technique was developed to visualize signals in living embryos. Embryos were collected on apple agar plates and aged to stage 9 to 10 (4-6 hr at 29°C). After dechorionation (5% sodium hypochlorite) embryos were strung (with a brush) in rows on apple agar blocs and immobilized on a cover slip, brushed with sticky glue (double stripped tape solubilized in heptane). Immobilized embryos on the cover slip were fixed on a plastic slide containing a hole in the middle (custom product of the garage of the Gene Center). The cover slip was attached to the slide with nail polish and embryos were mounted in Halocarbon 95 oil (*Halocarbon Products Corporation*, New Jersey, USA) to prevent them from drying. Using an inverse confocal microscope, with the objective underneath the slide made this construction necessary.

Neuroblasts were identified by the following criteria: delamination from the symmetrically dividing neuroectodermal cells, asymmetric cell division, giving rise to two differently sized daughter cells and asymmetric localization of proteins such as Miranda.

5.5.3 Fluorescence Recovery After Photobleaching

All fluorescence recovery after photobleaching (FRAP) experiments were done by point bleaching of 1 sec with maximum laser intensity using the advanced time laps tool. Recovery period was measured at lower laser intensity in time intervals of 3.25 sec. For calculating half time of recovery images were imported into "image J" (developed by Wayne Rasband, free download: http://rsb.info.nih.gov/ij/) and subtracted for background. The resulting curves were fitted to a single exponential function y=A(1-e-kt) with Origin 5.0 (Originlab) from which the FRAP half time t(1/2)= ln(2)/k was calculated. Images were imported into Adobe Photoshop, assembled in Adobe Illustrator, and converted to QuickTime movies.

5.6 Molecular Biology

5.6.1 Polymerase Chain Reaction (PCR)

PCR is based on the enzymatic amplification of a DNA fragment that is flanked by two short synthetic oligonucleotides. These so-called "primer" hybridize to the opposite strands of the target sequence and then synthesize the complementary DNA sequence by DNA polymerase. Each duplication cycle consists of three precisely timed consecutive reactions: denaturation, annealing, and extension. At each stage of the process, the number of copies is doubled. The reactions are controlled by changing the temperature using a special heat-stable polymerase (White et al., 1989).

5.6.1.1 Conditions

To avoid any contamination PCR grade water and filter tips were used. All other reagents (enzymes, buffers, nucleotides) were purchased from *Fermentas GmbH,* St. Leon-Rot, Germany. A standard PCR program was used for generating template DNA for *in vitro* transcription of Myosin VI RNA (Pfu) and for establishing oligonucleotide probes for *in situ* hybridization of Miranda RNA (Taq). Elongation time was adjusted, depending on the length of the fragment and depending of the type of polymerase (Pfu or Taq).

Conditions for *UAS Mira* 2-5

95°C	2 min		**50µl reaction volume**	
95°C	1 min		5µl	10xPfu buffer with 25 mM $MgSO_4$
53°C $_{\pm 5°C}$	1 min		1µl	10 mM dNTP Mix
72°C	2 min	10 cycles	2.5µl	10 µM primer frw
95°C	1 min		2.5µl	10 µM primer rev
47°C $_{\pm 5°C}$	1 min		37µl	H_2O (PCR grade)
72°C	2 min	25 cycles	1µl	template DNA (20 µg/µl)
72°C	5 min		1µl Pfu Polymerase (2.5 U/µl)	
4°C	forever		**∑= 50µl**	

5.6.1.2 Primer

Table 8: Nucleotide sequence of primer used for PCR.

Restriction sites are underlined. Following abbreviations were used: amino acid (aa), enhanced green fluorescence protein (eGFP), forward (frd), full length (fl), miranda (Mira), reverse (rev), sequence primer (Seq).

Name	Length (bp)	Sequence (5´→3´)	Enzyme	Application
mira-2 frw	20	ATCTCGAGTCTTTCTCCAAG	XhoI	Miranda C-terminal deletion analysis (aa 1-314)
mira-2 rev	22	ATGGTACCTTATCTGGAGATTC	KpnI	Miranda C-terminal deletion analysis (aa 1-314)
mira-3 frw	20	ATCTCGAGTCTTTCTCCAAG	XhoI	Miranda C-terminal deletion analysis (aa 1-314)
mira-3 rev	23	ATGGTACCTTAATAAATTCTCAC	KpnI	Miranda C-terminal deletion analysis (aa 1-314)
mira-4 frw	23	TCTCGAGGACAAAAAGTCAAAG	XhoI	Miranda C-terminal deletion analysis (aa 83-204)
mira-4 rev	22	ATGGTACCTTATCTGGAGATTC	KpnI	Miranda C-terminal deletion analysis (aa 83-204)
mira-5 frw	21	ATCTCGAGAGTGAGAATTTAT	XhoI	Miranda C-terminal deletion analysis (aa 206-314)
mira-5 rev	22	ATGGTACCTTATCTGGAGATTC	KpnI	Miranda C-terminal deletion analysis (aa 206-314)
eGFP frd	27	ATAGAATTCGTAACGATGGTGAGCAAG	EcoRI	eGFP tag for Miranda deletion analysis constructs
*eGFP*rev	24	TTACTCGAGGTCGACCTTGTACAG	XhoI	eGFP tag for Mira deletion analysis constructs
Seq*eGFP*	18	AACGGCATCAAGGTGAAC		sequence primer eGFP

jaguar1 frd	57	GGATCCTAATACGACTCACTATAGG GAGACCACCTAATCAAATATAGTTAT ATTTAC	*myosinVI* RNAi
jaguar1 rev	57	GGATCCTAATACGACTCACTATAGG GAGACCACTCAGATCCGAAAATCTT CGAGCCC	*myosin VI* RNAi
Seq 1	18	TTACAAGGACCACTGCAT	sequence primer eGFP
Seq 2	20	TTGTAACAGGAATACTGCAG	sequence primer Mira2-5
In-situ frd	50	GGATCCTAATACGACTCACTATAGG GAGAACAAATTCGAAAATGTCTTT	primer for Miranda *in-situ* hybridization
In-situ rev	50	CATACGATTTAGGTGACACTATAGA AGAGTTCATGTCCACCATGTAGGC	primer for Miranda *in-situ* hybridization

5.6.2 Sequencing

Sequencing of DNA was performed by the Blum group, located at the Gene Center Munich.

5.6.3 Competent Bacteria

For generation of Ca^{2+} competent bacteria 200 ml TY medium were inoculated with 2 ml of an *E. coli* DH5α over night culture (1:100 dilution) and shaken for 2-3 hr at 37°C. At OD_{600} of 0.4-0.6 (BioPhotometer, *Eppendorf,* Hamburg, Germany) the bacteria culture was cooled on ice water and centrifuged for 10 min at 4°C at 13.000 rpm. The pellet was resuspended in 30 ml TfBI and incubated for 10 min on ice. Subsequently the cells were again centrifuged for 10 min at 4°C at 13.000 rpm. The pellet was resuspended in 4 ml TfBII, aliquoted in 100 µl, shock frozen in liquid nitrogen and stored at -80°C.

Solutions:

TY-Medium: 2 % (w/v) bactotrypton; 0.5 % bactoyeast; 0.1 M NaCl; 10 mM $MgSO_4$;

TfBI: 100 mM KCl; 50 mM $MnCl_2$; 30 mM potassium acetate; 10 mM $CaCl_2$; 15% glycerol; pH 5.8;

TfBII: 10 mM MOPS; 10 mM KCl; 75 mM $CaCl_2$; 15 % glycerol; pH 7.0;

5.6.4 Transformation

For the transformation of $CaCl_2$-competent cells between 1-10 µl of the ligation reaction or alternatively 1 µg DNA was used. 100 µl aliquots of competent cells were thawed on ice before adding the DNA. After incubating 30 min on ice, bacteria were heat-pulsed at 42°C for exactly 90 sec and cooled down on ice for 2 min. 900 µl of pre-warmed Luria broth (LB) medium was added to each tube (1:10 dilution) and shaken for 30 min at 37°C (200-225 rpm). Of each transformation 50 and 200 µl were plated on LB agar plates containing 100 µg/ml ampicillin or 50 µg/ml kanamycin, respectively, and incubated at 37°C over night.

Solutions:

- **LB:** 1 % bactotrypton, 0,5 % bactoyeast, 1 % NaCl;
- **LB-Agar:** 6.3 g agar/300 ml LB;

- **Ampicillin:** 100 mg/ml stock solution in H_2O;
- **Kanamycin:** 100mg/ml stock solution in H_2O;

5.6.5 Preparation of Plasmid DNA

For each plasmid mini preparation 5 ml of overnight culture were used. The preparation was done according to the QIAprep Spin Miniprep Kit manual. For plasmid midi preparations, 50 ml of overnight culture were used. The preparation was done according to the HiSpeed Plasmid Midi Kit manual.

5.6.6 Ligation

The amount of vector and insert used for ligation was adjusted depending on the sizes of vector and insert fragments:

mass fragment [ng] = 100[ng] vector x length fragment [bp] x 6/ length vector [bp]

The ligation reaction was performed in a total volume of 20 µl at 17 or 22°C for 2-20 hr.

If the Rapid Ligation Kit was used the reactions were done according to the manufacturer's protocol.

5.6.7 Restriction Digest

Restriction digests for subsequent cloning were done at 37°C in a total volume of 50-100 µl containing 5-15 µg plasmid DNA and 1-5 µl of the corresponding enzyme/s. Digestion time varied from 2-12 hr.

5.6.8 *In vitro* Transcription

For *in vitro* transcription of *myosin VI* RNA the following reagents were pipetted together:

4 µl double-stranded cDNA (0.5 µg/µl)

20 µl transcription buffer (5x)

3 µl RNAse inhibitor

20 µl NTP: 5 µl ATP; 5 µl GTP; 5 µl CTP; 5 µl UTP (100 mM)

3 µl T7 RNA Polymerase

52 µl nuclease free H_2O

The reaction was incubated for 12 hr at 37°C. Then 4 µl DNase I was added to each sample and incubated for 30 min at 37°C. To purify the RNA a phenol-chloroform extraction and ethanol precipitation was performed.

5.7 Biochemistry

5.7.1 Production of *Drosophila* Embryo Extract

To obtain *Drosophila* embryo extract (DEX) large amount of Oregon R flies were kept in "biochemistry cages" (5.2.1) and embryos were collected on apple agar plates. As mentioned above (5.4.1) they were dechorinated in 5% sodiumhypochlorite for 2 min, shock frozen in liquid nitrogen and stored at -80°C if not used directly. Embryos were solubilized 1:2 in *Drosophila* embryo buffer (DEB). Protease- , phosphatase-, and RNAse-inhibitors as well as dithiothreitol (DTT) were added freshly to DEB each time. Embryos were shattered using a glass homogenizatior with a tight and a loose stirrer. Triton-X 100 was added to a final concentration of 0.5% and proteins were extracted by incubating the mixture on an "overhead" rotator at 4°C for 1 hr. To separate the pellet from the supernatant centrifugation for 30 min at 4°C (Rotanta 460 R, *Hettich Zentrifugen*, Tuttlingen, Germany) was performed. Supernatant was passed through a "Schleicher and Schüll" filter and the resulting solution was called DEX. To compare protein input and adjust antibody for immunoprecipitation (IP) the concentration of DEX was determined by Bradford assay.

Solutions:

- **Drosophila embryo buffer (DEB):**

25 mM hepes, 50 mM KCl, 1 mM $MgCl_2$, 250 mM sucrose, pH 7.5, sterile;

Additives (freshly added): 1 mM DTT, 40 U/µl RNAse inhibitor, 1x complete protease inhibitors, 40 mM p-nitrophenylphosphate, 2 mM sodium pyrophosphate, 2 mM orthovanadat, 50 mM sodium fluoride;

5.7.2 Immunoprecipitations

5.7.2.1 Principle

Immunoprecipitation (IP) involves the interaction between a protein and its specific antibody, the separation of these immune complexes with Protein G or Protein A, and the subsequent analysis by SDS-PAGE. This technique provides a rapid and simple means to separate a specific protein from whole cell lysates or culture supernatants. Additionally, IPs can be used to confirm the identity or study biochemical characteristics, post-translational modifications, and expression levels of proteins (Sweeney et al., 1996).

5.7.2.2 Immunoprecipitation of Miranda

Depending on the experiments DEX was split and incubated with 5-10 µg rabbit anti Miranda antibody (C-terminal) or, as a control, with slightly more (6-11 µg) preimmunserum of the same rabbit. The DEX-antibody/ DEX-preimmunserum incubation was performed over night at 4°C on a rotator. Protein A sepharose beads were blocked with 1% bovine serum albumin (BSA) for 1 hr at 4°C and subsequently washed 5 x with DEX. 10 µl of equilibrated beads were added to each of the samples and incubated for 1 hr at 4°C (beads bind to the constant region of the antibodies). The antibody-beads complex was centrifuged at 2000 rpm at 4°C for 5 min and subsequently washed 6 x 10 min at 4°C on the rotator. For dephosphorylating proteins beads were incubated with 2 µl Calf Intestine Alkaline Phosohatase (CIAP) for 1 hr at 37°C and again washed 4 x 5 min with DEB at 4°C on the rotator. Supernatant was removed and beads were prepared for the acrylamid gel.

Solutions:

- **Dephosphorylation solution**:
  2 µl CIAP (1 U/µl), 1.5 µl CIAP reaction buffer (10 x), 11.5 µl H_2O;

5.7.3 SDS-PAGE and Western Blotting

5.7.3.1 Sample Preparation

Supernatant of Protein A Sepharose beads resulting from an IP was removed gently. Beads were incubated with 20-40 µl 1 x SDS sample buffer including freshly added 100 mM DTT. Probes were heated at 95°C for 5 min and centrifuged at 13000 rpm. 10-25 µl of the supernatant was then loaded on a polyacrylamide gel. Liquid samples were diluted in 1 x sodium dodecyl sulphate (SDS) sample buffer (1:2) including 100 mM DTT, boiled, centrifuged and loaded on a polyacrylamide gel.

5.7.3.2 Gel Electrophoresis

For polyacrylamide gels the „Mini Trans-blot“ system (*BIO Rad*, Munich, Germany) was used following the instructions of the manufacturer. Ingredients for the running- and stack gel were pipetted together. Directly after pouring the running gel it was coated with isopropanol. After polymerization the alcohol was removed and the stack gel was added on top. “Spacer” of the glass slide were adjusted to the size of the combs (1 or 1.5 mm). Combs were removed after polymerization. Gel was incorporated into gel cambers filled with SDS running buffer. After loading the samples and protein marker the gel was run at 100 volt per gel.

Solutions:

Running gel 8%: 4.6 ml H_2O, 2.7 ml acrylamid (30%), 2.5 ml 1.5 M Tris (pH 8.8), 100 µl SDS (10%), 100 µl APS (10%), 6 µl TEMED;

Stack gel 5%: 1.4 ml H_2O, 330 µl acrylamid (30%), 250 µl 1.0 M Tris (pH 6.8), 20 µl SDS (10%), 20 µl APS (10%), 2 µl TEMED;

Running buffer: 25 mM Tris, 0.19 M glycin, 0.1% SDS;

5.7.3.2.1 Blotting, Blocking and Staining

Semi-dry blotting was used to transfer proteins to a membrane. Eight filter papers, the gel and a nitrocellulose membrane were incubated in transfer buffer for 10 min. Polyvinylidene fluoride (PVDF) membranes were activated in 100% methanol, followed by transfer buffer before used. The "sandwich" was prepared as follows: 4 filter papers on the bottom, the membrane, the gel and again 4 filter papers on top. Air bubbles were squeezed out using a Pasteur-pipette. Gels were blotted 11 volt for 1h. After the transfer the membrane was blocked for 1 hr at RT in 5% milk powder solubilized in washing buffer. For "Phosphorylation" experiments blocking was performed alternatively with 3% Bovine serum albumin (BSA, *DIANOVA*, Hamburg, Germany). The membrane was then incubated O/N at 4°C with the first antibody diluted in washing buffer. After subsequent washing steps of 2 x 2 min and 4 x 10 min at RT, second antibody in the corresponding dilution was incubated for 1 hr at RT. The blots were then washed again 3 x 5 min in washing buffer.

Solutions:

- **Transfer buffer:** 1% Tris glycine, 10% methanol;
- **Washing buffer:** 1x PBS, 0,05% Tween, pH 7,4;

5.7.3.2.2 Developing

For the immunodetection the ECL Western Blotting Detection Kit *(Amersham* purchased from *Invitrogen,* Karlsruhe, Germany) was used. Detection solutions A and B were mixed in a ratio of 1:1, for each blot 1 ml solution was used. The blot was placed protein side up on a saran wrap on the bench, detection solution was pipetted onto it and incubated for 1 min at room temperature. Excess liquid was removed and the blot was placed in a clear plastic bag without bubbles between the blot and the plastic cover. The wrapped blot was placed in an X-ray film cassette. In the dark room, a sheet of autoradiography film was placed on top of the membrane for 15 sec to 10 min, depending on the intensity of the expected signal.

6 RESULTS

6.1 Regulation of Miranda Localization by Myosin Dependent Mechanism

Asymmetric cell division (ACD) is an important prerequisite to generate cellular diversity. It is the primary mechanism used by neural progenitor cells to form the central and peripheral nervous systems. It has been shown that the adaptor protein Miranda plays a major role in establishing asymmetric cell fate by localizing cell fate determinants such as Staufen, Prospero and Brat to one side of the cell (3.3.2). Upon cytokinesis these cell fate determinants are inherited by only one daughter cell, which thereby switches its fate. Immunohistochemical analysis of fixed embryonic tissue already indicated that Miranda shows a very complex localization during mitosis: it localizes either to the apical or basal pole along the actin cortex or to the cytoplasm (Figure 10 E-H) (Shen et al., 1997; Fuerstenberg et al., 1998; Petritsch et al., 2003). However, experiments on fixed tissue only provide static images of single samples and are prone to produce fixation artifact.

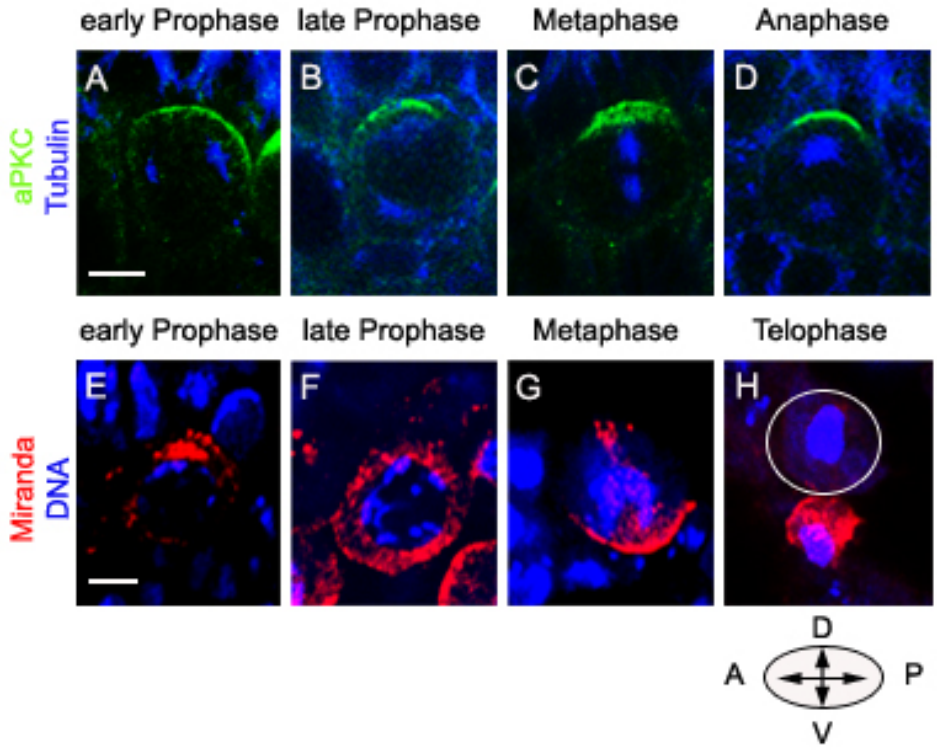

Figure 10: Protein localization in fixed embryonic neuroblasts.

(A-H) In contrast to Miranda (E-H), aPKC (green) (A-D) stays apical throughout mitosis. Miranda (red) forms an apical crescent in early prophase and sparing the nucleus in late prophase. It localizes as the characteristic basal crescent in metaphase and is inherited by the basal ganglion mother cell (GMC) in telophase (E-H). Pictures E-F were published in Petritsch et al., 2003.

To determine the sequence of Miranda localization during consecutive steps in mitosis, a live imaging approach was developed to study Miranda movement during mitosis in real-time. Using time-lapse confocal microscopy the temporal sequence of Miranda localization was investigated. A full length Miranda-GFP construct was expressed in living embryos, using the UAS-GAL4 system (Brand and Perrimon, 1993).

6.1.1 Underlying Genetic Mechanism: The UAS-GAL4 system

The UAS-GAL4 system in *Drosophila* (Brand and Perrimon, 1993), allows selective expression of any gene of interest in a time and tissue specific manner. This technique relies on the generation of transgenic fly lines that carry "activator" or "effector" constructs (Figure 11). Activator lines express a yeast transcription factor, GAL4, under the control of a specific promoter. Effector lines contain DNA-binding motifs (upstream activator sequence (UAS)) for GAL4 and are linked to the gene of interest. By crossing these two fly lines, the effector gene is transcribed, controlled by the activator´s promoter in the F1.

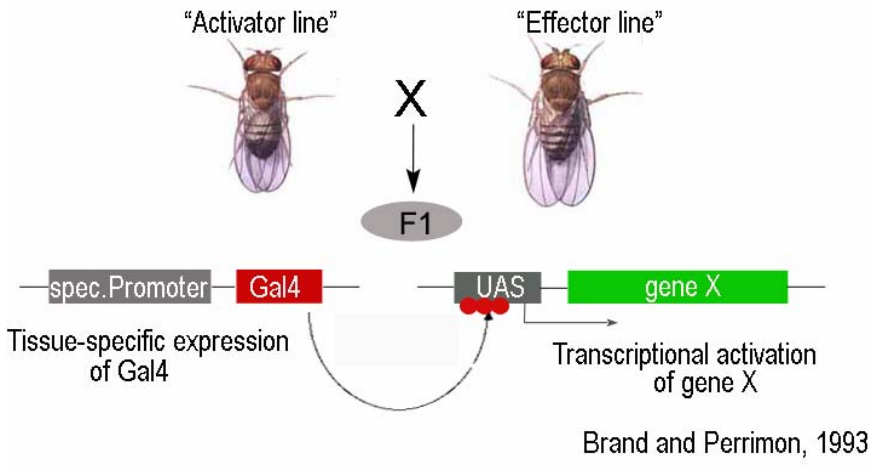

Figure 11: The UAS-GAL4 system for directed gene expression.

The UAS-GAL4 System in *Drosophila* (Brand and Perrimon, 1993), requires two transgenic fly lines. The "Activator" line expresses GAL4 under the control of a specific promoter, whereas the "Effector" line carries the gene of interest linked to an upstream activator sequence (UAS). After crossing the two lines, GAL4 binds to the UAS and induces the expression of a construct under the control of a specific GAL4 promoter in the F1 generation.

GAL4 was identified in *Saccharomyces cerevisiae*, as a regulator of genes induced by galactose (GAL) (Laughon et al., 1984). The 881 amino acids long protein regulates the transcription of the divergently transcribed GAL10 and GAL1 genes by directly binding to four related 17 base pair (bp) sites located between these loci (Duffy, 2002). These sites define an UAS

element, analogous to an enhancer element defined in multicellular eukaryotes, which is essential for the transcriptional activation of GAL4 regulated genes. The yeast transcription factor GAL4 is inactive in *Drosophila*. Thus, GAL4 can be expressed under the control of *Drosophila*-specific promoters with little effect upon the organism.

6.1.2 Miranda Localizes via the Cytoplasm to the Basal Cortex

Full length Miranda-GFP was expressed under the control of *neuralized*-GAL4, which drives expression specifically in neuroblasts and neuroepithelial cells. Using non-invasive time-lapse confocal microscopy Miranda was followed through mitosis in living embryos. Miranda-GFP shows uniform cytoplasmic localization, sparing the nucleus, in prophase of neuroepithelial cells (Figure 12 A; 0'00''). Presumably around the time of nuclear envelope breakdown (NEB) Miranda-GFP fills the entire cell as a 'cytoplasmic cloud' (Figure 12 A, arrow) before it accumulates in the basal crescent (Figure 12 A, 1´34´´). Upon cytokinesis, the basal Miranda crescent is cut in half in neuroepithelial cells (Figure 12 A; 7'50'') and symmetrically distributed to the two daughter cells. In neuroblasts cytoplasmic Miranda–GFP accumulates apically in prophase before NEB occurs (Figure 12 C, white arrows). The 'cytoplasmic cloud' (Figure 12 C ; white arrow, 5'08''), already observed in epithelial cells, persists for about 2 min before Miranda-GFP accumulates in the basal crescent (Figure 12 C, 7'09''). Upon cytokinesis, Miranda is inherited by the smaller, basal daughter cell in the neuroblast mitosis (Figure 12 C; 11'37''). As reported previously, Partner of Numb (PON)-GFP, by contrast, is primarily cortically localized throughout cell division in neuroepithelial cells and neuroblasts (Figure 12 B, D) (Lu et al., 1999) before it becomes restricted to a basal cortical crescent (Figure 12 B, 6´02´´; Figure 12 D, 8´31´´). As Miranda, PON is inherited symmetrically in epithelial cells (Figure 12 B, 7´37´´) and asymmetrically by the GMC in neuroblasts (Figure 12 D, 10´59´´) upon cytokinesis.

Miranda is very dynamically localized to a cytoplasmic cloud before metaphase. This cytoplasmic cloud feeds protein into the basal crescent. Correlated with an increase of the Miranda-GFP signal at the basal cortex (Figure 12 A; 1'34'' and Figure 12 C; 7'09''), the cytoplasmic signal decreases, suggesting that Miranda-GFP moves via the cytoplasm to the basal cortex in both cell types. The cytoplasmic cloud leads to Miranda crescent formation twice as fast in neuroepithelial cells (average =50 sec) than in neuroblasts (average=2 min). The data show that while Miranda and PON colocalize to a basal crescent in metaphase they use different routes to translocate to the basal side.

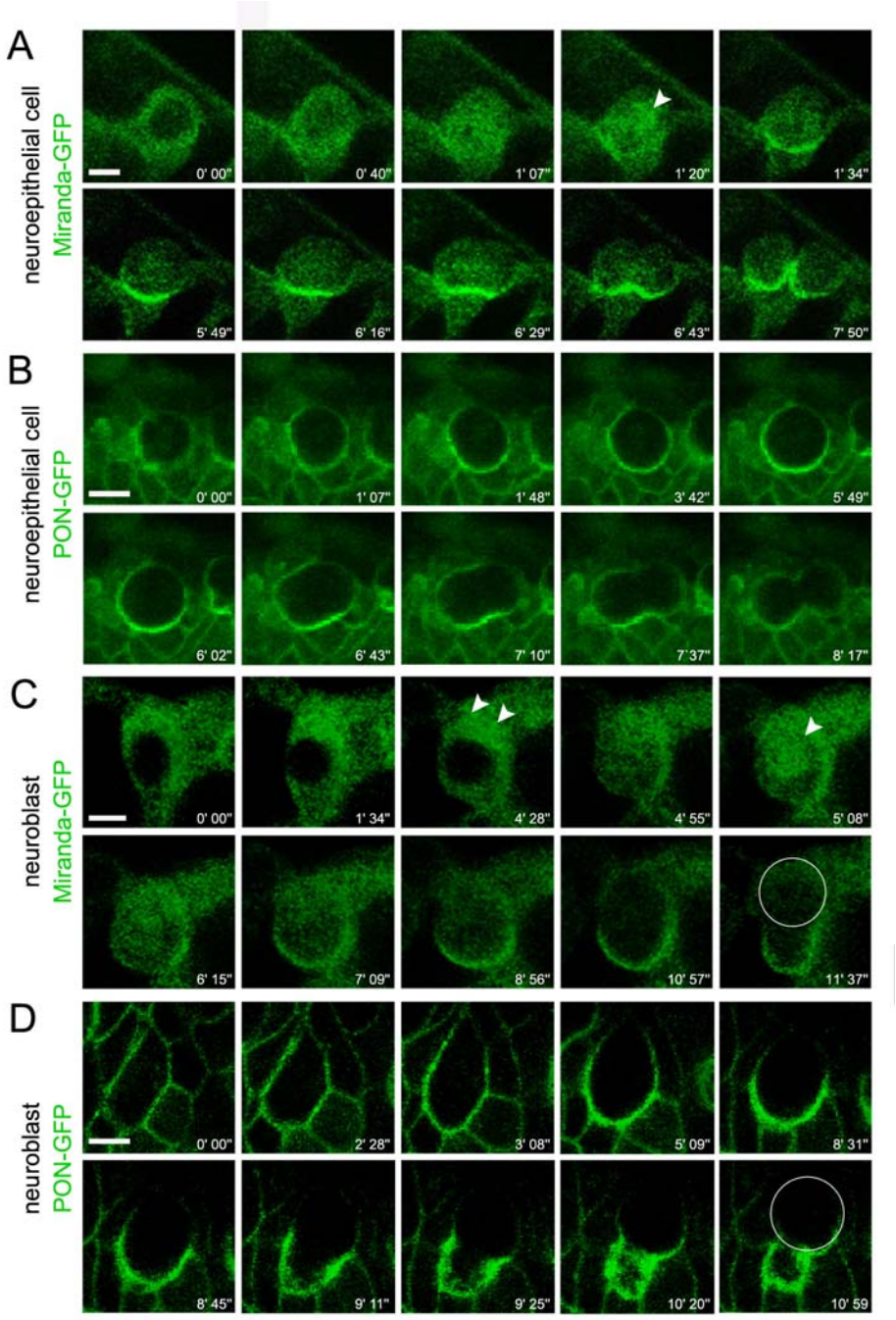

Figure 12: Miranda different from PON moves via the cytoplasm to the basal side of the cell.

(A-D) Time series of stage 9-10 embryos expressing either Miranda-GFP or PON-GFP. Single neuroepithelial cells or neuroblasts were followed through mitosis using time-lapse confocal microscopy. Images from a single confocal plane were recorded every 13.5 sec. Scale bars represent 5 µm. Apical is up in all images.

(A,C) Full length Miranda-GFP showes cytoplasmic localization (white arrow) during pro/metaphase, in neuroblasts (C) as well as in neuroepithelial cells (A). First Miranda spares the nucleus (0´00´´), and then it spreads into the entire cytoplasm (arrow). Miranda accumulates apically in neuroblasts (C, white arrows) but not in neuroepithelial cells (A) before filling the entire cytoplasm (white arrows) and accumulating into a tight basal crescent in metaphase. (B,D) Full length PON-GFP, different from Miranda, remaines at the cortex during mitosis of neuroepithelial cells (B) and neuroblasts (D).

While PON-GFP moves preferentially along the cortex, Miranda-GFP dynamically localizes to the cytoplasm and the cortex suggesting two routes for proteins during asymmetric cell division of *Drosophila* neuroblasts.

a) moving along the cortex as shown for PON-GFP
b) moving through the cytoplasm as shown for Miranda-GFP.

Contrary to earlier results in fixed embryonic neuroblasts (Figure 10, Figure 13), the time lapse experiments show that Miranda does not localize to an apical crescent in prophase neuroblasts. Miranda-GFP spares the nucleus and infrequently accumulates at the apical pole of the neuroblast (Figure 12 C, arrows). Apical accumulation of Miranda was mainly detected in delaminating neuroblasts, which might inherit Miranda from neuroepithelial cells (data not shown).

6.1.3 Mechanism of Dynamic Miranda Localization

It is known from studies on fixed embryonic tissue that proper Miranda localization requires an intact actin cytoskeleton (Knoblich et al., 1997) and depends on Myosin II (Barros et al., 2003) and Myosin VI (Petritsch et al., 2003). These data indicate that Miranda molecules probably move by active transport to the basal side of the cell, presumably associated with cell organelles such as the endoplasmatic reticulum (ER). However, the asymmetric localization of Miranda can also be explained by one or a combination of the following mechanisms: asymmetric localization and local translation of *miranda* mRNA, passive diffusion (3 dimensional in the cytosol or 2 dimensional along the cortex) and trapping of Miranda protein by basally localized anchor molecules, or protein targeting to the membrane followed by selective degradation at one side of the cortex.

6.1.3.1 Miranda is not Associated with the Endoplasmatic Reticulum

The nature of the cytoplasmic cloud could be a result of Miranda associated with cell organelles as the endoplasmatic reticulum (ER) during neuroblast mitosis. Similar to Miranda, segregation of ER into daughter cells is a dynamic process requiring the actin cytoskeleton with motor proteins to stabilize and transport ER tubules (Bannai et al., 2004). Intriguingly, the ER is not always symmetrically inherited by daughter cells. In early *C. elegans* embryos it is asymmetrically distributed by a Par protein-dependent mechanism (Poteryaev et al., 2005). To investigate the localization and segregation of the ER in dividing neuroblast cells, embryos

were fixed and stained with a KDEL antibody (Figure 13). This antibody recognizes the aminoacid sequence lysine- aspartic acid- glutamic acid- leucine (KDEL), which is present at the carboxy-terminus of soluble ER resident proteins and some membrane proteins. Similar to Miranda protein in fixed embryonic tissue, the ER appeares to be apically enriched during delamination and in early prophase. In pro/metaphase, the ER is distributed in the cytoplasm, partly overlapping with Miranda protein mainly in the apical half of the cells. However, while Miranda forms a basal crescent in late metaphase and is inherited by the basal ganglion mother cell (GMC), the ER remaines localized in the cytoplasm being more concentrated in the apical half of the cell and thus becomes mainly inherited by the neuroblast. Thus, the ER is not part of the "cytoplasmic cloud" moving Miranda molecules through the cytoplasm.

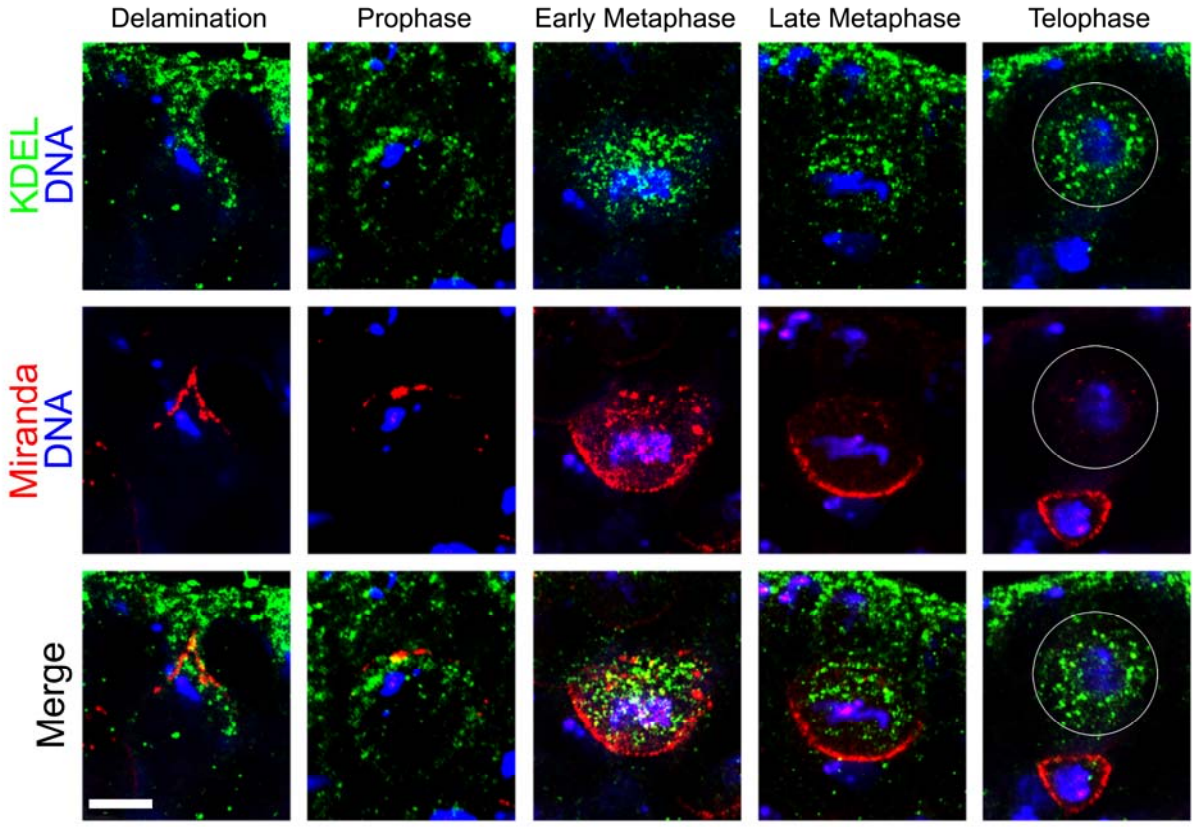

Figure 13: The ER in neuroblasts is apically localized throughout neuroblast division.
Wild type embryos were stained with anti-Miranda (red) and anti-KDEL (green) antibody. DNA is in blue. Scale bar represent 5µm. Miranda and the ER accumulate apically during delamination and early prophase and partially overlap (white arrows). In early metaphase, the ER is distributed in the cytoplasm, still partially overlapping with Miranda protein, but remaines in the cytoplasm and more concentrated in the apical half of the cell so that it is primarily inherited by the neuroblast daughter upon cytokinesis (white circle).

6.1.3.2 *miranda* mRNA and Protein Show Distinct Localization

To test alternative possibilities for Miranda localization such as localized translation and/or degradation, it was first analyzed whether Miranda localization depends on asymmetric *de novo* protein synthesis during mitosis. If *de novo* protein synthesis contributes to asymmetric Miranda localization, *miranda* mRNA should be detected at the basal pole. Localized translation on the basal pole could give rise to a typical basal metaphase crescent. *miranda* mRNA localization was determined by fluorescent *in situ* hybridization was tested and compared to Miranda protein localization (Figure 14). In prophase *miranda* mRNA accumulates around the apical pole and partially colocalizes with Miranda protein (Figure 14 A). While Miranda protein is removed from the apical side as mitosis proceeds and becomes restricted to a basal crescent, *miranda* mRNA remains apically localized in metaphase and anaphase (Figure 14 B,C). As the cell undergoes cytokinesis, *miranda* mRNA is exclusively inherited by the neuroblast whereas Miranda protein is found in the ganglion mother cell (GMC) only (Figure 14 D). The absence of *miranda* mRNA at the basal side of the cell supports the hypothesis that Miranda protein but not its mRNA is localized to the basal side. Miranda protein exists in one pool that is translated on the apical pole and is "transported" to the basal side via the cytoplasm.

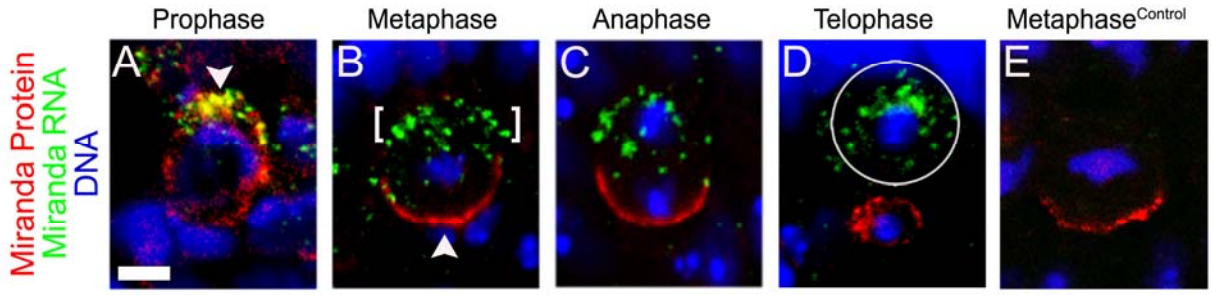

Figure 14: *miranda* mRNA stays apical during mitosis.

(A-D) Double labeling of *miranda* mRNA (green) by *in situ* hybridization and Miranda protein (anti-Miranda antibody; red) during neuroblast mitosis of wild type stage 9/10 embryos. Projections of confocal sections of neuroblasts are shown. Scale bars represent 5 µm. Apical is up in all images.

miranda mRNA is asymmetrically localized to the apical pole and cell throughout neuroblast division. In prophase mRNA and protein colocalize at the apical pole (A, arrow), while in metaphase *miranda* mRNA stays apically localized (B, white bracket) but Miranda protein becomes localized to a basal crescent (B, white arrow). *miranda* mRNA is inherited by the larger neuroblast (D, circle) while Miranda protein is inherited by the ganglion mother cell (C,D). (E) No signal for *miranda* mRNA can be detected using a sense RNA probe as a control.

6.1.3.3 Miranda is not Locally Degraded at the Apical Side of the Cell

As an alternative to local translation, Miranda protein may be selectively degraded by the 26S proteasome at the apical side of dividing neuroblasts in prometaphase in order to become basally enriched in metaphase. The 26S proteasome is present in the nucleus and cytosol of all cells and selectively degrades proteins modified by conjugation with ubiquitin. Mutations in the 26S proteasome affect cell fate decisions in the sensory organ precursor lineage of the developing pupae presumably because the Notch receptor is targeted for degradation (Schweisguth, 1999). To investigate whether the 26S proteasome locally degrades Miranda on the apical cortex and contributes to its asymmetric localization, Miranda localization was studied in embryos carrying a dominant temperature-sensitive (DTS) proteasome mutation in the ß2 proteasome subunit gene, *DTS5* (Figure 15) (Schweisguth, 1999). At the restrictive temperature (29°C) Miranda protein is still properly localized, in wild type embryos (Figure 15 A,B), in heterozygous embryos carrying a genomic allele of the *DTS5* mutant (Figure 15 C,D) as well as in embryos expressing a copy of the *DTS5* mutant in neuroblasts under control of a UAS-promoter and *prospero*-GAL4 (Figure 15 G,H). As a positive control cyclin B was used, which is known to be degraded during metaphase in a proteasome-dependent pathway (Alberts et al., 2002). Taking advantage of the UAS-GAL4 system it was shown that at the restrictive temperature (29°C) cyclin B is not degraded any more (Figure 15 K,L). In contrast, Miranda is still properly localized at the restrictive temperature in mutants with downregulated proteasome activity (Figure 15, G,H) (Schweisguth, 1999), suggesting that degradation might not contribute to Miranda asymmetric localization. In embryos kept at a lower temperature (18°C) and therefore showing functional proteasome activity (Figure 15 I,J), Cyclin B is degraded and no longer present in telophase neuroblasts (Figure 15 J).

6.1.3.4 Distinct Modes of Miranda Localization in the Cytoplasm and on the Cortex

The nature of Miranda movement was further studied by FRAP experiments in living embryos. Miranda protein could either freely diffuse in the cytoplasmic cloud or could be actively transported through the cytoplasm e.g. by myosin motor proteins. Likewise, it is unknown how Miranda protein interacts with the basal cortex to form the crescent. Previous data have shown that proper Miranda localization depend on an intact actin cytoskeleton (Knoblich et al., 1997). To investigate whether Miranda is immobilized at the cortex by a static anchor or moves within the limits of the basal crescent, as has been shown for PON (Lu et al., 1999) Fluorescence Recovery after Photobleaching (FRAP) of Miranda-GFP was performed during live cell imaging.

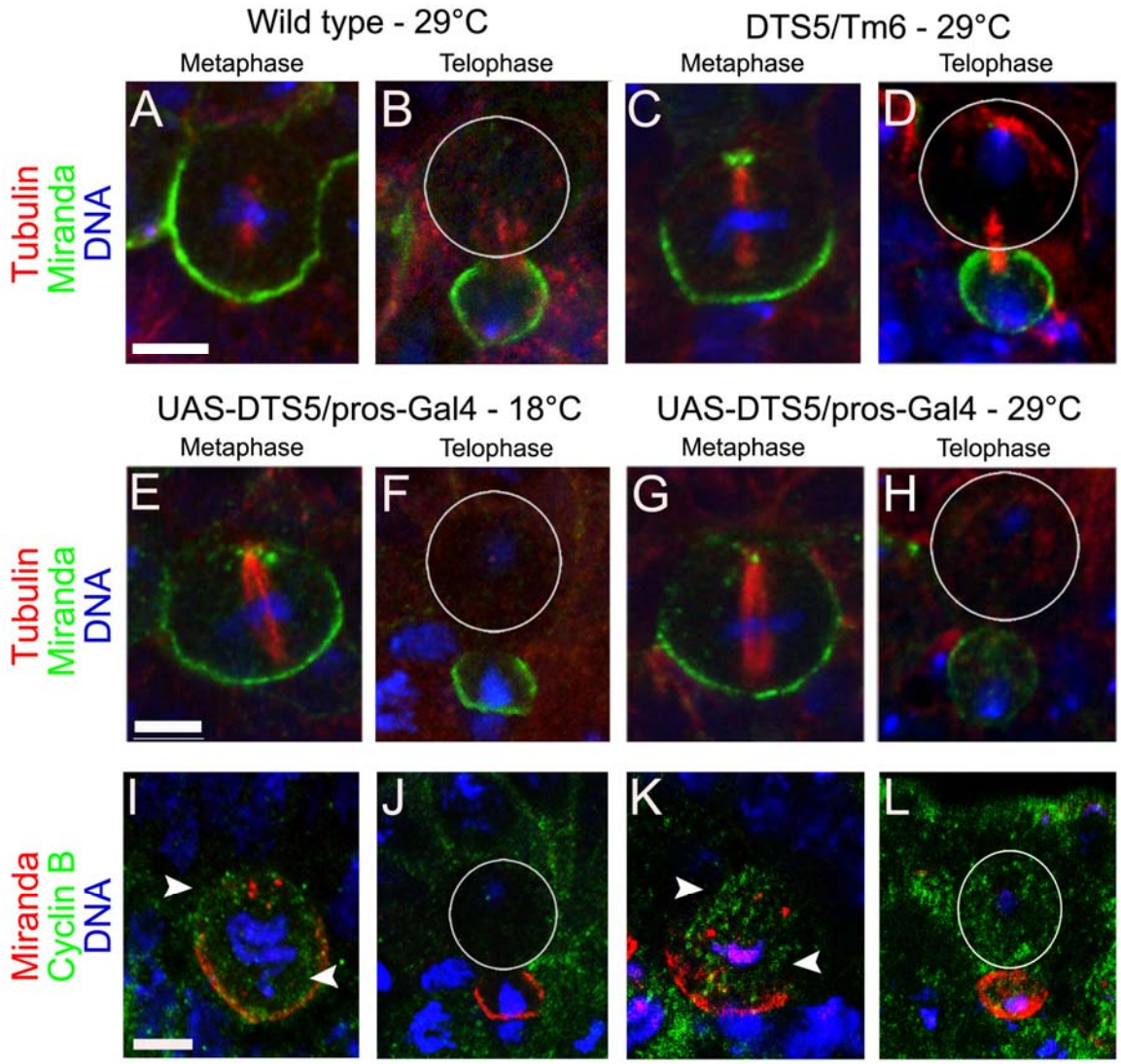

Figure 15: Miranda localizes asymmetrically independent of proteasome activity.

(A-L) Embryos were fixed and stained with antibodies against either Miranda (green) and tubulin (red) (A-H) or Miranda (red) and cyclin B (green) (I-L). DNA is blue. Scale bar represents 5 µm. White circles indicate the neuroblast. Embryos expressing DTS5, a dominant negative and temperature-sensitive form of a proteasome subunit, show correct Miranda localization at the restrictive temperature (29°C) (C,D). As observed in wild type neuroblasts Miranda localized in a tight metaphase crescent before being inherited by the ganglion mother cell in telophase (A,B). Miranda is still localized correctly in embryos expressing *DTS5* specifically in neuroblasts under control of a UAS-promoter and *prospero*-GAL4 at the permissive (E,F) as well as at the restrictive (G,H) temperature. In contrast, cyclin B (green), charging the cytoplasm in metaphase (I,K, arrows) is degraded in anaphase at the permissive (J) but not the restrictive temperature (L).

Miranda-GFP flies were combined with flies expressing Histone-RFP, revealing a *Drosophila* line, which coexpresses Miranda-GFP and Histone-RFP (crossing scheme not shown). The expression of Histone-RFP enabled to visualize DNA condensation during mitosis. The motility of cortical Miranda-GFP (Figure 16 A-D) was calculated after selectively bleaching a region of interest (ROI) within either the basal crescent (B) or the cytoplasmic regions (Figure 16 E,G). Recovery of the fluorescent signal by Miranda-GFP molecules moving into the ROI from adjacent areas was quantified. Interestingly, Miranda is motile at the basal cortex but only within the limits of the basal crescent (Figure 16 C,D). Indicated by their half time of recovery values ($t_{½}$Miranda = 6.76+/-0.66 sec compared to $t_{½}$PON = 6.79+/-0.43 sec) both proteins exhibit similar kinetics (Figure 16 J,L), suggesting that they interact with cortical regions by a similar mechanism. Since Myosin II is thought to repulse Miranda and PON from the apical cortex (Barros et al., 2003) (Figure 17) the recovery of cortical spaghetti-quash (Sqh), the regulatory light chain of Myosin II fused to GFP was determined. The recovery behavior of Sqh-GFP is similar although not identical to Miranda and PON-GFP (Figure 16 L; $t_{½}$MyoII = 5.73+/-0.40 sec) showing that Miranda moves slightly slower than Myosin II. Very fast movement of eGFP with $t_{½}$ of less than one second ($t_{½} < 1$ sec) indicates free and unrestrictedly three-dimensional diffusion. Proteins which interact with subcellular structures, such as the actin cytoskeleton or the membrane, or are bound to other slower moving proteins (e.g. myosins) show slower kinetics and hence a longer halftime of recovery (Lippincott-Schwartz et al., 2001). In contrast to cortically localized Miranda it was impossible to significantly reduce the fluorescent signal when bleaching a cytoplasmic ROI either on the apical or the basal half of the cell (Figure 16 E-H) using the same parameters as for cortical bleaching (see Experimental Procedures). Higher bleaching intensity could not be used due to an overall loss of fluorescent signal (data not shown). The first post-bleach recording of cytoplasmic Miranda shows an almost fully recovered ROI (Figure 16 E-H) indicative of rapid movement of Miranda molecules with a $t_{½}$ smaller than 1.5 sec. This suggests that Miranda diffuses unrestrictedly in the cytoplasm and is not immobilized by binding to subcellular structures such as the Golgi or the ER. To confirm this data, the recovery of cytoplasmic Miranda was compared with that of a freely diffusing protein such as eGFP. The eGFP signal fully recovers before the first post-bleach recording (Figure 16 K). FRAP analysis showed that during its cytoplasmic phase Miranda moves unrestrictedly within the cytoplasm with kinetics similar to eGFP molecules, suggesting that it might be part of a freely diffusing complex. On the cortex, the majority of Miranda is bound to the actin cytoskeleton but is able to move within the limits of the basal crescent similar to PON.

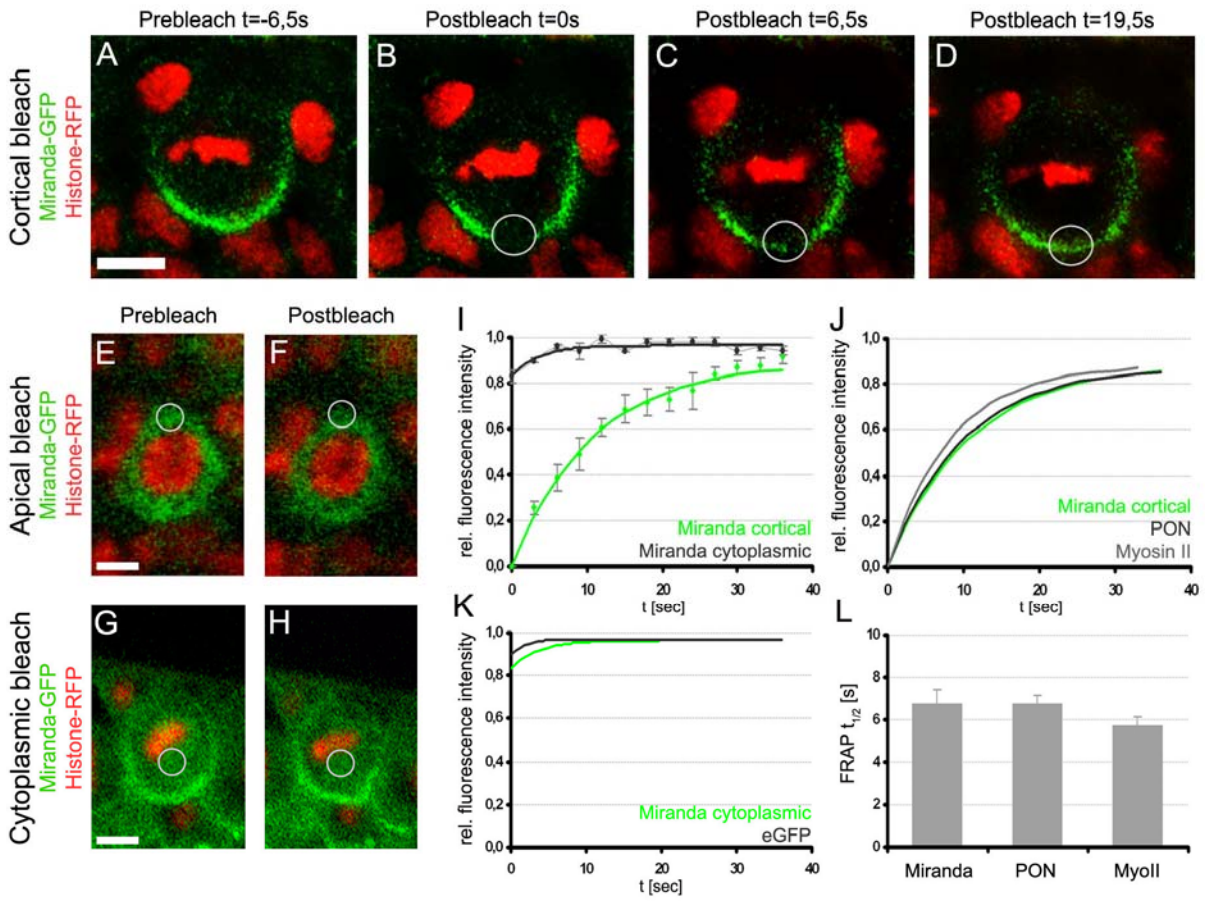

Figure 16: Miranda diffuses freely in the cytoplasm but shows spatially limited and slower movement at the cortex.

(A-D) FRAP of Miranda-GFP in a metaphase crescent (A) in dividing neuroblasts coexpressing Miranda-GFP and Histone-RFP. (B) The region of interest (ROI) was selected in the center of the basal metaphase crescent (white circle) and bleached by a high-intensity laser beam for 1 sec. Subsequent scanning of the area revealed a complete loss of GFP signal within the ROI. (C) Recovery of GFP signal within the ROI resulting from Miranda-GFP molecules moving into the area from surrounding unbleached regions were detected 6.5 sec after bleaching and filled the area completely at 19.5 sec after bleaching (I and J; green curve). (E-H) Cytoplasmic Miranda diffuses freely. Cytoplasmic Miranda on the apical pole (E) and on the basal half of the neuroblast (G) was bleached in a ROI as indicated by the white circles and recovery was recorded. Only a small reduction in the GFP signal was detected on the apical (F) and the basal (H) side indicative of a fast recovery of the GFP signal. (I-L) Mobility of Miranda protein depends on its subcellular location. Quantification of FRAP shows that while cytoplasmic Miranda diffuses freely, the cortical fraction is less mobile (I) and appears to be present in actin-associated complexes, similar to PON and Myosin II (J,L). Corresponding FRAP curves showed similar but not identical kinetics for all cortically localized Miranda, PON and Sqh, the regulatory light chain of Myosin II, respectively: Half-time of recovery is around 7 sec (n=10) for Miranda-GFP ($t_{1/2}$ Miranda = 6.76+/-0.66 sec) and for PON-GFP ($t_{1/2}$ PON = 6.79+/-0.43 sec). Sqh-GFP ($t_{1/2}$ Sqh = 5.73+/-0.40 sec) recoveres slightly faster (J,L). (K) Cytoplasmic Miranda (n=10) and eGFP alone (n=10) show very fast recovery ($t_{1/2}$ < 1.5 s) indicative of three-dimensional diffusion. Scale bars represent 5 µm in A, E and G.

6.1.3.5 Myosin II and Myosin VI Act at Distinctive Steps During ACD

The barbed end-directed motor Myosin II as well as the pointed end-directed motor Myosin VI have been implicated in regulating proper localization of Miranda to a basal crescent (Peng et al., 2000; Barros et al., 2003; Petritsch et al., 2003). The temporal and spatial order of the interaction of the two myosins with opposite polarity with Miranda *in vivo* is not fully understood. To address this question Miranda localization in the absence of Myosin II and Myosin VI, was studied, by using time-lapse confocal imaging.

Miranda localization was monitored after Myosin II activity was inhibited by injecting the Rho-kinase kinase inhibitor (RKI) Y-27632 (Barros et al., 2003) into living embryos expressing Miranda-GFP under the control of *scabrous*-GAL4 and Histone-RFP. Consistent with our earlier observations (Figure 12), in embryos injected with buffer only (control; Figure 17 A-D), Miranda-GFP moves to the cytoplasm in late prophase (Figure 17 A) before forming a metaphase crescent (Figure 16 B) and is inherited by the GMC daughter in telophase (Figure 17 C,D). Dividing neuroblasts in the absence of Myosin II activity however, show cortical Miranda localization throughout mitosis (Figure 17 E,F) and lack asymmetric distribution of the protein in anaphase and telophase (Figure 17 G,H). RKI-injected neuroblasts still undergo cytokinesis presumably due to residual Myosin II activity. These data show that (1) Myosin II is required to remove Miranda from the (apical) cortex in late prophase and (2) is a prerequisite for the formation of the cytoplasmic cloud by Miranda protein in late prophase without which the basal crescent in metaphase is not being formed. The data are consistent with earlier results from fixed embryonic tissue depicting steady-state images showing of cortically localized Miranda in metaphase neuroblasts of spaghetti squash (Sqh) mutants, lacking the regulatory light chain of Myosin II (Barros et al., 2003). By live imaging of Miranda localization in dividing neuroblasts, the temporal order of Myosin II activity can be specified. It cannot be excluded that Myosin II is also required for Miranda localization in metaphase to restrict the basal crescent.

To analyze the function of Myosin VI *in vivo*, RNAi in living embryos was performed. Embryos expressing Miranda-GFP/*sca*-GAL4 and Histone-RFP were injected with dsRNA complementary to Myosin VI (Figure 17 I-L). Interestingly, Miranda is completely mislocalized to the cytoplasm in all phases of neuroblast mitosis suggesting that Myosin VI is essential for cortical localization of Miranda (Figure 17 I-L).

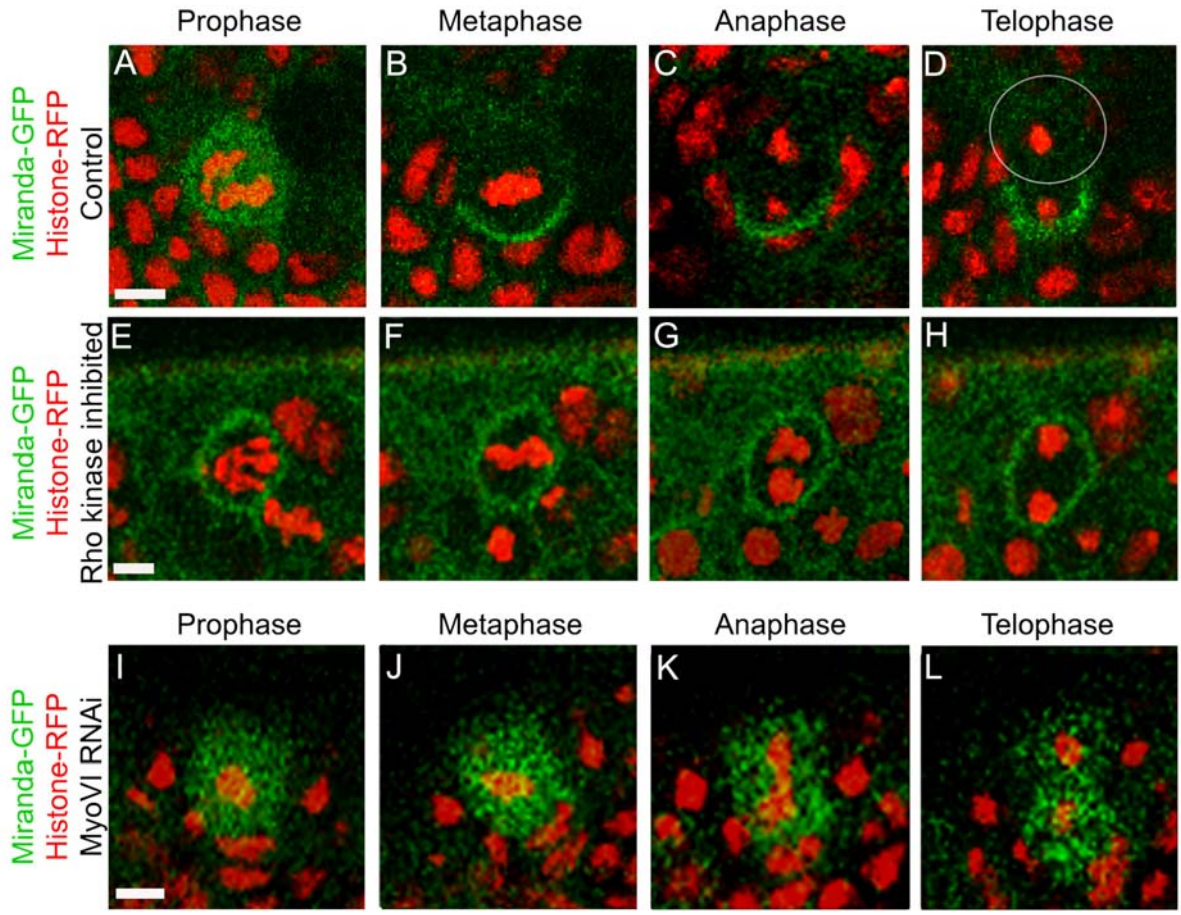

Figure 17: Myosin II and Myosin VI are required for proper Miranda localization.

(A-L) Live imaging in embryos coexpressing Miranda-GFP and Histone-RFP. Embryos were injected with buffer as a control (A-D), Rho-kinase Kinase Inhibitor (RKI) to inhibit Myosin II (E-H) or *myosin VI* dsRNA to downregulate Myosin VI (I-L), respectively. (A-D) In buffer control injected embryos, Miranda protein localizes normally from the apical side throughout the cytoplasm to the basal cortex. (E-H) When Myosin II is downregulated, Miranda remains cortically localized throughout mitosis and does not form a cytoplasmic cloud or a basal crescent. (I-L) Reduced Myosin VI activity on the other hand shows Miranda mislocalized to the cytoplasm and no cortical association throughout mitosis. Scale bars represent 5µm in A, E and I.

In summary Myosin VI is required for interaction of Miranda with the cortex in late prophase and metaphase and Myosin II in contrast is required to exclude Miranda from the cortex in late prophase. Earlier data of fixed embryonic tissue have shown that Miranda is mislocalized to the cytoplasm when Myosin VI activity is reduced (Petritsch et al., 2003). However, by applying live analysis of Miranda localization in dividing neuroblasts it was possible to dissect the timing of myosin activity at distinctive steps during asymmetric localization of Miranda in dividing neuroblasts.

6.1.3.6 PON Localization Depends on Myosin II but not on Myosin VI

The pointed end-directed Myosin motor Myosin VI has been shown earlier to be required for basal protein localization (Petritsch et al., 2003). Thus, it was tested whether PON localization is affected when Myosin VI activity is downregulated. In embryos lacking zygotic Myosin VI, the mitotic spindle is misoriented resulting in a misorientation of the division plane by 90° (Petritsch et al., 2003). PON protein however, is still localized to a cortical crescent in metaphase but the crescent is now positioned lateral to the epithelial surface presumably due to a general loss of proper apical-basal polarity (data not shown).

In an alternative approach, double-stranded RNA complementary to parts of the Myosin VI RNA to downregulate Myosin VI activity (Myosin VI RNA interference or RNAi) was injected. Similar to a loss of zygotic Myosin VI, Myosin VI RNAi lead to a misorientation of the cleavage plane, indicating that Myosin VI function was indeed reduced (Figure 18 A-D). PON protein however still formed a cortical crescent in metaphase at the lateral side of the metaphase neuroblast and is asymmetrically localized to the basal daughter cell upon cytokinesis (Figure 18 C). Thus, in contrast to its function in localizing Miranda, Myosin VI is not required for localization of PON in a cortical metaphase crescent, which suggests that this Myosin differentially regulate adaptor proteins during neuroblast division.

The Brand lab (Barros et al., 2003) has shown that Myosin II is required to properly localize Miranda and the cell fate determinant Numb to the basal cortex by excluding them from the apical cortex rather than by active transport. In hypomorphic maternal mutants for Spaghetti squash (Sqh), representing the regulatory light chain of Myosin II, the actin cytoskeleton is disrupted and consequently, Miranda is mislocalized to the mitotic spindle whereas Numb is mislocalized uniformly to the cytoplasm. Likewise, downregulation of Myosin II by inhibition of its upstream regulator Rho-kinase leads to mislocalization of Numb and Miranda uniformly around the cortex. Since PON is required for timely localization of Numb to the basal cortex in metaphase, it was tested whether Myosin II regulates PON localization as well. In order to selectively test the requirement of Myosin II for PON localization, Rho-kinase inhibitor Y-27632 was injected into embryos expressing PON-GFP under the control of the *scabrous*-GAL4 promoter in neuroblasts and neuroepithelial cells. In living embryos PON was remained uniformly localized around the entire cortex during mitosis when Myosin II activation is impaired (Figure 18 D-F). Thus, Myosin II is indeed required for proper localization of PON to a basal crescent, presumably by cortical exclusion of PON from the apical pole in prophase.

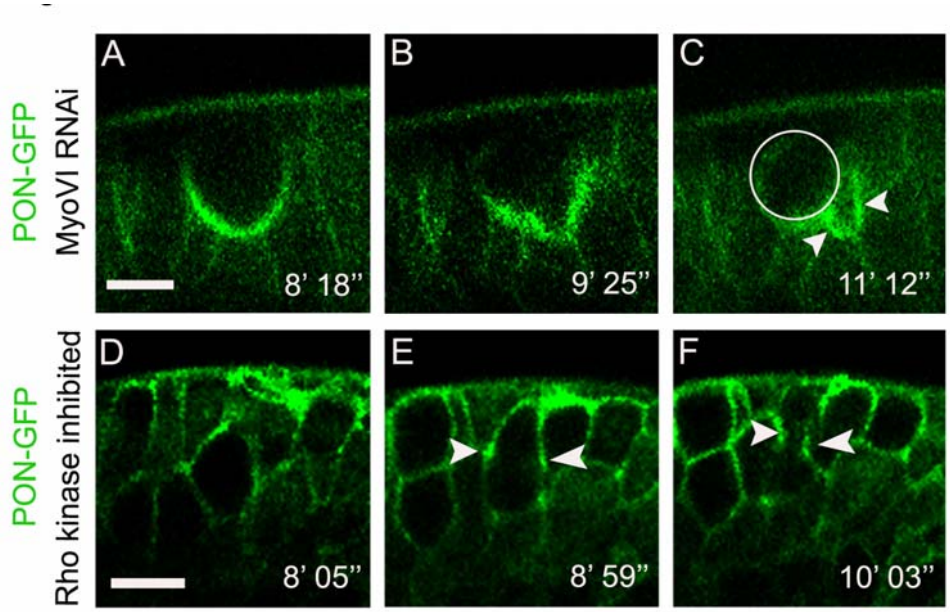

Figure 18: Localization of PON-GFP in embryos with reduced myosin activity.

(A-F) Localization of PON-GFP was examined by time-lapse microscopy. Scale bars represent 5µm.

(A-C) Albeit reduced Myosin VI activity resultes in spindle misorientation by 90°C (C), PON is still restricted to a basal crescent (B, C).

(D-F) PON-GFP is mislocalized to the cortex (D) throughout mitosis and concentrates at the cleavage furrow (E, F, arrows) in neuroblasts where Myosin II is inhibited.

6.1.3.7 The N-terminal 300 Amino Acids of Miranda are Required for Interaction with the Cortex

Miranda is a modular scaffolding protein with distinct functional domains (3.3.2.3). The N-terminus is required for cortical and asymmetric localization of Miranda. The N-terminal 298 amino acids of Miranda are sufficient to interact directly with Myosin VI *in vitro* (Petritsch et al., 2003). Here, the N-terminal localization domain was dissected into smaller functional subdomains to identify a minimal motif for asymmetric localization. Earlier studies of Miranda mutants expressing Miranda protein shorter than 300 amino acid have been hampered by the low abundance of these truncated proteins (Fuerstenberg et al., 1998; Matsuzaki et al., 1998). To circumvent low expression levels, transgenic flies were generated expressing truncated versions of the asymmetric localization domain of Miranda fused to GFP under control of the UAS/*prospero*-GAL4 in neuroblasts. As previously shown, the N-terminal 400 amino acids of Miranda interact with the cortex and form a basal metaphase crescent in 57 % of metaphase neuroblasts (Miranda-1; Figure 19 A,B,C). Contrary to published results (Fuerstenberg et al., 1998; Shen et al., 1998) the first 300 amino acid of Miranda N-terminus are not sufficient for its asymmetric localization. Miranda-2 (Figure 19 B, aa 1-300) localizes

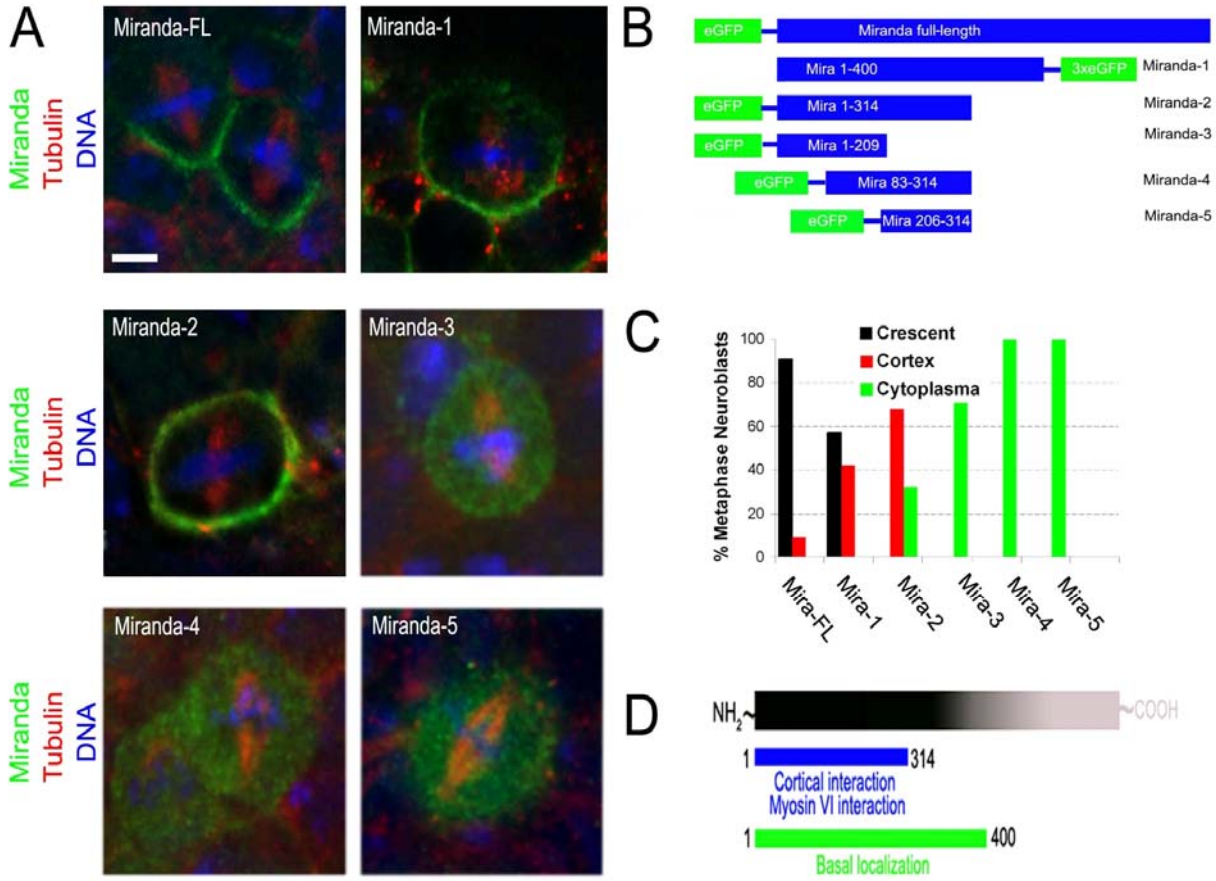

Figure 19: Cortical interaction of Miranda protein is mediated by its first 300 amino acids.

(A-C) Deletion analysis of the Miranda N-terminus in transgenic embryos expressing truncated versions of Miranda driven by *scabrous*-GAL4 and *prospero*-GAL4, respectively. Miranda-GFP fusion proteins were detected by anti-GFP antibody staining of fixed transgenic embryos. Full length Miranda fused to GFP recapitulates normal asymmetric Miranda localization in metaphase neuroblasts (A). The N-terminal 400 amino acids (Miranda-1) are also sufficient for crescent formation (A). The N-terminal 300 amino acids (Miranda-2) are insufficient for proper Miranda localization to a metaphase crescent (A), but merely mediate cortical interaction. Additional deletion of peptides from Miranda-2 either on the N-terminal or C-terminal side result into a fully cytoplasmic localization (Miranda-3, -4 and -5). Scale bar represents 5 µm.

(B) Schematic of truncated Miranda transgenes fused to GFP either on the N-terminus (Miranda- 2, -3, -4 and -5) or on the C-terminus (Miranda-1).

(C) Quantification of mislocalization of truncated Miranda protein in metaphase neuroblasts. 90% of Miranda full length localizes properly to a basal metaphase crescent, while only 57% of Miranda-1 and no Miranda-2 display normal basal protein localization. Fragments shorter than 300 amino acids are cytoplasmic suggesting that amino acid 200-300 are critical for proper cortical interaction.

(D) Scheme of cortical and asymmetric localization domains within the Miranda N-terminus.

uniformly around the cortex in the majority of metaphase neuroblasts (68 %, Figure 19 A,C) or to the cytoplasm (32%; Figure 19 A,C). This suggests that the area between aa 300 to 400 substantially contributes to asymmetric protein localization. Alternatively, the complete N-terminal 400 amino acids might be required for its asymmetric localization. Transgenic strains expressing Miranda-3 (Figure 19 B, aa 1-209), Miranda-4 (Figure 19 B, aa 83-204) and Miranda-5 (Figure 19 B, aa 206-314), respectively, display Miranda-GFP localization solely in the cytoplasm (Figure 19 A), similar as observed in embryos with reduced Myosin VI activity. This demonstrates that amino acids 1-300 are sufficient but also essential for cortical interaction of Miranda (Figure 19 D). Our data also infer that the N-terminal Myosin VI binding domain of Miranda which lies within amino acid 1-300 needs to be intact to mediate proper interaction of Miranda with the cortex and strengthens the hypothesis that Myosin VI brings Miranda to a cortical anchor.

6.2 Miranda is Required for Embryonic Development

Zygotic Miranda is important for the asymmetric cell division of neuroblasts. Analysis of several Miranda mutations encoding a series of C-terminally truncated proteins revealed perturbed cellular morphology (Ikeshima-Kataoka et al., 1997; Fuerstenberg et al., 1998). In homozygous embryos neuroectodermal cells are irregular sized and spaced, neuroblasts are elongated. In embryos heterozygous for any of the Miranda mutations cell morphology is normal demonstrating that wild-type Miranda protein can rescue the phenotype (Fuerstenberg et al., 1998). Analysis of Miranda mutations allowed discovering that the lack of Miranda function has an effect on CNS development. In *miranda* mutants where Prospero fall off the cortex, axon tracts are grossly defective, longitudinal connectives are generally either broken or severely reduced in width and commissures are often partially or completely fused (Ikeshima-Kataoka et al., 1997). *miranda* ^{ZZ176} represents a “loss of function” allele. A 169bp deletion causes a frame shift followed immediately by a stop codon. This produces a truncated protein containing the N-terminal 446 amino acids but lacking the C-terminal 384 amino acids, including the Prospero binding domain (Ikeshima-Kataoka et al., 1997; Matsuzaki et al., 1998). Since *miranda*^{ZZ176} is homozygous lethal the generation of germline clones displays the only possibility to examine the role of Miranda during early development.

6.2.1 Underlying Genetic Mechanism: The FLP/FRT System

Mosaic flies consist of two types of cells, somatic cells which are heterozygous for a mutation, therefore are viable and homozygous mutant germline cells to eliminate maternal contri-

bution (Perrimon, 1998). Using the yeast site-specific recombination FLP/FRT system (Golic and Lindquist, 1989) in combination with cell markers (Xu and Rubin, 1993), non-recombinant cells can be readily identified (Figure 20). To control the induction of mitotic recombination at specific stages a FLP (flippase) recombinase is mostly expressed under the control of a heat shock promoter (heat-shock flippase (hs-flp)) (Theodosiou and Xu, 1998). Although hs-flp lacks spatial control, one can sometimes choose heat shock window to favor the generation of clones in desired cell type. Only cells undergoing active proliferation are likely to be targets for mitotic recombination (Lee et al., 1999).

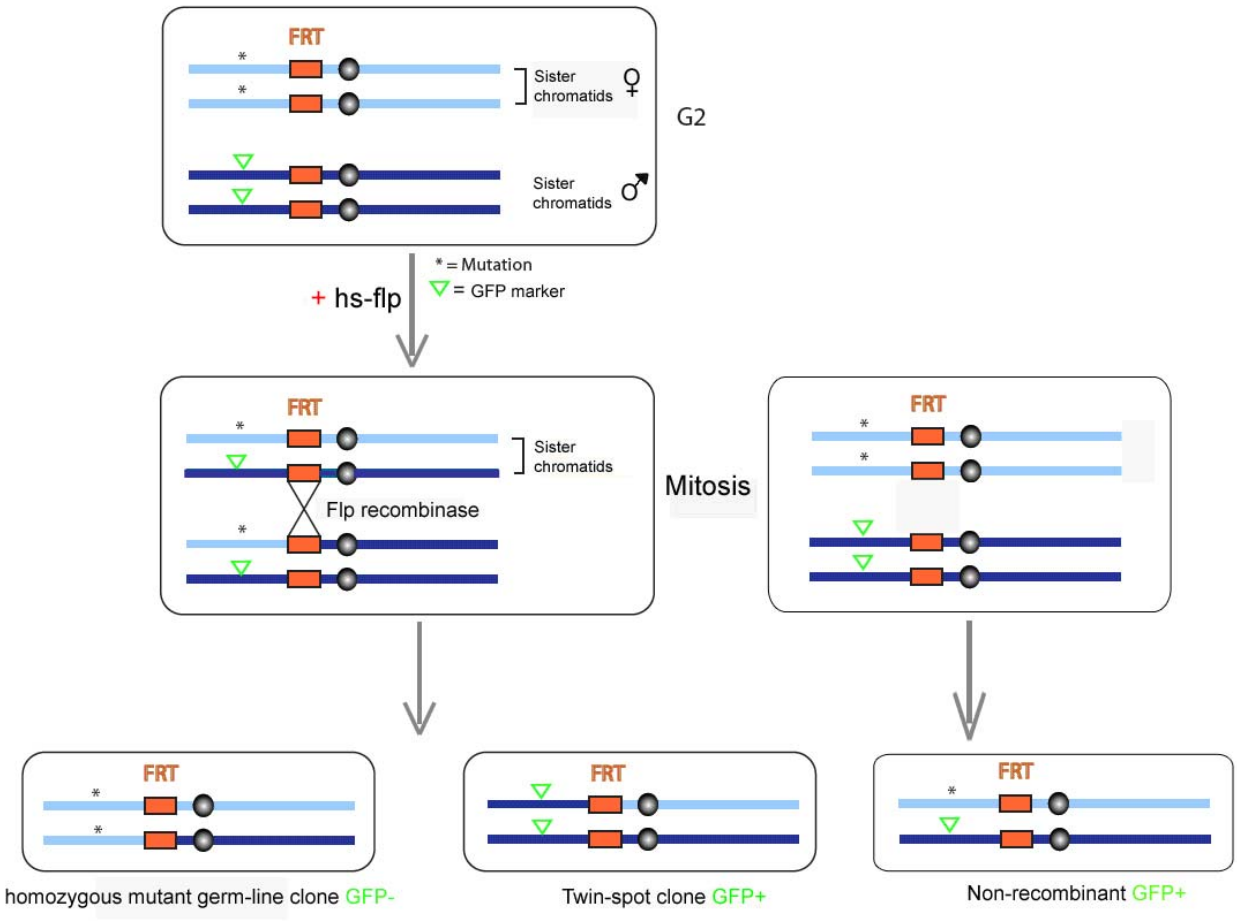

Figure 20: The FLP/FRT system to generate germline clones.

Flp recombinase mediates recombination between Flp target sites (FRT) on homologues chromosomes during mitosis. This site-specific recombination can be used to make the region that lies distal to the FRT site homozygous for a lethal mutation. A heat shock promoter (hs-flp) restricts recombination to germline cells. The homozygous mutant germline clone can be detected by the absence of GFP expression.

The FLP recombinase mediates site-specific recombination between two flippase recognition target (FRT) sites located at identical positions on homologue chromosomes because homolog chromosomes are paired in mitotic cells in *Drosophila*. The tissue that develops during expression of the FLP recombinase becomes homozygous for the region of the chromosome arm that lies distal to the FRT side. The embryos from the homozygous mutant germ-line clones can be selected by the absence of maternal GFP and screened for phenotypes (St Johnston, 2002).

6.2.2 Cross Breeding to Generate *miranda*^{ZZ176} Germline Clones

To perform crosses virgins of *miranda*^{ZZ176} balanced and holding a Flp recombinase under the control of a heat shock promoter (hs-flp) were crossed against males with the FLP recognition sequence on the same position (82B) but instead of the Miranda allele depicting a GFP marker (nuclear localization signal (nls) GFP) (Figure 21). Since germ cells begin their development during the second instar larvae F1 embryos were heat shocked for 1 hr at 37°C in the water bath to induce recombination. Due to recombination between FRT sites, embryos homozygous in the nurse cells for the Miranda mutation do not provide any functional Miranda to their progenies ("maternal contribution"; see also 3.1.3). Hatched F1 flies were sorted due to the sex and the absence of the dominant marker Stubble (Sb) and Tubby (Tb) (5.3.2.3) localized on the balancer chromosomes. Therefore, only virgins holding the FRT sites were backcrossed against males heterozygous for the *miranda*^{ZZ176} mutation, balanced over "Krüppel-GFP" (KrG4GFP). F2 embryos without any GFP do not get any functional Miranda.

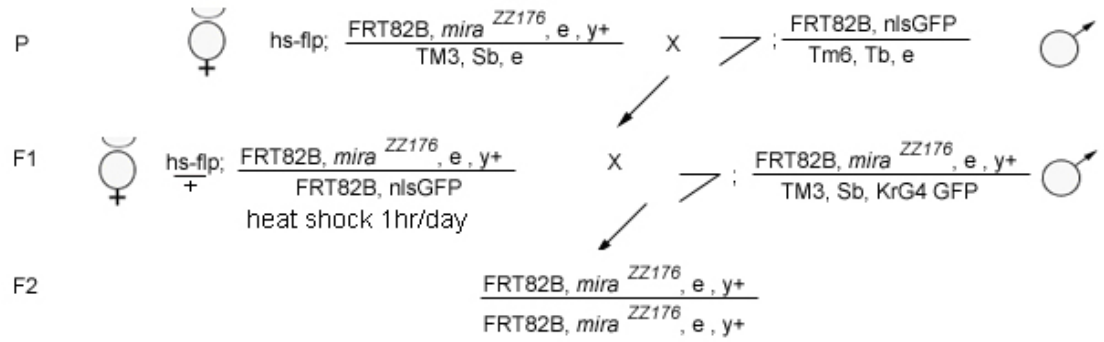

Figure 21: Crossing sheme for Miranda germline clones.

Virgins and males heterozygous for the *miranda* ^{ZZ176} mutation (*mira* ^{ZZ176}) were crossed. F1 flies were selected in absence of the dominant marker Stubble (Sb) and Tubbey (Tb). Selected F1 virgins were backcrossed against

males hereozygous for *mira* ^{ZZ176}. F2 embryos homozygous for the mutation were selected due to the absence of GFP and anlysed for phenotypes. Recombination between two FRTsides is controlled by a heat shock promoter (hs-flp).

6.2.3 Phenotype of *miranda*^{ZZ176} Germline Clones

miranda^{ZZ176} germline clones exhibit a strong phenotype: anterior-posterior (A/P) as well as dorsal-ventral (D/V) axes of the embryo are not defined (Figure 22 A,B). Compared to wild type embryos of the same age, the body shape of germline clones is modified.

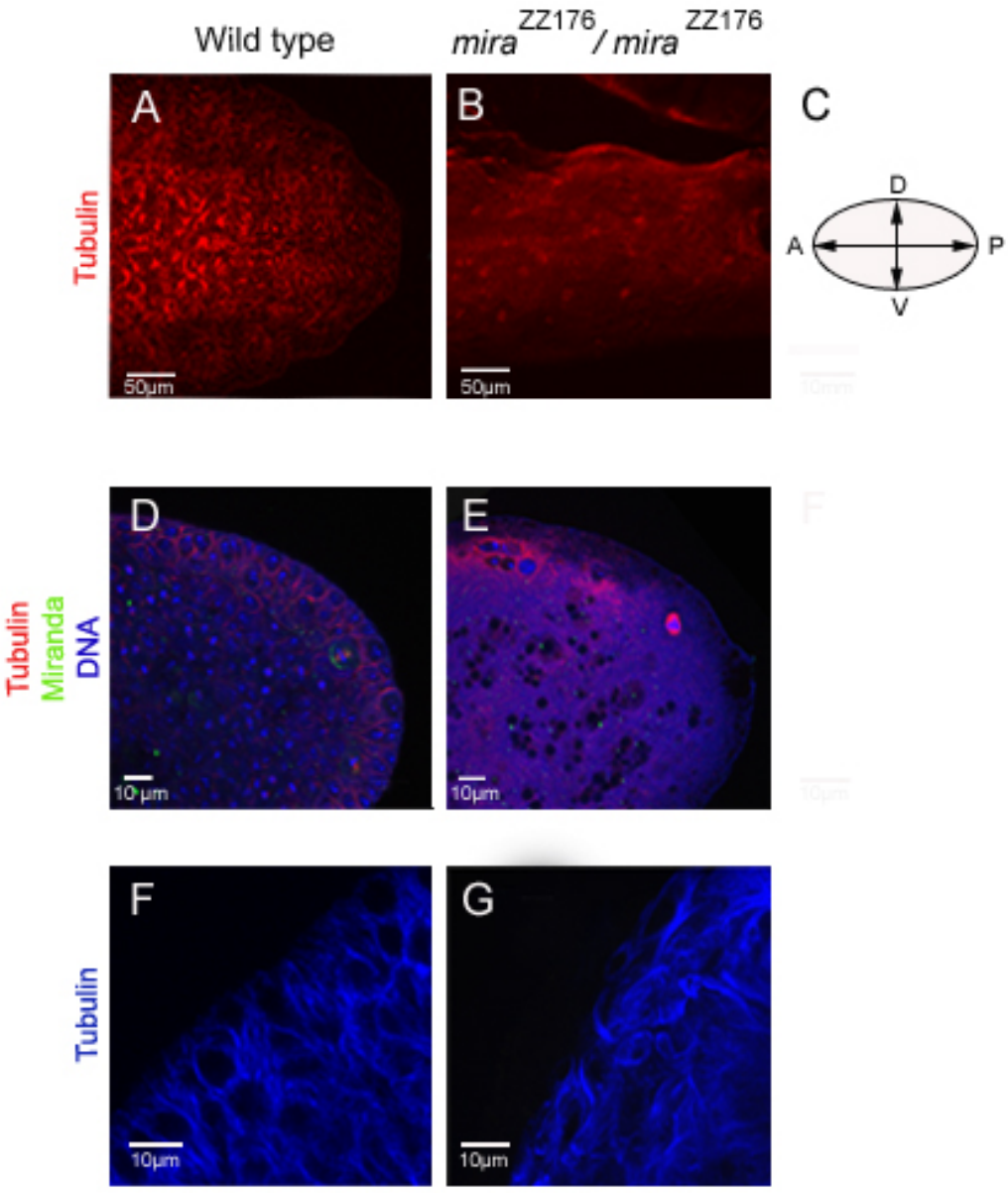

Figure 22*: miranda* ^{ZZ176} germline clones exhibit a strong phenotype.

(A-G) Stage 9-12 embryos were fixed, stained, and analyzed by confocal microscopy. (C) Anterior (A) is left, posterior (P) right, dorsal (D) up and ventral (V) down.

(A,D,F) Compared to wild type embryos *miranda*^{ZZ176} germline clones exhibit abnormalities concerning axis determination (B), cell morphology and spindle formation (F,G).

Posterior side of the embryo, rounded in wild type embryos (Figure 22 A), appears frayed and wavy in Miranda germline clones (Figure 22 B). As already observed for several *miranda* mutations single cell morphology is disturbed (Fuerstenberg et al., 1998). In wild type embryos, neuroectodermal cells show a stereotype columnar morphology (Figure 22 D,F). Strikingly in *miranda*^{ZZ176} germline clones epithelial cells and their spindle are strongly enlarged (Figure 22 E,G). Microtubules either show erratic patterning (Figure 20 G) or form clumps (Figure 20 E). These observed abnormalities depict the fundamental role of Miranda during early embryogenesis.

6.3 Regulation of Miranda Localization by Post-Translational Modifications

Since several kinases are involved in neuroblast division, it is quite conceivable that localization, degradation, or cargo binding of Miranda is regulated by phosphorylation. Atypical protein kinase C (aPKC) phosphorylates the cortical protein Lethal giant larvae (Lgl) and thereby alters the affinity of Lgl to the cortex (Betschinger et al., 2003). Interestingly, overexpression of a dominant negative form of aPKC results into a more severe phenotype than expression of non-phosphorylatable mutant of Lgl, leaving Miranda cytoplasmic (Betschinger et al., 2003). This implies that aPKC phosphorylation of more than the already identified sites within Lgl are crucial for proper asymmetric localization of Miranda. One possible scenario to explain the more sever phenotype obtained with the mutant of aPKC is that Lgl has additional, yet unidentified aPKC phosphorylation sites. Alternatively, aPKC phosphorylation of additional proteins, which regulate Miranda transport such as myosins or Miranda itself, might be necessary for proper basal transport of the protein. There are several putative consensus sites for aPKC phosphorylation present in Miranda. Additionally Miranda exhibits 6 putative cell cycle kinase CDC2 and 2 putative tyrosine phosphorylation sites.

Asymmetric protein localization is linked to mitosis. Inscuteable, exclusively expressed in neuroblasts, is proper localized only if CDC2 is functional (Tio *et al.*, 2001). Proper apical Inscuteable localization is necessary for apical-basal spindle orientation in neuroblasts (Kraut and Campos-Ortega, 1996; Kraut et al., 1996; Li et al., 1997). Since CdC2 is not phosphorylating Inscuteable (Knoblich et al., 1999; Tio et al., 1999). Miranda could be

a substrate for CDC2. An additional kinase, Rho-kinase kinase, is required for proper Miranda localization. Phosphorylation of the regulatory light chain (RLC) of Myosin II on serine 21 and threonine 20 induces a conformational change. Thereby Myosin II assembles into bipolar filaments and ATPase activity is increased (Tan et al., 1992). Rho-kinase kinase also inhibits myosin phosphatases, thereby preventing dephosphorylation of the RLC (Kimura et al., 1996). Reduced Rho-kinase kinase activity results in Miranda mislocalization. In metaphase neuroblasts Miranda is uniformly cortical and is not restricted to a basal crescent (Barros et al., 2003). Since there are several putative consensus sites for phosphorylation present in Miranda (Figure 23) it was tested whether Miranda is phosphorylated in embryonic extracts by using phosphospecific antibodies in immunoblots on immunoprecipitated Miranda.

MSFSKAKLKRFNDVDVAICGSPAASNSSAGSAGSATPTASSAAAAPPTVQPERKEQIEKFFKDAVRFASSSKEAK
EFAIPKEDKKSKGLRLFRTPSLPQRLRFRPTPSHTDTATGSGSGASTAASTPLHSAATTPVKEAKSASRLKGKEA
LQYEIRHKNELIESQLSQLDVLRRHVDQLKEAEAKLREEHELATSKTDRLIEALTSENLSHKALNEQMGQEHADL
LERLAAMEQQLQQQHDEHERQVEALVAESEALRLANELLQTANEDRQKVEEQLQAQLSALQADVAQAREHCSLEQ
AKTAENIELVENLQKTNASLLADVVQLKQQIEQDALSYGQEAKSCQAELECLKVERNTLKNDLANKCTLIRSLQD
ELLDKNCEIDAHCDTIRQLCREQARHTEQQQAVAKVQQQVESDLESAVEREKSYWRAELDKRQKLAENELIKIEL
EKQDVMVLLETTNDMLRMRDEKLQKCEEQLRNGIDYYIQLSDALQQQLVQLKQDMAKTITEKYNYQLTLTNTRAT
VNILMERLKKSDADVEQYRAELESVQLAKGALEQSYLVLQADAEQLRQQLTESQDALNALRSSSQTLQSEVSLKE
SLLHELLAGEAETLAKFNQIANSFQERIDGDAQLAHYHELRRKDETREAYMVDMKKALDEFATVLQFAQLELDNK
EQMLVKVREECEQLKLENIALKSKQPGSASLLGTP KANRSNTTDLEKIEDLLCDSELRSDCEKITTWLLNSSDK
CVRQDTTSEINELLSAGKSSPRPAPRTPKAAPHTPRSPRTPHTPRTPRSAASTPKKTVLFAGKENVPSPPQKQVL
KARNI

Figure 23: Miranda exhibits several putative consensus sited for phosphorylation.

Amino acids are designated with the common single letter code, X represents an arbitrary amino acid. Putative consensus sites are highlighted in color: CDC2 (S-X-R/K) (red), aPKC (T/S-P) (green) and tyrosine kinase sites (blue).

6.3.1 Miranda Encodes Four Isoforms

The *miranda* gene produces two different transcripts probably due to alternative splicing. The long form, which is 2956 nucleotides in length, encodes a protein with 830 amino acids. The short form has the same sequence apart from a 90-nucleotide internal deletion and encodes a protein with 800 amino acids (Shen et al., 1997). Anti-Miranda antibodies were used to extract protein complexes from *Drosophila* embryos (5.7.2.2). Subsequently samples were analyzed by SDS-PAGE and Western blotting (5.7.3). As already observed and identified by mass spectrometry (Petritsch et al., 2003) a quadruplet of Miranda isoforms is reproducibly immunoprecipitated (Figure 24, asterisk). As a control rabbit preimmune serum was added in excess (PreIS; 50 kDa band) and did not reveal any signal. Since phosphorylation increases the molecular weight of a protein, it results in a slower mobility in SDS-PAGE. Thus, the

duplet could represent phosphorylated and unphoshorylated forms of the short or long isoform of Miranda, respectively.

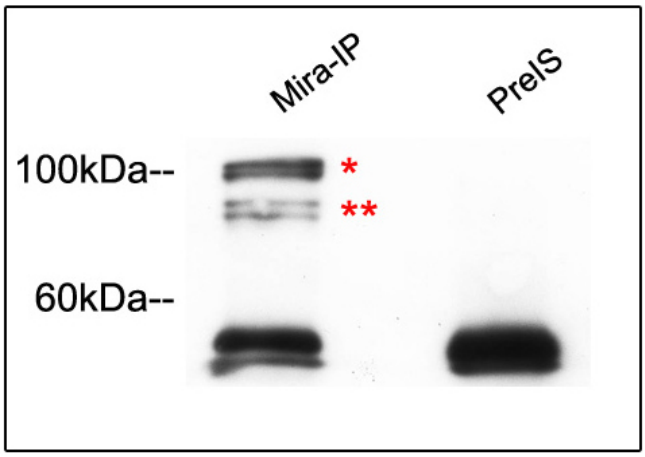

Figure 24: Miranda specifically immunoprecipitates.
Protein extracts from stage 5-15 embryos were subjected to immunoprecipitation with affinity purified anti-Miranda antibody (Mira-IP) or rabbit preimmune serum (PreIS). Western blots were probed with anti-Miranda antibody, revealing four specific Miranda isoforms between 80-100 kDa representing the long (830 aa asterisk) and the short (800 aa double asterisk) Miranda protein, and probably their phosphorylated isoforms. 50 kDa bands show the amount of antibody/PreIS used in the IP.

6.3.2 Miranda is Phosphorylated *In vivo*

Miranda was immunoprecipitated with an affinity purified Miranda antibody as described above (6.3.1). Immunoblots were probed with anti-phosphoserine, anti-phosphotyrosine, or anti-phosphothreonine to narrow down the putative phosphorylation sites of Miranda (Figure 25). The experiments revealed that Miranda is phosphorylated on all three residues *in vivo*. A phospho-specific Miranda signal is reproducibly detected. As expected preimmunserum (PreIS) does not precipitate any Miranda protein, indicating specificity of the Miranda antibody used for precipitation. As another control protein-A sepharose beads were treated with calf intestine alkaline phosphatase (CIAP) which almost diminishes the phosphospecific signal in the anti-Miranda immunoprecipitate. To investigate the physiological relevance of the identified phosphorylation all putative phosphorylation sites (Figure 23) need to be mutated.

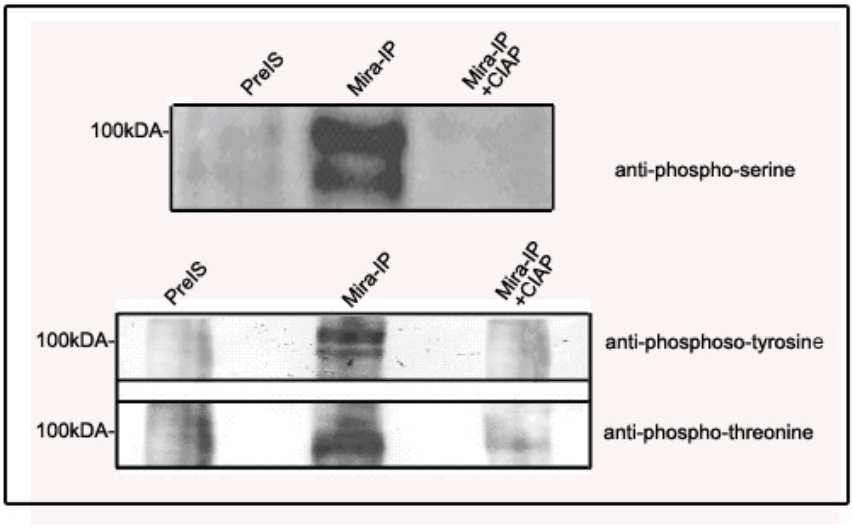

Figure 25: Miranda is phosphorylated on serine, tyrosine, and threonine.

Protein extracts from stage 5-15 embryos were subjected to immunoprecipitation with rabbit preimmune serum (PreIS) or affinity purified anti-Miranda antibody (Mira-IP). Treatment of protein-A sepharose beads with calf intestine alkaline phosphatase (CIAP) reduces the phosphospecific signal in the anti-Miranda immunoprecipitate. Western blots were probed with anti-phosphospecific antibodies.

7 DISCUSSION

7.1 Miranda Moves via the Cytoplasm to the Basal Side of the Cell

Miranda and PON are adaptor proteins for cell fate determinants regulating asymmetric cell division (ACD) in *Drosophila* neuroblast (Shen et al., 1997; Lu et al., 1998). Both proteins show dynamic localization, resulting in a metaphase crescent at the basal side of the cell and are asymmetrically inherited by the ganglion mother cell (GMC) only. Here it was shown for the first time, that that Miranda and PON take different routes to translocate to the basal crescent. In neuroepithelial cells and neuroblasts Miranda moved dynamically from the apical to the basal side of the cell via the cytoplasm, whereas PON localized exclusively cortical (Figure 12). This indicates that in *Drosophila* neuroblasts the localization of the two protein complexes (PON/Numb and Miranda/Prospero/*prospero*mRNA/Staufen/Brat) are regulated differently.

To assure that the "cytoplasmic cloud" was not an artifact due to overexpression different GAL4 lines were tested which all revealed identical results (data not shown). Protein expression, analyzed by western blot, reveales similar levels for endogenous Miranda and Miranda-GFP (Figure 26), indicating that Miranda-GFP reflects the localization of wild type protein. Moreover, cytoplasmic Miranda was detected in immunostainings of wild type embryos (Figure 27) as well.

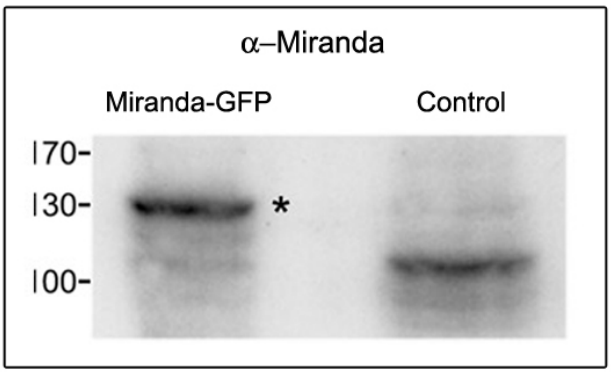

Figure 26: Miranda expression levels.

Immunoblots using a Miranda antibody reveal that the 130 kDa band (asterisk) representing Miranda-GFP is expressed specifically and at similar levels as endogenous Miranda (100 kDa, control lane).

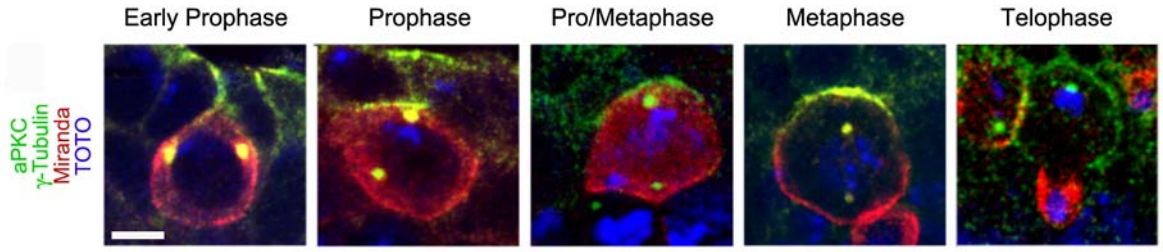

Figure 27: Miranda localization in wild type neuroblasts.

Miranda protein shows dynamic localization during neuroblast mitosis. Wild type embryos were fixed and stained with anti-Miranda (red), anti-aPKC (green) and anti-γTubulin (green) antibodies. DNA is blue. The scale bar is 5 µm. Projections of confocal sections are shown. Miranda spreads the entire cytoplasm in pro/metaphase neuroblasts and localizes as a tight basal crescent in metaphase.

The cytoplasmic phase of Miranda/Proteins observed in neuroblasts of the CNS may have a more general relevance: In *Drosophila* sensory organ precursor cells (SOP) of the PNS (Mayer et al., 2005) observed cytoplasmic pools of PON and NUMB. In *C. elegans*, directed by the conserved Par proteins, a polarized cytoplasmic flow moves P granules to the posterior cortex of the zygote (Cheeks et al., 2004). Par proteins, expressed in neuroblasts, are part of a conserved machinery for polarizing cells in *C. elegans*, *Drosophila, Xenopus*, and mammals (Solecki et al., 2006).

7.2 PON and Miranda Localization are Differently Regulated

Miranda was shown to interact with Numb *in vitro* (Shen et al., 1997) suggesting that they might indeed be in one complex with PON, which is a regulator of Numb localization. However, this interaction could be transient and restricted to their colocalization in the metaphase crescent. Additionally, asymmetric localization of Miranda in *numb* mutants is indistinguishable from that in wild-type embryos (Shen et al., 1997) and localization of Numb is not affected in *miranda* mutants (Ikeshima-Kataoka et al., 1997). Both findings argue against a functional interaction of Miranda and Numb. Myosin II and Myosin VI are both required for asymmetric localization of Miranda (6.1.3.5). It was unknown whether these myosins both regulate PON localization (6.1.3.6). In embryos lacking Myosin II, PON is improperly localized uniformly around the cortex and prevented from forming a basal crescent. Therefore PON-GFP becomes not asymmetrically segregated (Figure 18). This suggests that PON localization, similar to Miranda localization requires fully functional Myosin II. In neuroblasts with reduced Myosin VI activity PON, however, is still forming a basal metaphase crescent overlying the basal spindle pole (Figure 18). This indicates that PON localization, different

from Miranda localization, does not depend on Myosin VI. In addition to the localization pattern of PON and Miranda, the differences concerning Myosin VI activity strongly support the hypothesis of two different basal protein complexes in *Drosophila* neuroblasts. However, the localization of PON and Miranda also shows similarities. Asymmetric protein localization of both proteins does neither depend on asymmetrically localized RNA nor on local protein degradation (Figure 14, 15) (Lu et al., 1999).

7.3 *miranda* mRNA and the ER are Asymmetrically Inherited in *Drosophila* Neuroblasts

To test whether *miranda* mRNA is localized to the basal pole prior to Miranda protein contributing to basal Miranda protein localization, *in situ* hybridizations were performed using a Miranda-specific probe (Figure 14). While Miranda protein is apical and cytoplasmic in prophase before forming a basal metaphase crescent and being inherited by the ganglion mother cell only, *miranda* mRNA remains apically concentrated throughout the cell cycle and becomes inherited by the neuroblast daughter only (Figure 14). The data shown confirm earlier studies showing that *miranda* mRNA is apically localized and extend these studies by demonstrating that *miranda* mRNA remains apically localized as the cell undergoes cytokinesis whereby the RNA become inherited by the apical neuroblast daughter only. Thus *miranda* mRNA localization is not reflecting Miranda protein localization suggesting that they are independent from each other. In addition to Miranda *inscuteable* mRNA has been shown to become apically localized in neuroblasts (Hughes et al., 2004), which supports the stability of the apical protein complex with Pins, Gαi and Par proteins. While the Egalitarian/BicaudalD/dynein complex is required for apical localization of *inscuteable* mRNA, it is not necessary for *miranda* mRNA localization suggesting that different mechanism apply for the localization of these RNAs. It will be interesting in the future to determine the function of *miranda* mRNA localization, whether it depends on the apical complex and whether other motor proteins are required to establish this asymmetric localization. It has been shown earlier that *prospero* mRNA is localized to the basal side due to its association with the Miranda/Staufen complex which is supposed to serve as a back-up pool for Prospero protein perhaps in ganglion mother cells (Broadus et al., 1998). These data suggest that RNA localization do play a role during neuroblast division but are not as essential as localization of their encoded proteins.

The cortical endoplasmatic reticulum (ER) in yeast *S. cerevisiae* like the peripheral ER in mammalian cells undergoes tubular branching movements. It has been shown that ER tu-

bules become aligned along the mother-daughter axis during budding and are localized to the bud along polarized actin filaments by a Myosin V motor activity (Estrada et al., 2003). Although the structure and the dynamics of the ER vary between organisms its interaction with the cytoskeleton is consistent (Bannai et al., 2004). Interestingly, in the early *C. elegans* embryo the ER is asymmetrically localized by the Par proteins and shows dynamic localization (Poteryaev et al., 2005). In order to investigate the nature of the cytoplasmic movement of Miranda in pro/metaphase neuroblasts, localization of ER was determined during neuroblast division and found to remain apically concentrated and inherited mainly by the neuroblast daughter (Figure 13). Thus, Miranda transport occurs independently of ER dynamics in *Drosophila* neuroblasts.

7.4 Apical Degradation does not Contribute to Dynamic Miranda Localization

As an alternative explanation to active transport of the Miranda complex to the basal cortex, the importance of the proteasome and localized degradation on the apical cortex was investigated. In cell cycle mutant backgrounds, PON-GFP is mislocalized indicating that cell cycle events control cortical recruitment of PON at the entry of mitosis and the disassembly of PON crescent at the exit of mitosis (Lu et al., 1999). However, it was not determined whether the anaphase-promoting complex, some ubiquitin ligase, or components of the mitosis exit-signaling pathway are involved in disintegration of PON-GFP. Proteasome activity was specifically reduced in neuroblasts, however Miranda localization was not defect (6.1.3.3). As a control, Cyclin B, typically degraded during anaphase by the anaphase-promoting complex was enriched in telophase demonstrating function of the system (Figure 15). An intact proteasome has not been found to be necessary for Miranda localization under the conditions tested. These data argue that Miranda protein is being re-localized within the dividing neuroblast from the cytoplasm to the basal cortex and is not apically degraded by the proteasome.

7.5 Miranda Localization is Regulated by Diffusion, Myosin II, and Myosin VI

Time-lapse analysis of Miranda localization in the absence of Myosin II or Myosin VI allowed us to determine at which step during mitosis myosin activity is required to localize Miranda protein and go beyond earlier analysis of Miranda localization in fixed tissues (6.1.3.5). When Myosin II is inhibited by chemical inhibition of Rho-kinase kinase, Miranda is mislocalized uniformly around the cortex and not restricted to an apical crescent,

suggesting that Myosin II activity is required already prior to metaphase in prophase to exclude it from the baso-lateral cortex (Figure 17) but also in pro-metaphase to release Miranda to the cytoplasm. These data support and extend earlier studies (Barros et al., 2003) showing Miranda mislocalization uniformly around the cortex in metaphase when Myosin II was inhibited in neuroblasts from fixed embryonic tissue. Myosin II forms a complex with Miranda in embryonic extracts (Petritsch et al., 2003) and this might reflect the interaction of the two proteins in interphase and early prophase since at later stages they localize almost exclusively (Barros et al., 2003). Interestingly, recent data have shown that Myosin II itself is phosphorylated and inhibited by atypical PKC zeta in mammalian cells (Even-Faitelson and Ravid, 2006). However, a direct role of aPKC in inhibition of Myosin II activity has not been investigated in *Drosophila* neuroblast.

How is Myosin VI achieving cortical localization of Miranda? Myosin VI is a unique myosin because unlike most other myosin motors it moves *in vitro* towards pointed ends of actin filaments. Currently two major functions of Myosin VI are being discussed: It appears to be a cargo motor during the endocytic process due to its interaction with endosome vesicles (Buss et al., 2001; Aschenbrenner et al., 2003) and the ability of Myosin VI dimers to move processively in large steps *in vitro* (Park et al., 2006). Monomeric Myosin VI, however, is nonprocessive and it is currently unclear whether Myosin VI acts as a monomer or a dimer in a specific function. During sperm individualization in *Drosophila* Myosin VI also seems to act by binding of Myosin VI heads to actin for minutes and stabilizing actin at the cone front (Noguchi et al., 2006). A role for Myosin VI in anchoring cargo is supported by earlier data showing that cargo load slows Myosin VI kinetics (Scholz et al., 2005). Myosin VI is localized to particles mainly to the cytoplasm in *Drosophila* neuroblasts which accumulate in the basal half of the metaphase neuroblast coinciding in time and space with basal localization of Miranda (Petritsch et al., 2003). The FRAP analysis of Miranda protein kinetics in the cytoplasm suggest that Miranda is diffusing rather than being actively transported throughout the cytoplasm (Figure 16). Since Myosin VI itself does not form a tight basal crescent (Petritsch et al., 2003) and shows mainly cytoplasmic localization it is likely that Myosin VI takes Miranda from the cytoplasm to the cortex, where it is anchored by an unknown mechanism. Future studies of Myosin VI dynamics in dividing neuroblasts should address this question. While the search for homologues of asymmetrically localized proteins in mammalian stem cells is only beginning, researchers already dissect the molecular details of ACD in *Drosophila*. It will be interesting to study the degree of conservation of these mechanisms across species in the future.

7.6 Model of Miranda Localization

Based on published findings and the results presented above, following model of Miranda localization is proposed: Miranda is translated at the apical side of the neuroblast and assembles in a complex with Staufen and *prospero* mRNA, Prospero and perhaps Brat (Figure 28 A; Miranda complex). During late prophase Myosin II is activated on the apical side and mobilizes Miranda to the cytoplasm, excluding it from the apical cortex. In the cytoplasm, the Miranda complex diffuses three-dimensionally (Figure 28 B) and becomes captured by Myosin VI in the basal half of the metaphase neuroblast. Myosin VI either directly transports Miranda to a cortical anchor or provides a cytoplasmic anchor function to facilitate the interaction of Miranda with a basal cortical anchor (Fig 28 C). Different from Miranda, PON stays cortical during neuroblast mitosis (Figure 28 A-C). Since localization and regulation of Miranda and PON exhibit striking differences, it is likely that two protein complexes in *Drosophila* neuroblasts exist: PON/Numb and Miranda/Prospero/*prospero*mRNA/Staufen/ Brat.

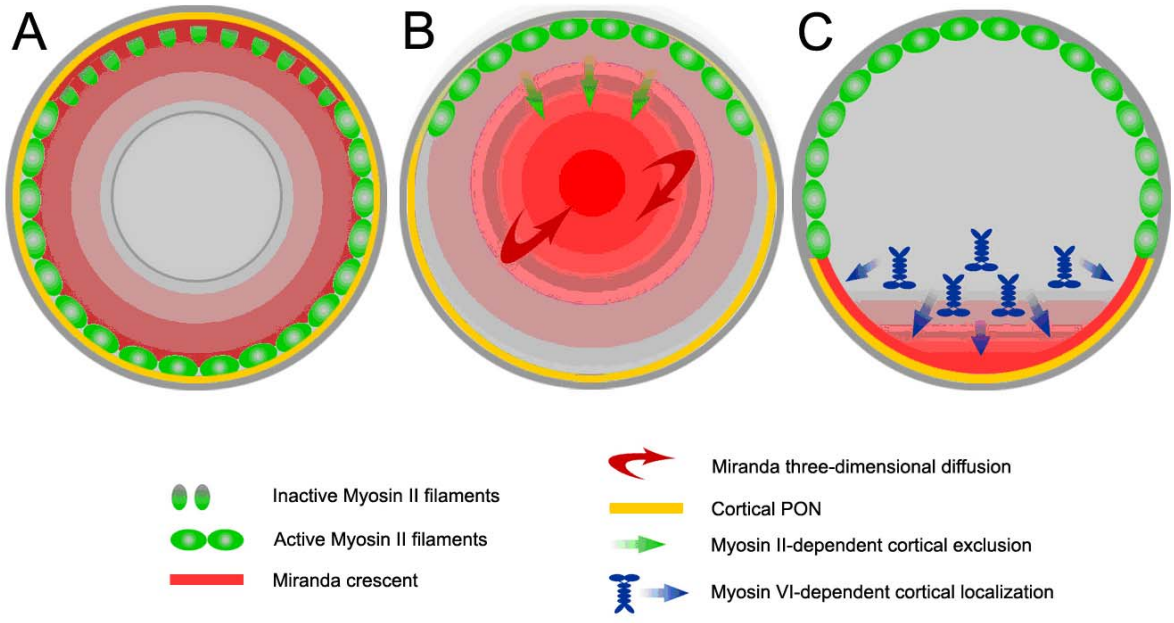

Figure 28: Model of Miranda localization by diffusion and myosin motors of opposite polarity.

7.7 Miranda is Essential During Early Embryogenesis

Miranda localizes asymmetrically in neuroectodermal epithelial cells and neuroblasts (Matsuzaki et al., 1998). Investigation of several Miranda mutations showed that Miranda is required for proper development of the CNS (Ikeshima-Kataoka et al., 1997). To overcome

maternal contribution which can mask the effect of mutations until stage 11 here, for the first time, Miranda germline clones were generated (6.2). The resulting embryos exerted severe defects in axis establishment, cellular morphology, and spindle formation (Figure 22). This demonstrates the fundamental function of Miranda during embryogenesis. However, these experiments have to be repeated to make sure that the observations are related to the absence of functional Miranda rather than the fixation procedure. So far, fixation artifacts cannot completely be excluded as spindle clumps, for instance, were also observed in earlier experiments with wild type embryos. Furthermore, dark areas that can be seen in the confocal microscope on the embryo surface appear with both germ line clones and wild type embryos. Although formaldehyde fixations effectively preserve cellular morphology since the original structure has been effectively locked in (Mason and O'Leary, 1991) this procedure may at the same time modify the antigen protein in its constitution or its conformation (Montero, 2003). In the case of the spindle, formaldehyde may have altered the microtubule structure and generate the observed clumps. Despite several approaches, it has not been possible to obtain large numbers of Miranda germline clones.

7.8 Miranda Localization may be Regulated by Phosphorylation

Little is known about the biochemical modifications that regulate Miranda localization. The tight correlation between mitosis, kinases and asymmetric protein localization suggest that mitosis specific posttranslational modifications like phosophorylation may be involved in regulating protein localization in *Drosophila* neuroblasts, as shown for Prospero and Lgl (Srinivasan et al., 1998; Betschinger et al., 2003). Cortical Prospero is highly phosphorylated compared to nuclear Prospero. One- and two-dimensional western analysis and phosphatase assays revealed several phosphoisoforms of Prospero (Srinivasan et al., 1998). Similar the additional protein bands which were repeatedly immunoprecipitated (Figure 24) might be Miranda phosophoisoforms. Since Miranda is phosphorylated on serine, threonine, and tyrosine (6.3.2), it was not possible to narrow down the phosphorylation sites. This has to be determined in the future by mutation of Miranda phosphorylation sites. Since the generation of transgenic flies is time-consuming, it will be easier to switch to an *in vitro* system. The Knoblich lab (Betschinger et al., 2003) successfully used *Drosophila* S2 cells to show that phosphorylated Lgl falls of the cortex.

Asymmetric localization of tyrosine kinases has been shown for mice: The receptor tyrosine kinase EGFR is asymmetrically distributed during mitosis of cortical progenitor cells in the ventricular and subventicular zone of forebrain. Higher concentration of EGFR in-

creases the probability that the cell is differentiating into an astrocyte. EGFR and Numb are inherited by the same daughter cell (Sun et al., 2005). Miranda exhibits only two tyrosine phosphorylation sides (Figure 23). Using the QuickChange II Site-Directed Mutagenesis Kit from *Stratagene* single and double phosphor-mutants can easily be obtained for generating UAS-transgenic lines. Expressing "phospho-dead" Miranda mutants specifically in neuroblasts will demonstrate the physiological relevance. Phosphorylation of Miranda may be required for binding to cargo proteins, cortical localization, or asymmetric localization. Alternatively, phosphorylation may also be the consequence.

7.9 Relevance of ACD for Mammalian Stem Cell Biology and Cancer

Mammalian stem cells localize proteins such as Numb and Inscuteable asymmetrically but the mechanism of asymmetric cell division in mammals has not been studied on a molecular level yet. However, several homologues of the fly asymmetric cell division machinery have been analyzed, indicating that considerable mechanistic conservation exists across species. Similar as in *Drosophila,* the mammalian Gβγ subunit of the heterotrimeric G-protein complex has been shown to regulate mitotic spindle orientation and cell fate during mouse cortical neurogenesis (Sanada and Tsai, 2005). Furthermore, mammalian aPKC, Par-3 and LGN, the mammalian homolog of Pins, are thought to be involved in ACD of basal epidermal progenitor cells (Lechler and Fuchs, 2005). Recently asymmetric stem cell divisions in *Drosophila* have been linked to cancer. Several studies showed how disrupting ACD could lead to uncontrolled proliferation. Transplantation studies of *Drosophila* larval brain tissue from *pins*, *miranda*, *numb*, or *prospero* mutants into wild-type adult abdomen, revealed an 100-fold larger abdomen compared to wild-type transplants (Caussinus and Gonzalez, 2005). Larval neuroblasts proliferation in *Drosophila* is regulated by segregating the growth inhibitor Brat and the transcription factor Prospero into only one daughter cell, the GMC, where they are required to inhibit self-renewal. In *bra*t or *prospero* mutants, both daughter cells grow and behave like neuroblasts leading to the formation of larval brain tumors (Betschinger et al., 2006; Lee et al., 2006).

The underlying molecular mechanism controlling self-renewal and proliferation in *Drosophila* may have a more general relevance and may be applied to other stem cells as well. There is not much know about the putative mammalian Brat homolog Tripartite motive proteins (Trim2,3 and 32) in cellular proliferation (van Diepen et al., 2005). However, the Prospero homolog Prospero-related homeobox1 (Prox1) has a conserved function in regulating retinal progenitor cell proliferation (Dyer et al., 2003). In addition, mutations in and aber-

rant DNA methylation of *prox1* have been observed in some liver tumors and lymphomas (Nagai et al., 2003; Schneider et al., 2006). Despite the recent progress, future extensive studies will be needed to fully elucidate the link between asymmetric cell division, stem cell proliferation, and cancer. Based on *Drosophila* neural stem cells this thesis provides insight to our general understanding of how stem and progenitor cells divide.

8 References

Akam, M. (1987). The molecular basis for metameric pattern in the Drosophila embryo. Development *101*, 1-22.

Alberts, Johnson, Lewis, Raff, Roberts, and Walter (2002). Molecular Biology of the Cell, 4 edn (New York, NY 10001-2299: Garland Science).

Anderson, K. V., Jurgens, G., and Nusslein-Volhard, C. (1985). Establishment of dorsal-ventral polarity in the Drosophila embryo: genetic studies on the role of the Toll gene product. Cell *42*, 779-789.

Artavanis-Tsakonas, S., Rand, M. D., and Lake, R. J. (1999). Notch signaling: cell fate control and signal integration in development. Science *284*, 770-776.

Aschenbrenner, L., Lee, T., and Hasson, T. (2003). Myo6 facilitates the translocation of endocytic vesicles from cell peripheries. Mol Biol Cell *14*, 2728-2743.

Baker, N. E. (1987). Molecular cloning of sequences from wingless, a segment polarity gene in Drosophila: the spatial distribution of a transcript in embryos. Embo J *6*, 1765-1773.

Bannai, H., Inoue, T., Nakayama, T., Hattori, M., and Mikoshiba, K. (2004). Kinesin dependent, rapid, bi-directional transport of ER sub-compartment in dendrites of hippocampal neurons. J Cell Sci *117*, 163-175.

Barros, C. S., Phelps, C. B., and Brand, A. H. (2003). Drosophila nonmuscle myosin II promotes the asymmetric segregation of cell fate determinants by cortical exclusion rather than active transport. Dev Cell *5*, 829-840.

Bartel, P., Chien, C. T., Sternglanz, R., and Fields, S. (1993). Elimination of false positives that arise in using the two-hybrid system. Biotechniques *14*, 920-924.

Betschinger, J., and Knoblich, J. A. (2004). Dare to be different: asymmetric cell division in Drosophila, C. elegans and vertebrates. Curr Biol *14*, R674-685.

Betschinger, J., Mechtler, K., and Knoblich, J. A. (2003). The Par complex directs asymmetric cell division by phosphorylating the cytoskeletal protein Lgl. Nature *422*, 326-330.

Betschinger, J., Mechtler, K., and Knoblich, J. A. (2006). Asymmetric segregation of the tumor suppressor brat regulates self-renewal in Drosophila neural stem cells. Cell *124*, 1241-1253.

Bhat, K. M. (1999). Segment polarity genes in neuroblast formation and identity specification during Drosophila neurogenesis. Bioessays *21*, 472-485.

Brand, A. H., and Perrimon, N. (1993). Targeted gene expression as a means of altering cell fates and generating dominant phenotypes. Development *118*, 401-415.

Brand, M., Jarman, A. P., Jan, L. Y., and Jan, Y. N. (1993). asense is a Drosophila neural precursor gene and is capable of initiating sense organ formation. Development *119*, 1-17.

Broadus, J., Fuerstenberg, S., and Doe, C. Q. (1998). Staufen-dependent localization of prospero mRNA contributes to neuroblast daughter-cell fate. Nature *391*, 792-795.

Brody, T., and Odenwald, W. F. (2000). Programmed transformations in neuroblast gene expression during Drosophila CNS lineage development. Dev Biol *226*, 34-44.

Buescher, M., Yeo, S. L., Udolph, G., Zavortink, M., Yang, X., Tear, G., and Chia, W. (1998). Binary sibling neuronal cell fate decisions in the Drosophila embryonic central nervous system are nonstochastic and require inscuteable-mediated asymmetry of ganglion mother cells. Genes Dev *12*, 1858-1870.

Buss, F., Arden, S. D., Lindsay, M., Luzio, J. P., and Kendrick-Jones, J. (2001). Myosin VI isoform localized to clathrin-coated vesicles with a role in clathrin-mediated endocytosis. Embo J *20*, 3676-3684.

Cai, Y., Yu, F., Lin, S., Chia, W., and Yang, X. (2003). Apical complex genes control mitotic spindle geometry and relative size of daughter cells in Drosophila neuroblast and pI asymmetric divisions. Cell *112*, 51-62.

Campos-Ortega, J. A. (1993). Mechanisms of early neurogenesis in Drosophila melanogaster. J Neurobiol *24*, 1305-1327.

Campos-Ortega, J. A., and Hartenstein, V. (1997). The Embryonic Development of Drosophila melanogaster (Berlin and New York: Springer-Verlag).

Cant, K., Knowles, B. A., Mooseker, M. S., and Cooley, L. (1994). Drosophila singed, a fascin homolog, is required for actin bundle formation during oogenesis and bristle extension. J Cell Biol *125*, 369-380.

Carmell, M. A., and Hannon, G. J. (2004). RNase III enzymes and the initiation of gene silencing. Nat Struct Mol Biol *11*, 214-218.

Carmena, A., Murugasu-Oei, B., Menon, D., Jimenez, F., and Chia, W. (1998). Inscuteable and numb mediate asymmetric muscle progenitor cell divisions during Drosophila myogenesis. Genes Dev *12*, 304-315.

Carmena, M., Gonzalez, C., Casal, J., and Ripoll, P. (1991). Dosage dependence of maternal contribution to somatic cell division in Drosophila melanogaster. Development *113*, 1357-1364.

Caussinus, E., and Gonzalez, C. (2005). Induction of tumor growth by altered stem-cell asymmetric division in Drosophila melanogaster. Nat Genet *37*, 1125-1129.

Cavaliere, V., Taddei, C., and Gargiulo, G. (1998). Apoptosis of nurse cells at the late stages of oogenesis of Drosophila melanogaster. Dev Genes Evol *208*, 106-112.

Cayouette, M., Whitmore, A. V., Jeffery, G., and Raff, M. (2001). Asymmetric segregation of Numb in retinal development and the influence of the pigmented epithelium. J Neurosci *21*, 5643-5651.

Cheeks, R. J., Canman, J. C., Gabriel, W. N., Meyer, N., Strome, S., and Goldstein, B. (2004). C. elegans PAR proteins function by mobilizing and stabilizing asymmetrically localized protein complexes. Curr Biol *14*, 851-862.

Chia, W., and Yang, X. (2002). Asymmetric division of Drosophila neural progenitors. Curr Opin Genet Dev *12*, 459-464.

Clevers, H. (2005). Stem cells, asymmetric division and cancer. Nat Genet *37*, 1027-1028.

Cooley, L., Verheyen, E., and Ayers, K. (1992). chickadee encodes a profilin required for intercellular cytoplasm transport during Drosophila oogenesis. Cell *69*, 173-184.

Cubas, P., de Celis, J. F., Campuzano, S., and Modolell, J. (1991). Proneural clusters of achaete-scute expression and the generation of sensory organs in the Drosophila imaginal wing disc. Genes Dev *5*, 996-1008.

D'Alessio, M., and Frasch, M. (1996). msh may play a conserved role in dorsoventral patterning of the neuroectoderm and mesoderm. Mech Dev *58*, 217-231.

de-la-Concha, A., Dietrich, U., Weigel, D., and Campos-Ortega, J. A. (1988). Functional Interactions of Neurogenic Genes of Drosophila Melanogaster. Genetics *118*, 499-508.

Doe, C. Q., and Bowerman, B. (2001). Asymmetric cell division: fly neuroblast meets worm zygote. Curr Opin Cell Biol *13*, 68-75.

Doe, C. Q., Chu-LaGraff, Q., Wright, D. M., and Scott, M. P. (1991). The prospero gene specifies cell fates in the Drosophila central nervous system. Cell *65*, 451-464.

Dominguez, M., and Campuzano, S. (1993). asense, a member of the Drosophila achaete-scute complex, is a proneural and neural differentiation gene. Embo J *12*, 2049-2060.

Duffy, J. B. (2002). GAL4 system in Drosophila: a fly geneticist's Swiss army knife. Genesis *34*, 1-15.

Duffy, J. B., Kania, M. A., and Gergen, J. P. (1991). Expression and function of the Drosophila gene runt in early stages of neural development. Development *113*, 1223-1230.

Dyer, M. A., Livesey, F. J., Cepko, C. L., and Oliver, G. (2003). Prox1 function controls progenitor cell proliferation and horizontal cell genesis in the mammalian retina. Nat Genet *34*, 53-58.

Estrada, P., Kim, J., Coleman, J., Walker, L., Dunn, B., Takizawa, P., Novick, P., and Ferro-Novick, S. (2003). Myo4p and She3p are required for cortical ER inheritance in Saccharomyces cerevisiae. J Cell Biol *163*, 1255-1266.

Even-Faitelson, L., and Ravid, S. (2006). PAK1 and aPKCzeta regulate myosin II-B phosphorylation: a novel signaling pathway regulating filament assembly. Mol Biol Cell *17*, 2869-2881.

Fire, A., Xu, S., Montgomery, M. K., Kostas, S. A., Driver, S. E., and Mello, C. C. (1998). Potent and specific genetic interference by double-stranded RNA in Caenorhabditis elegans. Nature *391*, 806-811.

Foley, K., and Cooley, L. (1998). Apoptosis in late stage Drosophila nurse cells does not require genes within the H99 deficiency. Development *125*, 1075-1082.

Frohnhofer, H. G., Lehmann, R., and Nusslein-Volhard, C. (1986). Manipulating the anteroposterior pattern of the Drosophila embryo. J Embryol Exp Morphol *97 Suppl*, 169-179.

Fuerstenberg, S., Peng, C. Y., Alvarez-Ortiz, P., Hor, T., and Doe, C. Q. (1998). Identification of Miranda protein domains regulating asymmetric cortical localization, cargo binding, and cortical release. Mol Cell Neurosci *12*, 325-339.

Fuse, N., Hisata, K., Katzen, A. L., and Matsuzaki, F. (2003). Heterotrimeric G proteins regulate daughter cell size asymmetry in Drosophila neuroblast divisions. Curr Biol *13*, 947-954.

Garcia-Bellido, A. (1979). Genetic Analysis of the Achaete-Scute System of DROSOPHILA MELANOGASTER. Genetics *91*, 491-520.

Garcia-Bellido, A., and Santamaria, P. (1978). Developmental analysis of the achaete-scute system of *Drosophila melanogaster*. Genetics *88*, 469-486.

Ghysen, A., and Dambly-Chaudiere, C. (1989). Genesis of the Drosophila peripheral nervous system. Trends Genet *5*, 251-255.

Gigliotti, S., Rotoli, D., Graziani, F., and Malva, C. (2003). Oogenesis in Drosophila melanogaster: a model system for studying cell differentiation and development. Ital J Biochem *52*, 104-111.

Golic, K. G., and Lindquist, S. (1989). The FLP recombinase of yeast catalyzes site-specific recombination in the Drosophila genome. Cell *59*, 499-509.

Gönczy, P., and Rose, L. (2005). Asymmetric cell division and axis formation in the embryo. In Wormbook: The C. elegans Research Community).

Grumbling, G., Strelets, V., and Consortium, T. F. (2006). FlyBase: anatomical data, images and queries. Nucleic Acids Research *34*

Gutjahr, T., Patel, N. H., Li, X., Goodman, C. S., and Noll, M. (1993). Analysis of the gooseberry locus in Drosophila embryos: gooseberry determines the cuticular pattern and activates gooseberry neuro. Development *118*, 21-31.

Gutzeit, H. O. (1986). The role of microfilaments in cytoplasmic streaming in Drosophila follicles. J Cell Sci *80*, 159-169.

Hartenstein, V. (1993). Atlas of Drosophila Development Cold Spring Harbor Laboratory Press).

Hirata, J., Nakagoshi, H., Nabeshima, Y., and Matsuzaki, F. (1995). Asymmetric segregation of the homeodomain protein Prospero during Drosophila development. Nature *377*, 627-630.

Hughes, J. R., Bullock, S. L., and Ish-Horowicz, D. (2004). Inscuteable mRNA localization is dynein-dependent and regulates apicobasal polarity and spindle length in Drosophila neuroblasts. Curr Biol *14*, 1950-1956.

Ikeshima-Kataoka, H., Skeath, J. B., Nabeshima, Y., Doe, C. Q., and Matsuzaki, F. (1997). Miranda directs Prospero to a daughter cell during Drosophila asymmetric divisions. Nature *390*, 625-629.

Isshiki, T., Pearson, B., Holbrook, S., and Doe, C. Q. (2001). Drosophila neuroblasts sequentially express transcription factors which specify the temporal identity of their neuronal progeny. Cell *106*, 511-521.

Isshiki, T., Takeichi, M., and Nose, A. (1997). The role of the msh homeobox gene during Drosophila neurogenesis: implication for the dorsoventral specification of the neuroectoderm. Development *124*, 3099-3109.

Izumi, Y., Ohta, N., Itoh-Furuya, A., Fuse, N., and Matsuzaki, F. (2004). Differential functions of G protein and Baz-aPKC signaling pathways in Drosophila neuroblast asymmetric division. J Cell Biol *164*, 729-738.

Jan, Y. N., and Jan, L. Y. (1998). Asymmetric cell division. Nature *392*, 775-778.

Jarman, A. P., Grau, Y., Jan, L. Y., and Jan, Y. N. (1993). atonal is a proneural gene that directs chordotonal organ formation in the Drosophila peripheral nervous system. Cell *73*, 1307-1321.

Jimenez, F., Martin-Morris, L. E., Velasco, L., Chu, H., Sierra, J., Rosen, D. R., and White, K. (1995). vnd, a gene required for early neurogenesis of Drosophila, encodes a homeodomain protein. Embo J *14*, 3487-3495.

Justice, N., Roegiers, F., Jan, L. Y., and Jan, Y. N. (2003). Lethal giant larvae acts together with numb in notch inhibition and cell fate specification in the Drosophila adult sensory organ precursor lineage. Curr Biol *13*, 778-783.

Kaltschmidt, J. A., and Brand, A. H. (2002). Asymmetric cell division: microtubule dynamics and spindle asymmetry. J Cell Sci *115*, 2257-2264.

Kaltschmidt, J. A., Davidson, C. M., Brown, N. H., and Brand, A. H. (2000). Rotation and asymmetry of the mitotic spindle direct asymmetric cell division in the developing central nervous system. Nat Cell Biol *2*, 7-12.

Kambadur, R., Koizumi, K., Stivers, C., Nagle, J., Poole, S. J., and Odenwald, W. F. (1998). Regulation of POU genes by castor and hunchback establishes layered compartments in the Drosophila CNS. Genes Dev *12*, 246-260.

Karcavich, R. E. (2005). Generating neuronal diversity in the Drosophila central nervous system: a view from the ganglion mother cells. Dev Dyn *232*, 609-616.

Kimple, R. J., Willard, F. S., Hains, M. D., Jones, M. B., Nweke, G. K., and Siderovski, D. P. (2004). Guanine nucleotide dissociation inhibitor activity of the triple GoLoco motif protein G18: alanine-to-aspartate mutation restores function to an inactive second GoLoco motif. Biochem J *378*, 801-808.

Kimura, K., Ito, M., Amano, M., Chihara, K., Fukata, Y., Nakafuku, M., Yamamori, B., Feng, J., Nakano, T., Okawa, K., *et al.* (1996). Regulation of myosin phosphatase by Rho and Rho-associated kinase (Rho-kinase). Science *273*, 245-248.

Knoblich, J. A. (2001). Asymmetric cell division during animal development. Nat Rev Mol Cell Biol *2*, 11-20.

Knoblich, J. A., Jan, L. Y., and Jan, Y. N. (1995). Asymmetric segregation of Numb and Prospero during cell division. Nature *377*, 624-627.

Knoblich, J. A., Jan, L. Y., and Jan, Y. N. (1997). The N terminus of the Drosophila Numb protein directs membrane association and actin-dependent asymmetric localization. Proc Natl Acad Sci U S A *94*, 13005-13010.

Knoblich, J. A., Jan, L. Y., and Jan, Y. N. (1999). Deletion analysis of the Drosophila Inscuteable protein reveals domains for cortical localization and asymmetric localization. Curr Biol *9*, 155-158.

Knust, E. (1994). Cell fate choice during early neurogenesis in Drosophila melanogaster. Perspect Dev Neurobiol *2*, 141-149.

Kornberg, T. (1981). Engrailed: a gene controlling compartment and segment formation in Drosophila. Proc Natl Acad Sci U S A *78*, 1095-1099.

Kraut, R., and Campos-Ortega, J. A. (1996). inscuteable, a neural precursor gene of Drosophila, encodes a candidate for a cytoskeleton adaptor protein. Dev Biol *174*, 65-81.

Kraut, R., Chia, W., Jan, L. Y., Jan, Y. N., and Knoblich, J. A. (1996). Role of inscuteable in orienting asymmetric cell divisions in Drosophila. Nature *383*, 50-55.

Kuchinke, U., Grawe, F., and Knust, E. (1998). Control of spindle orientation in Drosophila by the Par-3-related PDZ-domain protein Bazooka. Curr Biol *8*, 1357-1365.

Laski, F. A., Rio, D. C., and Rubin, G. M. (1986). Tissue specificity of Drosophila P element transposition is regulated at the level of mRNA splicing. Cell *44*, 7-19.

Laughon, A., Driscoll, R., Wills, N., and Gesteland, R. F. (1984). Identification of two proteins encoded by the Saccharomyces cerevisiae GAL4 gene. Mol Cell Biol *4*, 268-275.

Lechler, T., and Fuchs, E. (2005). Asymmetric cell divisions promote stratification and differentiation of mammalian skin. Nature *437*, 275-280.

Lee, C. Y., Wilkinson, B. D., Siegrist, S. E., Wharton, R. P., and Doe, C. Q. (2006). Brat is a Miranda cargo protein that promotes neuronal differentiation and inhibits neuroblast self-renewal. Dev Cell *10*, 441-449.

Lee, T., Lee, A., and Luo, L. (1999). Development of the Drosophila mushroom bodies: sequential generation of three distinct types of neurons from a neuroblast. Development *126*, 4065-4076.

Leptin, M. (1999). Gastrulation in Drosophila: the logic and the cellular mechanisms. Embo J *18*, 3187-3192.

Li, P., Yang, X., Wasser, M., Cai, Y., and Chia, W. (1997). Inscuteable and Staufen mediate asymmetric localization and segregation of prospero RNA during Drosophila neuroblast cell divisions. Cell *90*, 437-447.

Lieber, T., Kidd, S., Alcamo, E., Corbin, V., and Young, M. W. (1993). Antineurogenic phenotypes induced by truncated Notch proteins indicate a role in signal transduction and may point to a novel function for Notch in nuclei. Genes Dev *7*, 1949-1965.

Lindsley, D. L., and Zimm, G. G. (1992). The Genome of *Drosophila Melanogaster* (London: Academic Press).

Lippincott-Schwartz, J., Snapp, E., and Kenworthy, A. (2001). Studying protein dynamics in living cells. Nat Rev Mol Cell Biol *2*, 444-456.

Loncar, D., and Singer, S. J. (1995). Cell membrane formation during the cellularization of the syncytial blastoderm of Drosophila. Proc Natl Acad Sci U S A *92*, 2199-2203.

Lu, B., Ackerman, L., Jan, L. Y., and Jan, Y. N. (1999). Modes of protein movement that lead to the asymmetric localization of partner of Numb during Drosophila neuroblast division. Mol Cell *4*, 883-891.

Lu, B., Jan, L., and Jan, Y. N. (2000). Control of cell divisions in the nervous system: symmetry and asymmetry. Annu Rev Neurosci *23*, 531-556.

Lu, B., Roegiers, F., Jan, L. Y., and Jan, Y. N. (2001). Adherens junctions inhibit asymmetric division in the Drosophila epithelium. Nature *409*, 522-525.

Lu, B., Rothenberg, M., Jan, L. Y., and Jan, Y. N. (1998). Partner of Numb colocalizes with Numb during mitosis and directs Numb asymmetric localization in Drosophila neural and muscle progenitors. Cell *95*, 225-235.

Ma, C., Zhou, Y., Beachy, P. A., and Moses, K. (1993). The segment polarity gene hedgehog is required for progression of the morphogenetic furrow in the developing Drosophila eye. Cell *75*, 927-938.

Mahowald, A. P., and Kambysellis, M. P. (1980). Oogenesis, Vol 2 (London: TRF Wright).

Mason, J. T., and O'Leary, T. J. (1991). Effects of formaldehyde fixation on protein secondary structure: a calorimetric and infrared spectroscopic investigation. J Histochem Cytochem *39*, 225-229.

Matsuzaki, F., Ohshiro, T., Ikeshima-Kataoka, H., and Izumi, H. (1998). miranda localizes staufen and prospero asymmetrically in mitotic neuroblasts and epithelial cells in early Drosophila embryogenesis. Development *125*, 4089-4098.

Matzke, M. A., and Birchler, J. A. (2005). RNAi-mediated pathways in the nucleus. Nat Rev Genet *6*, 24-35.

Mayer, B., Emery, G., Berdnik, D., Wirtz-Peitz, F., and Knoblich, J. A. (2005). Quantitative analysis of protein dynamics during asymmetric cell division. Curr Biol *15*, 1847-1854.

Mazumdar, A., and Mazumdar, M. (2002). How one becomes many: blastoderm cellularization in Drosophila melanogaster. Bioessays *24*, 1012-1022.

McCall, K., and Steller, H. (1998). Requirement for DCP-1 caspase during Drosophila oogenesis. Science *279*, 230-234.

McDonald, J. A., and Doe, C. Q. (1997). Establishing neuroblast-specific gene expression in the Drosophila CNS: huckebein is activated by Wingless and Hedgehog and repressed by Engrailed and Gooseberry. Development *124*, 1079-1087.

Mellerick, D. M., and Nirenberg, M. (1995). Dorsal-ventral patterning genes restrict NK-2 homeobox gene expression to the ventral half of the central nervous system of Drosophila embryos. Dev Biol *171*, 306-316.

Merrill, P. T., Sweeton, D., and Wieschaus, E. (1988). Requirements for autosomal gene activity during precellular stages of Drosophila melanogaster. Development *104*, 495-509.

Montero, C. (2003). The antigen-antibody reaction in immunohistochemistry. J Histochem Cytochem *51*, 1-4.

Morrison, S. J., and Kimble, J. (2006). Asymmetric and symmetric stem-cell divisions in development and cancer. Nature *441*, 1068-1074.

Muskavitch, M. A. (1994). Delta-notch signaling and Drosophila cell fate choice. Dev Biol *166*, 415-430.

Nagai, H., Li, Y., Hatano, S., Toshihito, O., Yuge, M., Ito, E., Utsumi, M., Saito, H., and Kinoshita, T. (2003). Mutations and aberrant DNA methylation of the PROX1 gene in hematologic malignancies. Genes Chromosomes Cancer *38*, 13-21.

Noguchi, T., Lenartowska, M., and Miller, K. G. (2006). Myosin VI stabilizes an actin network during Drosophila spermatid individualization. Mol Biol Cell *17*, 2559-2571.

Novotny, T., Eiselt, R., and Urban, J. (2002). Hunchback is required for the specification of the early sublineage of neuroblast 7-3 in the Drosophila central nervous system. Development *129*, 1027-1036.

Ohshiro, T., Yagami, T., Zhang, C., and Matsuzaki, F. (2000). Role of cortical tumour-suppressor proteins in asymmetric division of Drosophila neuroblast. Nature *408*, 593-596.

Okada, M. (1998). Germline cell formation in Drosophila embryogenesis. Genes Genet Syst *73*, 1-8.

Park, H., Ramamurthy, B., Travaglia, M., Safer, D., Chen, L. Q., Franzini-Armstrong, C., Selvin, P. R., and Sweeney, H. L. (2006). Full-length myosin VI dimerizes and moves processively along actin filaments upon monomer clustering. Mol Cell *21*, 331-336.

Parks, S., Wakimoto, B., and Spradling, A. (1986). Replication and expression of an X-linked cluster of Drosophila chorion genes. Dev Biol *117*, 294-305.

Parmentier, M. L., Woods, D., Greig, S., Phan, P. G., Radovic, A., Bryant, P., and O'Kane, C. J. (2000). Rapsynoid/partner of inscuteable controls asymmetric division of larval neuroblasts in Drosophila. J Neurosci *20*, RC84.

Pearson, B. J., and Doe, C. Q. (2003). Regulation of neuroblast competence in Drosophila. Nature *425*, 624-628.

Peng, C. Y., Manning, L., Albertson, R., and Doe, C. Q. (2000). The tumour-suppressor genes lgl and dlg regulate basal protein targeting in Drosophila neuroblasts. Nature *408*, 596-600.

Perrimon, N. (1998). Creating mosaics in Drosophila. Int J Dev Biol *42*, 243-247.

Petritsch, C., Tavosanis, G., Turck, C. W., Jan, L. Y., and Jan, Y. N. (2003). The Drosophila myosin VI Jaguar is required for basal protein targeting and correct spindle orientation in mitotic neuroblasts. Dev Cell *4*, 273-281.

Petronczki, M., and Knoblich, J. A. (2001). DmPAR-6 directs epithelial polarity and asymmetric cell division of neuroblasts in Drosophila. Nat Cell Biol *3*, 43-49.

Portin, P. (2002). General outlines of the molecular genetics of the Notch signalling pathway in Drosophila melanogaster: a review. Hereditas *136*, 89-96.

Poteryaev, D., Squirrell, J. M., Campbell, J. M., White, J. G., and Spang, A. (2005). Involvement of the actin cytoskeleton and homotypic membrane fusion in ER dynamics in Caenorhabditis elegans. Mol Biol Cell *16*, 2139-2153.

Qin, H., Percival-Smith, A., Li, C., Jia, C. Y., Gloor, G., and Li, S. S. (2004). A novel transmembrane protein recruits numb to the plasma membrane during asymmetric cell division. J Biol Chem *279*, 11304-11312.

Rhyu, M. S., Jan, L. Y., and Jan, Y. N. (1994). Asymmetric distribution of numb protein during division of the sensory organ precursor cell confers distinct fates to daughter cells. Cell *76*, 477-491.

Riechmann, V., and Ephrussi, A. (2001). Axis formation during Drosophila oogenesis. Curr Opin Genet Dev *11*, 374-383.

Romani, S., Campuzano, S., Macagno, E. R., and Modolell, J. (1989). Expression of achaete and scute genes in Drosophila imaginal discs and their function in sensory organ development. Genes Dev *3*, 997-1007.

Sanada, K., and Tsai, L. H. (2005). G protein betagamma subunits and AGS3 control spindle orientation and asymmetric cell fate of cerebral cortical progenitors. Cell *122*, 119-131.

Schaefer, M., Petronczki, M., Dorner, D., Forte, M., and Knoblich, J. A. (2001). Heterotrimeric G proteins direct two modes of asymmetric cell division in the Drosophila nervous system. Cell *107*, 183-194.

Schaefer, M., Shevchenko, A., Shevchenko, A., and Knoblich, J. A. (2000). A protein complex containing Inscuteable and the Galpha-binding protein Pins orients asymmetric cell divisions in Drosophila. Curr Biol *10*, 353-362.

Schneider, M., Buchler, P., Giese, N., Giese, T., Wilting, J., Buchler, M. W., and Friess, H. (2006). Role of lymphangiogenesis and lymphangiogenic factors during pancreatic cancer progression and lymphatic spread. Int J Oncol *28*, 883-890.

Schober, M., Schaefer, M., and Knoblich, J. A. (1999). Bazooka recruits Inscuteable to orient asymmetric cell divisions in Drosophila neuroblasts. Nature *402*, 548-551.

Scholz, T., Altmann, S. M., Antognozzi, M., Tischer, C., Horber, J. K., and Brenner, B. (2005). Mechanical properties of single myosin molecules probed with the photonic force microscope. Biophys J *88*, 360-371.

Schuldt, A. J., Adams, J. H., Davidson, C. M., Micklem, D. R., Haseloff, J., St Johnston, D., and Brand, A. H. (1998). Miranda mediates asymmetric protein and RNA localization in the developing nervous system. Genes Dev *12*, 1847-1857.

Schupbach, T., and Wieschaus, E. (1986). Germline autonomy of maternal-effect mutations altering the embryonic body pattern of Drosophila. Dev Biol *113*, 443-448.

Schweisguth, F. (1999). Dominant-negative mutation in the beta2 and beta6 proteasome subunit genes affect alternative cell fate decisions in the Drosophila sense organ lineage. Proc Natl Acad Sci U S A *96*, 11382-11386.

Shen, C. P., Jan, L. Y., and Jan, Y. N. (1997). Miranda is required for the asymmetric localization of Prospero during mitosis in Drosophila. Cell *90*, 449-458.

Shen, C. P., Knoblich, J. A., Chan, Y. M., Jiang, M. M., Jan, L. Y., and Jan, Y. N. (1998). Miranda as a multidomain adapter linking apically localized Inscuteable and basally localized Staufen and Prospero during asymmetric cell division in Drosophila. Genes Dev *12*, 1837-1846.

Shen, Q., Zhong, W., Jan, Y. N., and Temple, S. (2002). Asymmetric Numb distribution is critical for asymmetric cell division of mouse cerebral cortical stem cells and neuroblasts. Development *129*, 4843-4853.

Siegrist, S. E., and Doe, C. Q. (2005). Microtubule-induced Pins/Galphai cortical polarity in Drosophila neuroblasts. Cell *123*, 1323-1335.

Skeath, J. B. (1999). At the nexus between pattern formation and cell-type specification: the generation of individual neuroblast fates in the Drosophila embryonic central nervous system. Bioessays *21*, 922-931.

Skeath, J. B., and Carroll, S. B. (1994). The achaete-scute complex: generation of cellular pattern and fate within the Drosophila nervous system. Faseb J *8*, 714-721.

Skeath, J. B., and Thor, S. (2003). Genetic control of Drosophila nerve cord development. Curr Opin Neurobiol *13*, 8-15.

Solecki, D. J., Govek, E. E., Tomoda, T., and Hatten, M. E. (2006). Neuronal polarity in CNS development. Genes Dev *20*, 2639-2647.

Spana, E. P., and Doe, C. Q. (1995). The prospero transcription factor is asymmetrically localized to the cell cortex during neuroblast mitosis in Drosophila. Development *121*, 3187-3195.

Spana, E. P., Kopczynski, C., Goodman, C. S., and Doe, C. Q. (1995). Asymmetric localization of numb autonomously determines sibling neuron identity in the Drosophila CNS. Development *121*, 3489-3494.

Srinivasan, S., Peng, C. Y., Nair, S., Skeath, J. B., Spana, E. P., and Doe, C. Q. (1998). Biochemical analysis of ++Prospero protein during asymmetric cell division: cortical Prospero is highly phosphorylated relative to nuclear Prospero. Dev Biol *204*, 478-487.

St Johnston, D. (2002). The art and design of genetic screens: Drosophila melanogaster. Nat Rev Genet *3*, 176-188.

St Johnston, D., and Nuesslein-Volhard, C. (1992). The origin of pattern and polarity in the Drosophila embryo. Cell *68*, 201-219.

Struhl, G., and Adachi, A. (1998). Nuclear access and action of notch in vivo. Cell *93*, 649-660.

Sun, Y., Goderie, S. K., and Temple, S. (2005). Asymmetric distribution of EGFR receptor during mitosis generates diverse CNS progenitor cells. Neuron *45*, 873-886.

Sweeney, S. E., Halloran, P. J., and Kim, Y. B. (1996). Identification of a unique porcine Fc gamma RIIIA alpha molecular complex. Cell Immunol *172*, 92-99.

Tan, J. L., Ravid, S., and Spudich, J. A. (1992). Control of nonmuscle myosins by phosphorylation. Annu Rev Biochem *61*, 721-759.

Tautz, D., and Pfeifle, C. (1989). A non-radioactive in situ hybridization method for the localization of specific RNAs in Drosophila embryos reveals translational control of the segmentation gene hunchback. Chromosoma *98*, 81-85.

Temple, S. (2003). Embryonic stem cell self-renewal, analyzed. Cell *115*, 247-248.

Temple, S., and Alvarez-Buylla, A. (1999). Stem cells in the adult mammalian central nervous system. Curr Opin Neurobiol *9*, 135-141.

Theodosiou, N. A., and Xu, T. (1998). Use of FLP/FRT system to study Drosophila development. Methods *14*, 355-365.

Tio, M., Zavortink, M., Yang, X., and Chia, W. (1999). A functional analysis of inscuteable and its roles during Drosophila asymmetric cell divisions. J Cell Sci *112 (Pt 10)*, 1541-1551.

Urbach, R., and Technau, G. M. (2003). Segment polarity and DV patterning gene expression reveals segmental organization of the Drosophila brain. Development *130*, 3607-3620.

Vaessin, H., Grell, E., Wolff, E., Bier, E., Jan, L. Y., and Jan, Y. N. (1991). prospero is expressed in neuronal precursors and encodes a nuclear protein that is involved in the control of axonal outgrowth in Drosophila. Cell *67*, 941-953.

van Diepen, M. T., Spencer, G. E., van Minnen, J., Gouwenberg, Y., Bouwman, J., Smit, A. B., and van Kesteren, R. E. (2005). The molluscan RING-finger protein L-TRIM is essential for neuronal outgrowth. Mol Cell Neurosci *29*, 74-81.

Verheyen, E. M., and Cooley, L. (1994). Profilin mutations disrupt multiple actin-dependent processes during Drosophila development. Development *120*, 717-728.

Villares, R., and Cabrera, C. V. (1987). The achaete-scute gene complex of D. melanogaster: conserved domains in a subset of genes required for neurogenesis and their homology to myc. Cell *50*, 415-424.

von Ohlen, T., and Doe, C. Q. (2000). Convergence of dorsal, dpp, and egfr signaling pathways subdivides the drosophila neuroectoderm into three dorsal-ventral columns. Dev Biol *224*, 362-372.

Wakamatsu, Y., Maynard, T. M., Jones, S. U., and Weston, J. A. (1999). NUMB localizes in the basal cortex of mitotic avian neuroepithelial cells and modulates neuronal differentiation by binding to NOTCH-1. Neuron *23*, 71-81.

Wang, H., and Chia, W. (2005). Drosophila neural progenitor polarity and asymmetric division. Biol Cell *97*, 63-74.

Weigmann, K., Klapper, R., Strasser, T., Rickert, C., Technau, G. M., Jäckle, H., Janning, W., and Klämbt, C. (2003). FlyMove – a new way to look at development of Drosophila. Trends in Genetics *19*, 310-311.

Weiss, J. B., Von Ohlen, T., Mellerick, D. M., Dressler, G., Doe, C. Q., and Scott, M. P. (1998). Dorsoventral patterning in the Drosophila central nervous system: the intermediate neuroblasts defective homeobox gene specifies intermediate column identity. Genes Dev *12*, 3591-3602.

Wheatley, S., Kulkarni, S., and Karess, R. (1995). Drosophila nonmuscle myosin II is required for rapid cytoplasmic transport during oogenesis and for axial nuclear migration in early embryos. Development *121*, 1937-1946.

White, T. J., Arnheim, N., and Erlich, H. A. (1989). The polymerase chain reaction. Trends Genet *5*, 185-189.

Wieschaus, E. (1996). Embryonic transcription and the control of developmental pathways. Genetics *142*, 5-10.

Wodarz, A. (2005). Molecular control of cell polarity and asymmetric cell division in Drosophila neuroblasts. Curr Opin Cell Biol *17*, 475-481.

Wodarz, A., and Huttner, W. B. (2003). Asymmetric cell division during neurogenesis in Drosophila and vertebrates. Mech Dev *120*, 1297-1309.

Wodarz, A., Ramrath, A., Grimm, A., and Knust, E. (2000). Drosophila atypical protein kinase C associates with Bazooka and controls polarity of epithelia and neuroblasts. J Cell Biol *150*, 1361-1374.

Wodarz, A., Ramrath, A., Kuchinke, U., and Knust, E. (1999). Bazooka provides an apical cue for Inscuteable localization in Drosophila neuroblasts. Nature *402*, 544-547.

Wurmbach, E., Wech, I., and Preiss, A. (1999). The Enhancer of split complex of Drosophila melanogaster harbors three classes of Notch responsive genes. Mech Dev *80*, 171-180.

Xu, T., and Rubin, G. M. (1993). Analysis of genetic mosaics in developing and adult Drosophila tissues. Development *117*, 1223-1237.

Xue, F., and Cooley, L. (1993). kelch encodes a component of intercellular bridges in Drosophila egg chambers. Cell *72*, 681-693.

Yamashita, Y. M., Fuller, M. T., and Jones, D. L. (2005). Signaling in stem cell niches: lessons from the Drosophila germline. J Cell Sci *118*, 665-672.

Yu, F., Cai, Y., Kaushik, R., Yang, X., and Chia, W. (2003). Distinct roles of Galphai and Gbeta13F subunits of the heterotrimeric G protein complex in the mediation of Drosophila neuroblast asymmetric divisions. J Cell Biol *162*, 623-633.

Yu, F., Morin, X., Cai, Y., Yang, X., and Chia, W. (2000). Analysis of partner of inscuteable, a novel player of Drosophila asymmetric divisions, reveals two distinct steps in inscuteable apical localization. Cell *100*, 399-409.

Zhong, W., Jiang, M. M., Weinmaster, G., Jan, L. Y., and Jan, Y. N. (1997). Differential expression of mammalian Numb, Numblike and Notch1 suggests distinct roles during mouse cortical neurogenesis. Development *124*, 1887-1897.

9 ACKNOWLEDGEMENTS

I would like to thank **Dr. Claudia Petritsch** for the possibility to do my PhD in her lab, for the interesting project as well as for the strong support during the three years of my thesis. I would also like to thank all members of the **Gene Center Munich** (LMU) for the great atmosphere in this institute.

Special thanks to **Prof. Dr. Bertold Hock** for giving advice and being my "doctor father" as well as to **Prof. Dr. Angelika Schnieke** and **Prof. Dr. Dr. Johann Bauer** for attending my PhD committee.

Thanks to **Prof. Dr. Ralf Jansen** for his help at every opportunity. I would also like to thank **Prof. Dr. Heinrich Leonhardt** and his group for technical assistance concerning the FRAP experiments and **Dr. Takashi Suzuki** for help with the microinjections. Thanks also to **Dr. Stefan Heidmann** from the Lehner group for providing several fly stocks.

I would like to thank all my (former) lab colleagues **Ramona Heptner, Corinna Albers, Diana Langer, Tijana Radovicj, Stefan Dehmel, Tina Whiteus,** and **Birgit Czermin** for the great atmosphere and the good music. Special thanks to **Markus Waldhuber** for the great assistance on the "Miranda Project" and **Ingrid Fetka** for helping to generate the transgenic flies. Thanks to all people of the third floor for the help in several situations and the nice atmosphere especially during "coffee breaks" in the kitchen, notably **Geri Dobreva** and **Matthias Kieslinger** for their technical advice. Many thanks to **Tatiana Tomasi** from the MPI for the great help concerning never ending "fly" problems.

I would like to thank my former supervisor of the diploma thesis **Dr. Nicolai Obel** for correcting the abstract and **Hilary Stevens** for final proof reading.

Special thanks to my **Mother** and my **Father** and my whole family, "**Aunt", "Uncle", Serena, Tatjana** as well as **Kilian, Jürgen, "Oma", Stefan** and **Erika**, for being there for whenever I needed them.

Special thanks also to **Peter** for support in "good times and in bad times". I would like to thank **Auguste C.** especially for the her company in drinking red wine and our good old buddy **Peter Lehmann** (14.5%), as well as **Cesar** for his good company.

Special thanks also to **Alessandro** for all the "coffee breaks" during the last months, which made the writing more amusing.

Thanks to **Tom, Martha, Julia, Alex, Steph, Steffi, Bärbel** and all my friends.